AD: _____

AWARD NUMBER: W81XWH-16-1-0179

TITLE: Targeting Extracellular Histones with Novel RNA Bio-drugs for the Treatment of Acute Lung Injury

PRINCIPAL INVESTIGATOR: Francis Miller

RECIPIENT: Duke University
Durham, NC 27705

REPORT DATE: October 2018

TYPE OF REPORT: Annual

PREPARED FOR: U.S. Army Medical Research and Materiel Command
Fort Detrick, Maryland 21702-5012

REPORT DOCUMENTATION PAGE

Form Approved
OMB No. 0704-0188

1. REPORT DATE	2. REPORT TYPE	3. DATES COVERED
October 2018	Annual report	15 Sep 2017 - 14 Sep 2018

4. TITLE AND SUBTITLE
Targeting Extracellular Histones with Novel RNA Bio-drugs for the Treatment of Acute Lung Injury

5a. CONTRACT NUMBER

5b. GRANT NUMBER
W81XWH-16-1-0179

5c. PROGRAM ELEMENT NUMBER

6. AUTHOR(S)
Francis J Miller, MD

E-Mail: francis.miller@duke.edu;

5d. PROJECT NUMBER

5e. TASK NUMBER

5f. WORK UNIT NUMBER

7. PERFORMING ORGANIZATION NAME(S) AND ADDRESS(ES)

Duke University
200 West Main St
Suite 820 Erwin Square Plaza
Durham, NC 27705-0000

Subcontract to:
UNIVERSITY OF IOWA, THE
105 JESSUP HALL
IOWA CITY IA 52242-1316

8. PERFORMING ORGANIZATION REPORT NUMBER

9. SPONSORING / MONITORING AGENCY NAME(S) AND ADDRESS(ES)

U.S. Army Medical Research and Materiel Command
Fort Detrick, Maryland 21702-5012

10. SPONSOR/MONITOR'S ACRONYM(S)

11. SPONSOR/MONITOR'S REPORT NUMBER(S)

12. DISTRIBUTION / AVAILABILITY STATEMENT

Approved for public release; distribution unlimited

13. SUPPLEMENTARY NOTES

14. ABSTRACT

Extracellular histones have been proposed as the causative agent of acute lung injury (ALI). The goal of this proposal is to develop a therapeutic to neutralize (inactivate) circulating histones and prevent the morbidity and mortality associated with multiple organ dysfunction/acute respiratory distress syndrome (MODS/ARDS) occurring with ALI. To accomplish this goal, we developed novel bio-reagents (RNA aptamers) that bind to histones known to cause MODS/ARDS and ALI but do not bind to other serum proteins. The RNA aptamers were evaluated for their ability to inhibit histone-mediate 1. cytotoxicity, 2. platelet aggregation, 3. TLR activation and 4. calcium influx. In this report, we show that RNA aptamers protect from histone-mediated pulmonary cell toxicity and attenuate mortality and lung inflammation and tissue destruction in mice. Pulmonary delivery results in diffuse distribution and prolonged retention of aptamers in the lungs. Ongoing studies are evaluating the protective effects of aptamers in murine models of inhalation injury.

15. SUBJECT TERMS
Acute lung injury (ALI), acute respiratory distress syndrome (ARDS), multiple organ dysfunction syndrome, extracellular histones, circulating histones, histones

16. SECURITY CLASSIFICATION OF:			17. LIMITATION OF ABSTRACT	18. NUMBER OF PAGES	19a. NAME OF RESPONSIBLE PERSON
a. REPORT	b. ABSTRACT	c. THIS PAGE			USAMRMC
Unclassified	Unclassified	Unclassified	Unclassified	130	19b. TELEPHONE NUMBER *(include area code)*

TABLE OF CONTENTS

1. INTRODUCTION:

A challenging medical problem often observed in critically ill patients is that following a severe injury or illness, even those organs not directly affected by the original problem subsequently become dysfunctional. This condition, known as multiple organ dysfunction syndrome (MODS) may be reversible, but there is no treatment to prevent it from happening and of those that develop MODS, the risk of death is 40%. The most common organ involved in MODS is the lungs (referred to as acute respiratory distress syndrome or ARDS). Trauma (blast and explosive) has obvious relevance to the military; however, other equally relevant causes of MODS/ARDS are acute lung injury (ALI) from smoke/chlorine gas inhalation, burns, radiation, influenza and severe infection. Only recently have investigators recognized that each of these various conditions are caused by damaged tissues releasing histones into the circulation. Histones normally reside in the nucleus and partner with the DNA, but when extracellular histones have toxic effects to the lungs and other organs. The goal of this proposal is to develop a therapeutic to neutralize (inactivate) circulating histones and prevent the morbidity and mortality associated with MODS/ARDS and ALI that can be easily delivered in combat and field situations. To accomplish this goal, novel bio-reagents (RNA aptamers) that will bind to histones but not to other circulating proteins or cells will be tested in human cultured cells and in mice for their ability to prevent histone-mediated toxicity and ALI. Studies have successfully evaluated the effect of extracellular histones on endothelial cell calcium influx, TLR activation, cytotoxicity, and on platelet activation. Furthermore, additional characterization of RNA aptamers have been completed and have been found to attenuate cell death and platelet aggregation. In addition, we find that serum levels of circulating histones are associated with the severity of illness in patients. In mice, RNA aptamers attenuate the tissue injury and prevent death in mice injected intravenously with histones. These data have been submitted for publication at Nature Communications. Ongoing studies have shown that pulmonary delivery results in diffuse distribution and retention of RNA aptamers in the lung. In vivo experiments are testing the efficacy of these aptamer at preventing pulmonary inflammation and tissue disruption in response to smoke inhalation injury, chlorine gas injury and influenza. The project is on target for completion at the end of the funding period and we anticipate the publication of several manuscripts using the data derived from these studies. Since histones are highly conserved across species from yeast to humans, the bio-reagents developed and validated in this proposal can be immediately tested in preclinical animal models and human clinical trials. Furthermore, as a drug to prevent the development of MODS/ARDS and ALI in high risk patients, these bio-reagents have significant advantages as compared to other possible therapeutics because they are very stable and not as susceptible to fluctuations in temperature, do not require special handling conditions, do not cause allergic responses, and will be easy to deliver. In addition to having relevance to military situations, the therapeutics derived from this application would have wide benefit to the general population in reducing morbidity and mortality associated with MODS/ARDS and ALI.

2. KEYWORDS:

Acute lung injury (ALI), acute respiratory distress syndrome (ARDS), multiple organ dysfunction syndrome, extracellular histones, circulating histones, histones

3. ACCOMPLISHMENTS:

What were the major goals of the project?

The primary goal of this project is to test the efficacy of selective RNA aptamers to inactivate circulating histones and prevent the morbidity and mortality associated with ALI/ARD. More specifically, the major goals of this project are:

1. Identification of individual aptamer sequences capable of neutralizing one or multiple histone subtypes.
2. In vitro assessment of toxicity of histones on pulmonary endothelial and epithelial cells and efficacy of RNA aptamers.
3. Confirmation of aptamer binding to histones and neutralizing efficacy in blood from patients with ALI/ARD.
4. Proof-of-concept of in vivo efficacy of RNA aptamers in different preclinical models of ALI (smoke inhalation injury, chlorine gas inhalation and influenza).
5. Measurement of the half-life of RNA bio-drugs in human serum.
6. Toxicology/safety profile of the aptamers and assessment for non-specific immune activation.
7. Filing of intellectual property patent(s).

What was accomplished under these goals?

The methodology and the data supporting the accomplishments listed below are described in the attached manuscript (Urak et al) which was recently accepted for publication at *Nature Communications*. Figure numbers refer to the figure in the manuscript (see appendix).

- Identification of histone-specific RNA aptamers – Figure 1 and Supplemental Figures 1 and 2.
- High specificity binding of RNA aptamers to histones but not to serum proteins - Figure 2.
- Stability of RNA aptamers in human serum - Supplementary Figure 3.
- RNA aptamers inhibit histone-induced platelet aggregation – Figure 3 and Supplementary Figure 4. (SOW Major task 2)
- RNA aptamers inhibit histone-induced Toll like receptor (TLR) activation - Figure 3 and Supplementary Figure 4. (SOW Major task 2)
- RNA aptamers inhibit histone-mediated toxicity of endothelial cells - Figure 3. (SOW Major task 2)
- RNA aptamers inhibit histone-mediated extracellular calcium influx into endothelial cells - Figure 3. (SOW Major task 2)
- RNA aptamers prevent death in a murine model of MODS – Figure 4.
- RNA aptamers attenuate the histologic findings of vascular congestion, multifocal neutrophilic aggregates in vessels, thrombi, and in the lung in response to intravenous histones in mice – Figure 4 and Supplementary Figure 5.
- RNA aptamers partially attenuate TLR activation in the liver but not in lung or spleen in response to intravenous histones – Figure 4.

- Aptamers bind and neutralize histones generated in NETosis of human neutrophils – Figure 6.

In data currently being prepared for manuscript submission, we show that the RNA aptamers identified can detect low levels (< 10 µg/mL) of circulating histones in critically ill patient samples. This aptamer-based detection assay was orders of magnitude more sensitive at detecting circulating histones in serum compared to current antibody-based methods. This work was performed to allow completion of Major task #2, ex vivo studies to measure histone levels in blood from patients with acute lung injury (ALI). The "aptamer-based detection assay" was developed because our experience with the antibody-based methods were disappointing in that they appeared to lack expected sensitivity and because of difficulties obtaining reproducible quality antibody to histones.

In addition, using this aptamer-based detection assay, we find that serum histone levels are associated with patient severity of illness, as measured by the APACHE II score (Figure 1). (SOW Major task 2)

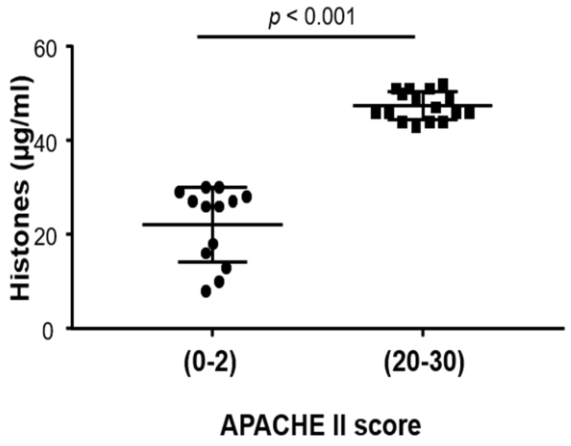

Figure 1. Circulating histone levels and severity of illness in patients using RNA aptamers for detection.

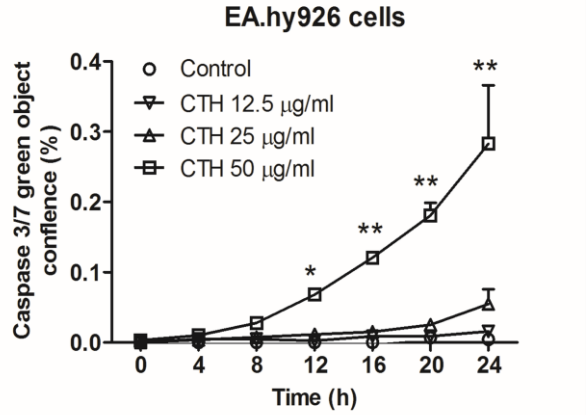

Figure 2. Dose dependent release of caspases by human endothelial cells in response to calf-thymus histones (CTH).

We have completed the studies showing the ability of RNA aptamers to inhibit histone-induced platelet aggregation (SOW Major task 2) and this data is shown in the Nature Communications manuscript (Figure 3 and Supplementary Figure 4). These studies of platelet aggregation were performed at Iowa with a collaborator. However, we have identified a new collaborator at Duke (site 1) to assist with performance of the platelet surface marker expression in response to aptamers and these studies will be completed within the next six months.

We are further characterizing the cytotoxic activity of histones on human endothelial and epithelial cells and the ability of RNA aptamers to protect from cell death when administered after the CTH. This protocol has clinical relevance and has not been sufficiently tested in the literature. Exposure of endothelial cells to calf thymus histones (CTH) results in a dose dependent release of caspases 3 and 7 (Figure 2). The treatment of cultured cells with RNA aptamers one hour after CTH protects cells from histone-mediated toxicity when analyzed at 24 hours (Figure 3). (SOW Major task 2)

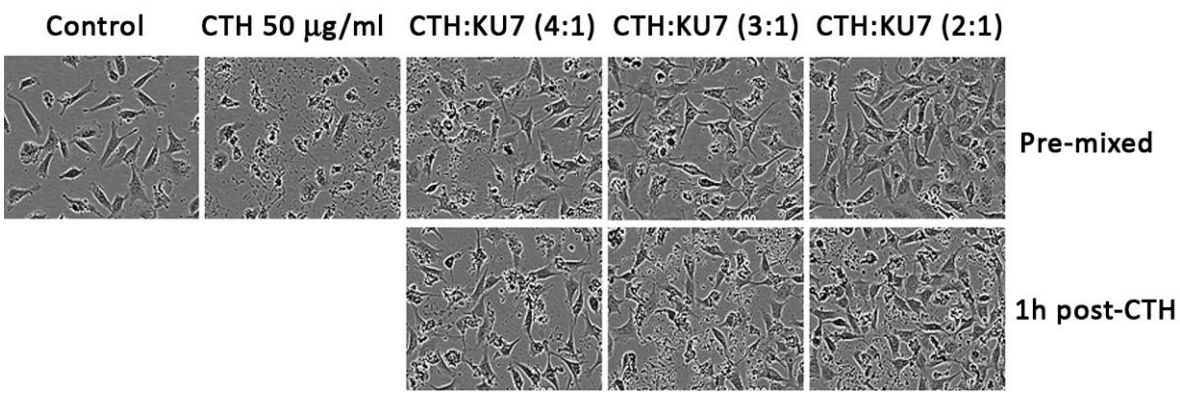

Figure 3. RNA aptamers protect from endothelial cell death when administered one hour after the CTH. Pictures obtained 24 hours after CTH. Rounded and shrunken cells indicated cell death.

Our data suggests that pulmonary epithelial cells are less sensitive to CTH in vitro as compared to endothelial cells (Figure 4). (SOW Major task 2)

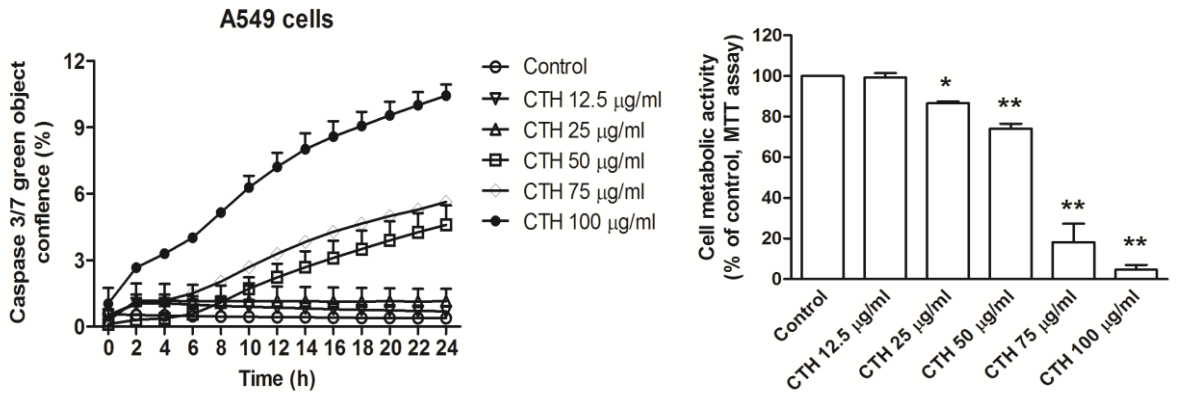

Figure 4. Dose-dependent histone mediated toxicity of human pulmonary epithelial cells as measured by caspase 3 and 7 release (left panel) and by MTT assay (right panel).

In addition, the administration of RNA aptamers one hour after CTH protects human epithelial cells from histone-mediated cell toxicity (Figure 5). (SOW Major task 3)

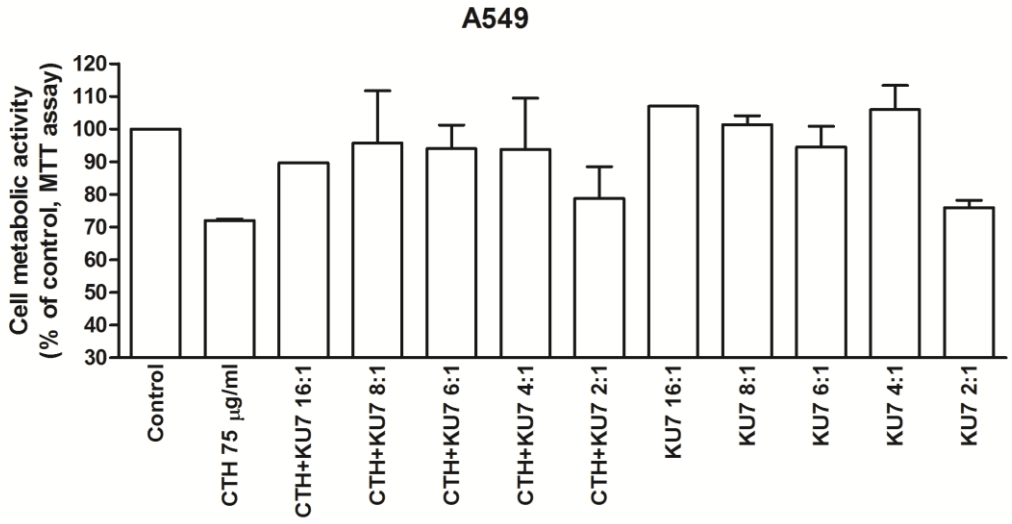

Figure 5. RNA aptamer (KU7) protects from histone-mediated toxicity (CTH 75 ug/ml) in human epithelial cells measured 24 hours after CTH by MTT assay. The RNA aptamers were added one hour after the CTH. The ratios indicate the relative molar amounts of histone to aptamer.

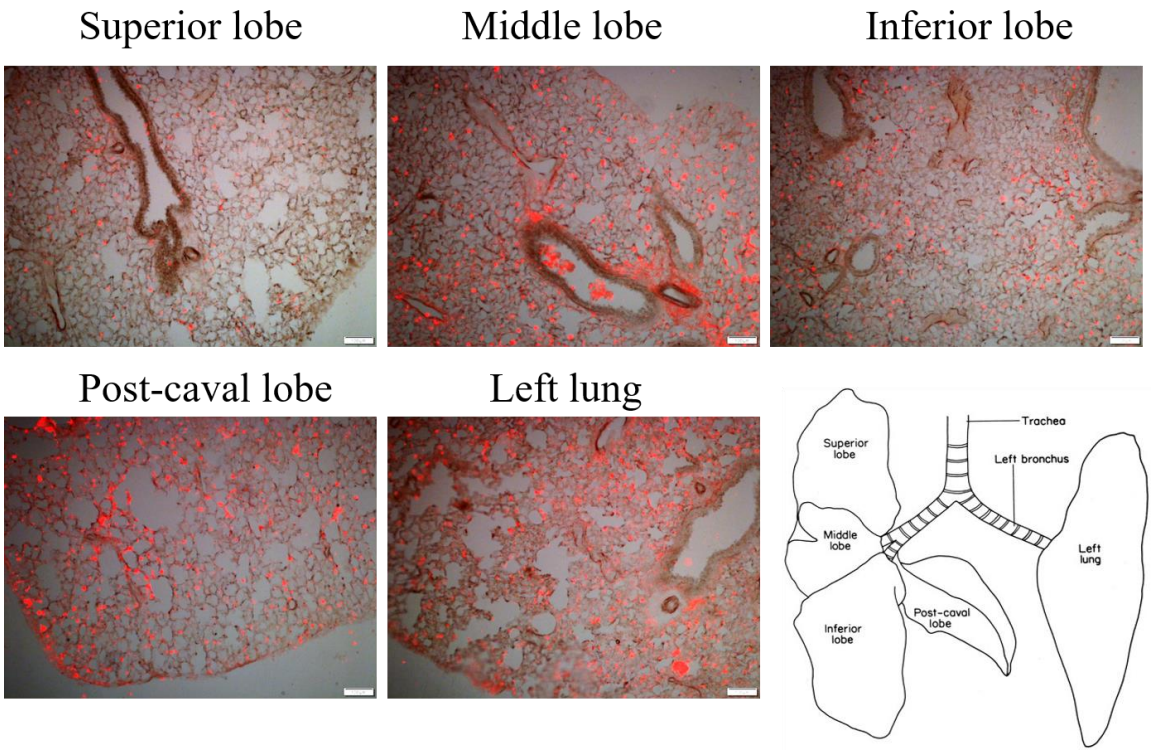

Figure 6. Fluorescent microscopy of mouse lung four hours after intratracheal delivery of fluorescent RNA aptamer KU7.

We examined the distribution and the retention of the RNA aptamers in the mouse lung following intratracheal (IT) delivery. Using a fluorescently labelled RNA aptamer, we detected diffuse alveolar distribution of the RNA aptamer at four hours following IT delivery throughout the entire lung (Figure 6). (SOW Major task 3) Importantly, retention of the aptamer was detected in the BALF and within the lung (fluorescence microscopy) at 24 hours following administration. This observation has important implications regarding the dosing of RNA aptamers for pulmonary injury.

SOW Major task 3 and 4 examine effect of anti-histone aptamers in models of acute lung injury. As a positive control, mice received histones into the lung. The direct administration of histones to the lungs by intratracheal delivery results in tissue destruction and inflammation within the lung tissue (Figure 7). Intratracheal delivery of histones (CTH) also causes an inflammatory infiltration into the lungs as measured by broncheoaveolar lavage and staining for white blood cells (Figure 8). Importantly, the RNA aptamer KU7 alone does not cause an inflammatory response when administered to the lungs of mice (Figure 8). (SOW Major task 3 and task 5) However, pre or post treatment with KU7 did not attenuated the inflammatory response to CTH. (SOW Major task 3) This may suggest that the KU7-histone complex elicits an inflammatory response in the lung. We have collected the lungs from these mice and processing for histologic analysis to determine whether the RNA aptamers protect from the histologic damage caused by CTH (as seen in Figure 7). (SOW Major task 3, 4)

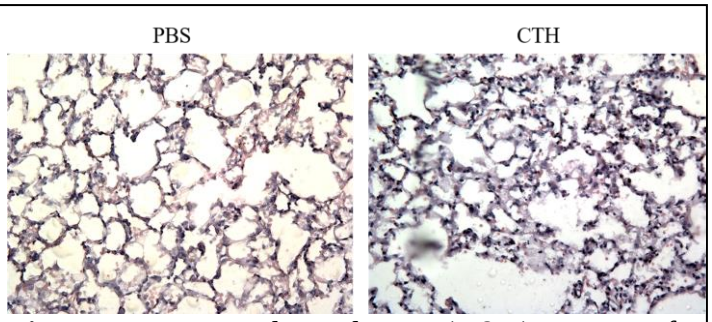

Figure 7. Hematoxylin and eosin (H&E) staining of mouse lung six hours after PBS (50 µl, left panel) or histones (CTH, 500 µg/50ul, right panel). Histones caused disruption of normal alveolar architecture and inflammatory cell infiltration. The platelet aggregation and hemorrhage seen in the lungs after intravenous delivery of histones was not observed.

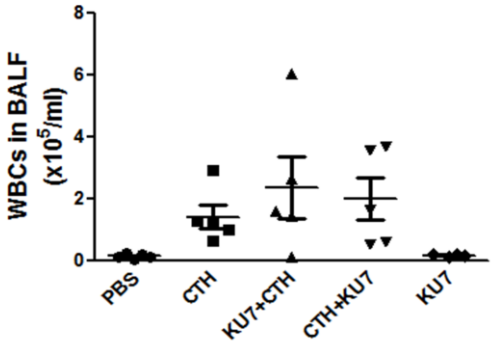

Figure 8. Inflammatory cell number in broncheo-alveolar lavage fluid (BLAF) of mice. Histones were administered to mice intratracheally (IT) and RNA aptamer KU7 given IT either 30 min before (KU7+CTH) or 30 minutes after (CTH+KU&)

We have initiated implementation of each of the three mouse models of acute lung injury (smoke inhalation, chlorine inhalation, and influenza). . (SOW Major task 3 and 4) As shown in Figure 9, the intratracheal delivery of smoke particulate matter when derived from flammable wood elicits an inflammatory cell infiltration into the BALF. In contrast, the smoke particulate matter from smoldering wood does not. We are in the process of measuring histone levels and histopathology in these lungs. (SOW Major task 3). Studies are planned that will test the efficacy of aptamer delivered into the lungs on reducing the inflammatory response.

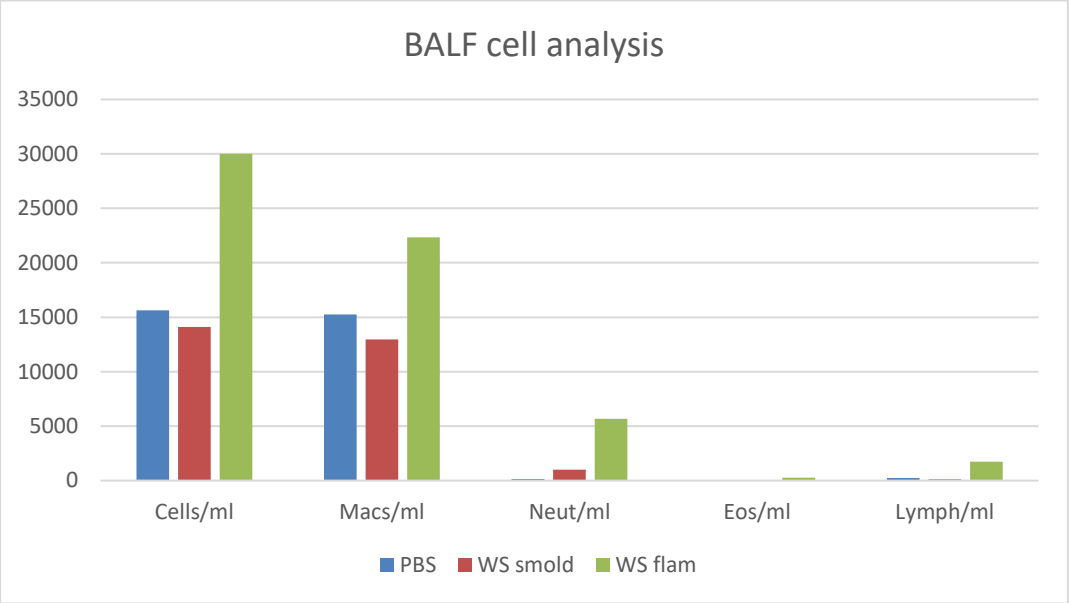

Figure 9. Flammable wood smoke particulate matter induces inflammatory infiltration into the lungs in mice 24-hours after intratracheal delivery.

We have also begun studies using the chlorine gas model of acute lung injury. (SOW Major task 3) In our early data, the inhalation of chlorine gas by mice predominantly causes large airway irritation. Evaluation of bronchoalveolar fluid suggests that the chlorine gas is not getting into the alveoli of the mice without causing severe large airway damage. We are attempting to change the dose and duration of chlorine gas in this model to induce the intended ALI.

We have also initiated experiments of influenza model of ALI in mice. We have procured the virus and are currently working with the core facility that will assist with these studies.

Finally, we have performed studies examining the safety of the aptamer (SOW Major task 5). Given the expense of humanized mice, our initial pilot studies have tested safety in C57BL6 mice. Our findings with these mice will allow for more focused studies in the humanized mice. In addition to the data in Figure 8, we have also tested the effect of aptamers on the induction of inflammatory gene expression in the lung, liver, kidney, and spleen. The data for liver and spleen are shown in figure 10. (SOW Major task 5). Organ weights were also obtained, and organ histology being processed. These data will be extended in humanized mice over the next year.

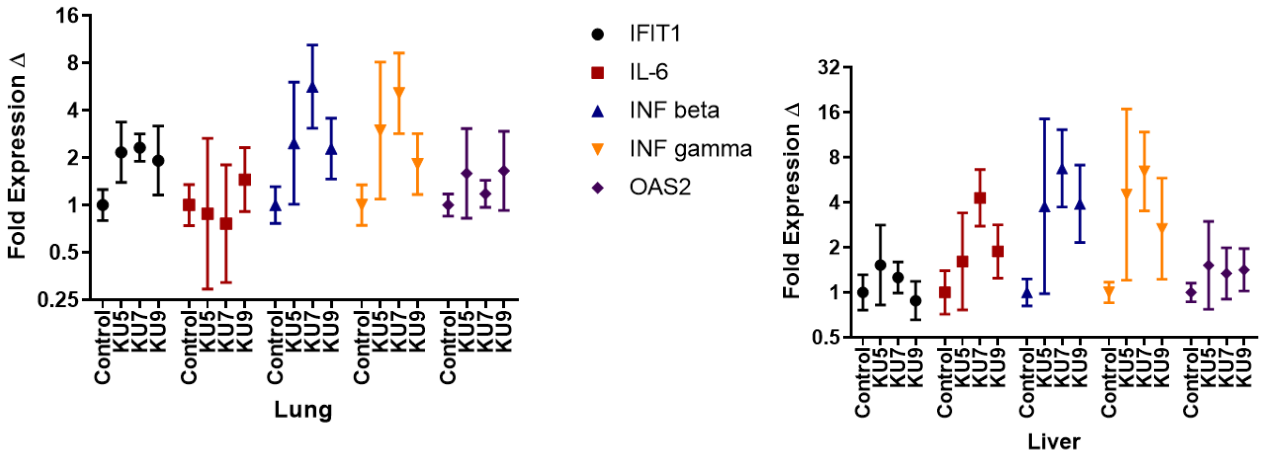

Figure 10. Quantitative PCR of inflammatory gene expression in lung (left) and liver (right) after administration of aptamer.

Approved SOW :

Specific Aim 1: In vitro characterization and optimization of RNA aptamers that selectively bind to human histone.	**Proposed Completion**	**Work Completed**	**Site 1 Initiating PI**	**Site 2 Partnering PI**
Major Task 1L Local IRB/IACUC Approval				
Local IRB approval		100%	Miller	Giangrande
Local IACUC approval		100%	Miller	Giangrande
Major Task 2: In vitro - functional efficacy of aptamers	*Months*	*Percent*	*Team*	*Team*
Measurement of calcium influx by fura-2 in human pulmonary microvascular endothelial cells.	1-12	100%	Miller	Giangrande
Measurement of TLR activation in human pulmonary microvascular endothelial cells	1-12	100%		Giangrande
Detection of cell toxicity Cell lines used: human pulmonary microvascular endothelial cells	1-12	100%	Miller	Giangrande
Measure platelet thrombi formation Human platelets (health donors)	6-18	100%		Giangrande Dayal
Measure platelet surface marker expression in human platelets (healthy donors)	6-18	50%	Miller	Giangrande Dayal
Ex vivo experiment using blood from patients with ALI	6-24	100%		Giangrande Comellas
Specific Aim 2: Evaluate efficacy and safety of histone-specific RNA aptamers in vivo	**Proposed Completion**	**Work Completed**	**Site 1 Initiating PI**	**Site 2 Partnering PI**
Major Task 3: Evaluation of efficacy in inhalation injury model (chlorine inhalation and smoke inhalation models)	*Months*	*Percent*	*Team*	*Team*
Assessment of minimal effective dose (MED) C57/BL6 mice	18-26	55%	Miller Tighe Gunn	
Assessment of alveoloar permeability and inflammation by bronchoalveolar lavage	18-26	50%	Miller Tighe	Giangrande
Lung histology by histopathologic staining and analysis	26-30	50%	Miller Tighe	Giangrande
Major Task 4: Evaluation of efficacy in influenza lung injury model	*Months*	*Percent*	*Team*	*Team*
Assessment of minimal effective dose (MED) C57/BL6 mice.	18-26	25%	Miller Tighe	Giangrande
Assessment of alveoloar permeability and inflammation by bronchoalveolar lavage	18-26	25%	Miller Tighe	Giangrande
Lung histology by histopathologic staining and analysis	26-30	0%	Miller Tighe	Giangrande
Major Task 5: Evaluation of safety	*Months*	*Percent*	*Team*	*Team*
Rising dose and repeated dose toxicology studies to establish a no observed adverse event level (NOAEL) in vitro and in vivo studies.	30-36	0%	Miller	Giangrande
Assessment of potential immunostimulation in humanized mice	30-36	25%		Giangrande

What opportunities for training and professional development has the project provided?

This project is the thesis project for Kevin Urak, a graduate student in Dr. Giangrande's research laboratory, with the expectation that he will defend his thesis in December 2018. Kevin has had the opportunity to present oral abstracts and posters at regional and national scientific conferences (see Research Products below and Appendix). Furthermore, the project is providing opportunities for new knowledge and training in techniques for members in both Drs. Giangrande and Miller's laboratories (see #7 Participants below).

How were the results disseminated to communities of interest?

Results have been presented at local, regional, and national scientific seminars. A manuscript is currently under review at Nature Communications. An abstract was submitted and will be presented as a poster at the 2018 Military Health System Research Symposium in Orlando, FL in August 2018.

What do you plan to do during the next reporting period to accomplish the goals?

The goals for reporting period 3 are outlined in the Table on page 10 for those experiments that are not yet completed. We anticipate completing all proposed studies by the end of the project.

4. IMPACT:

What was the impact on the development of the principal discipline(s) of the project?

Of relevance to the military, a challenging problem in individuals with severe tissue injury or critical illness is the potential that even those organs not directly affected by the original problem subsequently become dysfunctional (multiple organ dysfunction syndrome, or MODS). The example of trauma has obvious relevance to the military; however, other equally relevant causes of ALI leading to MODS/ARDS include smoke and chlorine gas inhalation, burns, radiation, and infection. The incidence of MODS/ARDS in military situations is difficult to assess because there are so many causes of it. For example, in burn patients, a recent study found an incidence of MODS/ARDS of 60% with a mortality of 65%. In patients with severe sepsis, MODS/ARDS develops in 50% and is responsible for most of the associated mortality. There is no effective pharmacotherapy to directly treat the underlying cause of MODS/ARDS and current therapy is directed at supportive care. However, if this study is successful then the RNA aptamers can be immediately tested in preclinical animal models and human clinical trials as a drug to prevent the development of MODS/ARDS and ALI in high risk patients. These bio-reagents have significant advantages as compared to other possible therapeutics because they are stable and not as susceptible to fluctuations in temperature, do not require special handling conditions, do not cause allergic responses, and will be easy to deliver.

What was the impact on other disciplines?

Nothing to report at this time. However, since histones are responsible for multiple diverse causes of MODS/ARDS, including trauma, burns, major surgery, pancreatitis, sepsis, ischemia/reperfusion, etc., if this study is successful than the findings will have potential broad application to many other disciplines.

What was the impact on technology transfer?

Nothing to report.

What was the impact on society beyond science and technology?

Nothing to report

5. CHANGES/PROBLEMS:

Changes in approach and reasons for change

Nothing to report.

Actual or anticipated problems or delays and actions or plans to resolve them

Experiments in the animal models of acute lung injury have taken longer than anticipated (see table of work accomplished in #3 above). This has been because of longer than anticipated time to schedule experiments with the Duke Rodent Inhalation Facility and for the processing and interpretation of histologic samples. Dr. Miller has redistributed Ms. Snow's efforts to increase efficiency of this proves and we anticipate the completion of the animal experiments by the end of the next reporting period.

Changes that had a significant impact on expenditures

Nothing to report.

Significant changes in use or care of human subjects, vertebrate animals, biohazards, and/or select agents

Nothing to report.

Significant changes in use or care of human subjects

Nothing to report.

Significant changes in use or care of vertebrate animals.

Nothing to report.

Significant changes in use of biohazards and/or select agents

Nothing to report.

6. PRODUCTS:

Manuscripts

1. Urak KT, Blanco GN, Shubham S, Lin L, Dassie JP, Thiel WH, Chen Y, Sonkar VK, Lei B, Murthy S, Gutierrez WR, Wilson ME, Stiber JA, Klesney-Tait J, Dayal S, Miller Jr FJ, Giangrande PH. RNA inhibitors of nuclear proteins responsible for multiple organ dysfunction syndrome. *Nature Communications*, 2018 (in revision). Acknowledgement of federal support- Yes.
2. Shubham S, Lin LH, Contreras P, Urak KT, Blanco G, Miller Jr FJ, Klesney-Tait J, Giangrande PH. Detection of extracellular histones in serum using RNA aptamers. 2018 (in preparation). Acknowledgement of federal support- Yes.

3. Lei B, Urak KT, Shubham S, Snow K, Klesney-Tait J, Stiber JA, Giangrande PH, Miller Jr FJ. RNA aptamers in treatment of histone-mediated acute lung injury. 2018 (in preparation). Acknowledgement of federal support- Yes.

Abstracts

1. Urak KT, Blanco G, Lin LH, Dassie J, Shubham S, Thiel WT, Chen Y, Sonkar V, Lei B, Gutierrez W, Wilson M, Stiber JA, Klesney-Tait J, Dayal S, Miller Jr FJ, Giangrande PH. RNA Inhibitors of Nuclear Proteins Implicated in Multiple Organ Dysfunction Syndrome. Molecular Therapy, 2018 May 1,Vol. 26, No. 5, pp. 37-37.
2. Miller Jr FJ, Urak KT, Blanco G, Lin LH, Lei B, Giangrande PH. RNA inhibitors of extracellular histones to prevent multiple organ dysfunction syndrome. Military Health System Research Symposium (MHSRS), 2018.

Oral Presentations

1. Urak KT, Blanco G, Lin LH, Dassie J, Shubham S, Thiel WT, Chen Y, Sonkar V, Lei B, Gutierrez W, Wilson M, Stiber JA, Klesney-Tait J, Dayal S, Miller Jr FJ, Giangrande PH. RNA Inhibitors of Nuclear Proteins Implicated in Multiple Organ Dysfunction Syndrome. American Society of Gene and Cell Therapy (ASGCT) annual meeting in Chicago IL, April 2018.
2. Urak KT, Blanco G, Lin LH, Dassie J, Shubham S, Thiel WT, Chen Y, Sonkar V, Lei B, Gutierrez W, Wilson M, Stiber JA, Klesney-Tait J, Dayal S, Miller Jr FJ, Giangrande PH. RNA Inhibitors of Nuclear Proteins Implicated in Multiple Organ Dysfunction Syndrome. University of Iowa Internal Medicine Research Day Award Presentations, Iowa City, IA. January 2018.
3. Urak KT, Blanco G, Lin LH, Dassie J, Shubham S, Thiel WT, Chen Y, Sonkar V, Lei B, Gutierrez W, Wilson M, Stiber JA, Klesney-Tait J, Dayal S, Miller Jr FJ, Giangrande PH. RNA Inhibitors of Nuclear Proteins Implicated in Multiple Organ Dysfunction Syndrome. Univ of Iowa Molecular Medicine Seminar, Iowa City, IA. January 2018.

Poster Presentations

1. Urak KT, Blanco G, Lin LH, Dassie J, Shubham S, Thiel WT, Chen Y, Sonkar V, Lei B, Gutierrez W, Wilson M, Stiber JA, Klesney-Tait J, Dayal S, Miller Jr FJ, Giangrande PH. RNA Inhibitors of Nuclear Proteins Implicated in Multiple Organ Dysfunction Syndrome. RNA Consortium, Iowa City, IA, May 2018.
2. Urak KT, Blanco G, Lin LH, Dassie J, Shubham S, Thiel WT, Chen Y, Sonkar V, Lei B, Gutierrez W, Wilson M, Stiber JA, Klesney-Tait J, Dayal S, Miller Jr FJ, Giangrande PH. RNA Inhibitors of Nuclear Proteins Implicated in Multiple Organ Dysfunction Syndrome. University of Iowa Internal Medicine Research Day, Iowa City, IA. October 2017.
3. Miller Jr FJ, Urak KT, Blanco G, Lin LH, Lei B, Giangrande PH. RNA inhibitors of extracellular histones to prevent multiple organ dysfunction syndrome. Military Health System Research Symposium (MHSRS) annual meeting, Orlando, FL, August 2018.

Website(s) or other Internet site(s)

Nothing to report.

Technologies or techniques

Nothing to report.

Inventions, patent applications, and/or licenses

Nothing to report.

Other Products

Nothing to report.

5. PARTICIPANTS & OTHER COLLABORATING ORGANIZATIONS

What individuals have worked on the project?

Name: Francis Miller, MD
No change.

Name: Kamie Snow
No change.

Name: Beilei Lei, PhD
Has increased effort to 8-person months.

Name: Michael Gunn, MD
No change.

Name: Alejandro Comellas, MD
No change.

Name: Sanjana Dayal, PhD
No change.

Has there been a change in the active other support of the PD/PI(s) or senior/key personnel since the last reporting period?

Nothing to report.

What other organizations were involved as partners?

Nothing to report.

6. SPECIAL REPORTING REQUIREMENTS

Collaborative award.

Independent reports are submitted for both the Initiating PI (Miller) and the Partnering PI (Giangrande). Specific tasks are indicated with the PI and research site in the table of "Research Specific Tasks" found in Section #3.

7. APPENDICES:

Appendices materials have been included.

RNA inhibitors of nuclear proteins responsible for multiple organ dysfunction syndrome

Short title: RNA inhibitors of extracellular histones

Kevin T Urak[1,2§], Giselle N Blanco[1§], Shambhavi Shubham[1§], Li-Hsien Lin[1], Justin P Dassie[1], William H Thiel[1,3], Yani Chen[1], Vijay Kumar Sonkar[1], Beilei Lei[4], Shubha Murthy[1], Wade R Gutierrez[5], Mary E. Wilson[1,6,7], Jonathan A Stiber[4], Julia Klesney-Tait[1], Sanjana Dayal[1], Francis J Miller Jr*[4,8,9] and Paloma H Giangrande*[1,2,3,10,11,12,13]

[1]*Internal Medicine, University of Iowa, Iowa City, IA, USA*
[2]*Molecular & Cellular Biology Program, University of Iowa, Iowa City, IA, USA*
[3]*Abboud Cardiovascular Research Center, University of Iowa, Iowa City, IA, USA*
[4]*Department of Medicine, Duke University, Durham, NC, USA*
[5]Medical Scientist Training Program, *University of Iowa, Iowa City, IA, USA*
[6]*Department of Microbiology, University of Iowa, Iowa City, IA, USA*
[7]*Veteran's Affairs Medical Center, University of Iowa, Iowa City, IA, USA*
[8]*Pharmacology and Cancer Biology Program, Duke University, Durham, NC, USA*
[9]*Deptartment of Medicine, Veterans Administration Medical Center, Durham, NC, USA*
[10]*Interdisciplinary Graduate Program in Genetics, University of Iowa, Iowa City, IA, USA*
[11]*Holden Comprehensive Cancer Center, University of Iowa, Iowa City, IA, USA*
[12]*Radiation Oncology, University of Iowa, Iowa City, IA, USA*
[13]*Environmental Health Sciences Research Center (EHSRC), University of Iowa, Iowa City, IA, USA*

[§] *Equal contribution*

***Corresponding authors:**
Paloma H Giangrande, PhD
University of Iowa
375 Newton Rd
5202 MERF
Iowa City, IA 52242
Phone: +1-319-384-3242 (office)
Fax: +1-319-353-5552
Email: paloma-giangrande@uiowa.edu

Francis J Miller, Jr., MD
Duke University
508 Fulton St, Bldg. 15,
Room 306, Durham, NC 27705
Phone: +1-919-668-2688 (office)
Email: francis.miller@duke.edu

ABSTRACT

Development of multiple organ dysfunction syndrome (MODS) is the most decisive clinical event following severe infection or extensive tissue injury to predict patient morbidity and mortality. Following cellular injury, nuclear proteins, of which histones are the most abundant, are released into the circulation and are crucial mediators of MODS. Unfortunately, available anti-histone therapies (e.g., heparin and toll-like-receptor blocking antibodies) have failed in clinical trials due to off-target effects causing bleeding and systemic toxicity. Here, we describe a novel therapeutic strategy for MODS based on chemically stabilized nucleic acid bio-drugs (aptamers). Systematic evolution of ligands by exponential enrichment (SELEX) technology was utilized to identify aptamers that selectively bind the histones implicated in MODS and do not bind to serum proteins. We demonstrate the efficacy of histone-specific aptamers in human cells and in a murine model of MODS. Given the many etiologies of MODS, these aptamers could have significant therapeutic impact on the treatment of numerous clinical conditions associated with this syndrome.

INTRODUCTION

Approximately 45% of patients who develop multiple organ dysfunction syndrome (MODS) will die due to acute secondary organ injury/failure.[1, 2] Survivors are at risk of developing persistent mental and physical impairments.[1] MODS occurs after a severe cytotoxic insult such as sepsis, trauma, ischemia/reperfusion (I/R) injury, pancreatitis, peritonitis, stroke, thrombosis, and autoimmune disease.[3-8] MODS is characterized by the release of molecular mediators from damaged tissues which create a domino effect including capillary leak, interstitial edema, hemorrhage and systemic inflammation.[9] MODS is primarily managed with supportive care, as there is no approved treatment to prevent or reverse it. The realization that damaged cells release their nuclear content into the circulation suggests nuclear proteins as potential therapeutic targets for MODS.[10, 11] Since histones are the most abundant proteins in the nucleus, they have been identified as potential therapeutic targets for MODS.

Histones are highly cationic intra-nuclear proteins that support the normal structural development of chromatin and regulation of gene expression. Histones and DNA-bound histones (nucleosomes) are released into the extracellular space during cell death processes including necrosis, apoptosis and neutrophil extracellular traps-induced cell death (NETosis). In the extracellular space, histones act as cytotoxic damage-associated molecular pattern (DAMP) proteins by activating Toll-like receptors (TLRs), promoting pro-inflammatory cytokine pathways and altering phospholipid membrane permeability.[13-17] In humans, the normal serum level of histones is very low (estimated at < 0.6 ng/mL).[18-20] However, serum levels as high as 3 ng/mL have been reported in critically ill patients, and correlate with hallmark features of MODS including, coagulopathy, endothelial dysfunction, and inflammation.[10, 21-23]

Several animal studies demonstrate that intravenous administration of exogenous histones is sufficient to cause a MODS-like phenotype.[13, 14, 24] Importantly, anti-histone treatments (e.g.,

histone neutralizing antibodies, activated protein C – APC, recombinant thrombomodulin and heparin) protect mice against secondary organ failure due to lethal endotoxemia, sepsis, ischemia/ reperfusion injury, trauma, pancreatitis, peritonitis, stroke, and thrombosis.[3-8] However, therapeutic approaches currently pursued in experimental models have marked limitations. For example, despite their use in laboratory experiments, TLR2/4 monoclonal antibodies (mAbs) to block extracellular histone signaling would cause substantial immunodeficiency in humans by inhibiting innate immune defenses after host infection. Similarly, anti-histone mAbs have been implicated in autoimmunity.[25, 26] Several other biologics that have demonstrated efficacy in animal models failed to provide therapeutic benefit in clinical trials (e.g. APC) and are associated with increased risk of bleeding (e.g. heparin and APC) or systemic toxicity (e.g. histone deacetylase inhibitors).[27, 28] In addition, many biologics require restrictive handling and storage, special dosing considerations, and risk allergic reactions (recombinant proteins and antibodies), which limit their use in field situations or small regional health clinics.[29, 30] Thus, the development of specific histone inhibitors is a unique clinical opportunity to interrupt a pathophysiologic cascade responsible for significant morbidity and mortality associated with MODS.

Chemically-stabilized nucleic acid bio-drugs (aptamers) are synthetic structure RNA or DNA oligonucleotide ligands that bind with high affinity and specificity to their targets.[31-33] As a therapeutic, aptamers possess several key advantages over other biologics including: ***1)*** they are self-refolding, single-chain, and redox-insensitive. Unlike proteins, aptamers tolerate pH and temperatures that proteins do not. ***2)*** They act as selective inhibitors of their target, eliminating potential for off-target effects. ***3)*** They are easy and economical to produce. Their production does not depend on bacteria, cell cultures or animals. ***4)*** Their small size leads to a high number of moles of target substance bound per gram of aptamer. Additionally, their transport properties allow for improved tissue penetration. ***5)*** They are stable at ambient temperature, yielding a

much longer shelf-life than other biologics, and can tolerate transportation without refrigeration. ***6)*** Cross-species reactive aptamers can be easily engineered, thus expediting testing of the same reagent in preclinical animal models and in future human clinical trials. The clinical potential of aptamers is also highlighted by the FDA approval of an aptamer-based drug for the treatment of macular degeneration and by clinical trials demonstrating the safety and efficacy of systemically administered aptamers.[34-40]

In this study, we developed a novel anti-histone therapeutic strategy to selectively neutralize extracellular histones implicated in MODS, based on aptamers. Because histones (cationic proteins) normally associate with DNA in the nucleosome, oligonucleotides such as aptamers (anionic molecules) have intrinsic high affinity for histones, making them an excellent reagent for binding and neutralizing extracellular histones and reducing the morbidity and mortality associated with MODS. In this study, we developed nuclease-resistant, 2′ fluoro-modified RNA aptamers with high affinity (K_D = nanomolar (nM)) for histones implicated in MODS (H3 and H4) with systematic evolution of ligands by exponential enrichment (SELEX).[41, 42] A key stringent negative selection step was introduced during the selection process, to favor the identification of aptamers that bound to histones, but not other proteins in human serum, thereby reducing potential side effects. The aptamers were evaluated for efficacy in human cells in culture and in a mouse model of MODS.

RESULTS

Identification of histone-specific RNA aptamers using SELEX

Two parallel selections were performed using the *in vitro* SELEX protocol to isolate RNA aptamers (51 nucleotides in length) that selectively bind to human histones implicated in MODS (H3 and H4) (**Fig. 1A**). To identify RNA sequences that specifically bind to histones, but not to proteins in serum, we introduced a stringent *negative selection* step against bovine serum albumin (BSA) and human IgG. (**Fig. 1A; Step 2**). RNAs that bound to serum proteins were removed (**Fig. 1A; Step 3**) and unbound RNA was recovered. To ensure the isolation of high-affinity binding RNAs to human histones, a *positive selection* step was performed using human recombinant histones H3 and H4 proteins (**Fig. 1A; Step 3**). Eight rounds of selection (against target histones H3 or H4) and negative selection (against BSA and human IgG) were performed (see **Supplementary Table 1**). Binding of the round 0 (R0) and round 8 (R8) RNA pools to histones H3 and H4 was verified using the double-filter binding assay (**Fig. 1B; top panels**). A leftward shift in the binding curve of the R8 RNA pools compared to the R0 RNA pools for both selections is indicative of enrichment of high-affinity binding RNA sequences. Importantly, the enriched R8 RNA pools did not bind to serum proteins (**Fig. 1B; bottom panels**) confirming specificity for histones. Equilibrium dissociation constants (K_D) for R0 and R8 RNA pools were determined using one site binding nonlinear regression curve fit (see **Supplementary Table 2**).

High throughput sequencing (Illumina) and bioinformatics analysis of selected RNA sequences from the selection rounds revealed that the selections converged between rounds 5 and 8 (**Fig. 1C**). Percent sequence enrichment (% enrichment) was measured to determine the evolution of each sequence family at the later rounds of selection. Percent sequence enrichment at each round of selection was measured by taking the total number of unique sequences in each round and dividing by the total number of sequences obtained in each round as previously described. For each selection, the 50% enrichment point is indicated by a grey dot (**Fig. 1C**). The top three

RNA sequences from each selection (H3 selection: KU4 – KU6; H4 selection: KU7 – KU9) were selected based on the following criteria: sequences that increase in abundance during the positive selection rounds (against target histones H3 or H4) but do not decrease in abundance during the negative selection rounds (against BSA and human IgG) (see **Supplementary Table** 1 for details on selection conditions). Individual RNA sequences are listed in **Supplementary Table 3**. Theoretical secondary structures for each of the six RNA aptamers were generated using Mfold.[44](**Supplementary Fig. 1**)

Next, the binding of single RNA aptamers isolated from the histone H3 and H4 selections was evaluated with Surface Plasmon Resonance (SPR) (**Fig. 2A**) and double-filter binding assay (**Supplementary Fig. 2**; data shown for aptamers KU7 and KU9). RNA aptamers were incubated with either calf thymus-derived histones (CTH) (top panels), recombinant human histone H4 (middle panels), or BSA (bottom panels) (**Fig. 2A**). As predicted, the RNA aptamers bound with high-affinity to both CTH histones and recombinant human histone H4, but not to BSA (**Fig. 2A**). Importantly, the aptamers bound equally well to both CTH and recombinant human histone H4 suggesting that the aptamers bind irrespective of post-translational modifications and are not species-specific. While aptamers KU7 and KU9 were derived from the H3 selection, we also evaluated binding of the RNAs to all histone subunits using the double-filter binding assay (**Supplementary Fig. 2A**). Of note, both aptamers bound with low nM affinity to histones, H1, H3, and H4 (major histones implicated in MODS). In contrast, while only aptamer KU7 bound to histone H2B, neither aptamer bound to histone H2A. In addition, equilibrium binding kinetics were determined for one of the aptamers (KU7). We observed similar (low nM) binding affinities at various time intervals (**Supplementary Fig. 2B**). Finally, as observed with SPR analysis (**Fig. 2**), no significant binding was observed to human serum or human albumin (**Supplementary Fig. 2C**), confirming specificity of the aptamers for histone

proteins *vs*. serum proteins. Together, these data highlight the potential safety of this approach for targeting extracellular histones, while minimizing unwanted off-target effects.

Based on the predicted secondary structures of the RNA aptamers (see **Supplementary Fig. 1**), we reasoned that two of the aptamers (KU7 and KU9) would be more stable in human serum compared to the other four aptamers (KU4, KU5, KU6, and KU8) and thus better suited for clinical applications. To assess their serum stability, RNA aptamers were incubated with 50% human serum for up to 28 days. Aliquots of the aptamer-serum solution, obtained at various time points, were resolved on a denaturing PAGE gel (8M urea 10% acrylamide) following staining with SYBR gold to visualize the RNAs (**Supplementary Fig. 3**). The amount of full-length aptamer was quantified for each time point by comparing the intensity of the bands to the "0 hour" time point using the Image Lab software. (**Fig. 2B**; data shown for aptamers KU5, KU7 and KU9). As predicted, aptamers KU7 and KU9 had superior serum stability profiles compared to the other aptamers tested (comparison shown for KU5 only).

In vitro efficacy of RNA aptamers

The release of histones from dying cells is associated with microvascular thrombosis and tissue ischemia.[7, 45] Histone H4 and, to a lesser extent H3, are responsible for directly inducing aggregation of human platelets. To determine whether the selected RNA aptamers inhibit adverse effects of extracellular histones, aptamers KU7 and KU9 were incubated with platelets derived from healthy human donors in the absence or presence of histone H4. We show that anti-histone aptamers KU7 and KU9 inhibit histone H4-induced platelet aggregation in a dose-dependent manner (**Fig. 3A**). In contrast, the aptamers did not inhibit platelet aggregation induced by collagen, even at the highest aptamer dose tested (**Fig. 3A**). Importantly, histone-induced platelet aggregation was significantly inhibited by aptamers KU7 and KU9 at a molar ratio of histone to aptamer of 1:1, 2:1 and, to a lesser extent, 4:1 (**Fig.3A**). Platelet

aggregometer graphs for the individual aptamers and RNA round pools are shown in **Supplementary Fig. 4A and B**.

In vivo, the release of extracellular histones in circulation results in an amplifying effect by promoting additional cell death and nuclear content release, as well as activation of TLRs resulting in pro-inflammatory cytokine production (interleukin-6, IL-6), enhanced inflammation and coagulation activation.[14, 21-23] We show that aptamers KU7 and KU9 inhibit calf thymus histone (CTH)-induced TLR activation as measured by IL-6 production (**Fig. 3B and Supplementary Fig. 4C; left panel**). Importantly, histone-induced TLR activation was significantly inhibited by aptamers KU7 and KU9 at a molar ratio of histone to aptamer of 1:1, 2:1, 4:1 (**Fig. 3B**). In contrast, the aptamers have no effect on lipopolysaccharide (LPS)-induced TLR activation (**Supplementary Fig. 4C; right panel**).

In addition to a heightened inflammatory response, high levels of extracellular histones are cytotoxic to endothelial and epithelial cells as well as several other cell types[3, 46-48]. We confirmed that administration of calf thymus histones to a human hybrid endothelial cell line (EA.hy926) causes dose-dependent cell death (**Fig. 3C; left panel**). Aptamers (KU7 and KU9) have a dose-dependent protective effect in neutralizing histone-induced cytotoxicity (**Fig. 3C; right panel**).

Extracellular histones appear to induce cytotoxicity through their interaction with phospholipids in the plasma membrane, leading to transmembrane conductance, calcium influx, cell swelling, and cytolysis [49-51]. We confirmed that administration of calf thymus histones to EA.hy926 cells resulted in increased intracellular calcium [Ca^{2+}] levels^{+}]) calcium influx (**Fig. 3D**). Importantly, aptamers significantly inhibit the histone-induced increase of intracellular calcium at molar ratio of histone to aptamer up to 4:1 with KU7 and 6:1 with KU9 as measured using the calcium

indicator Fura 2-AM. The aptamers alone had no effect on intracellular calcium levels (**Fig. 3D**). Together, these data confirm that the aptamers can prevent the functional effect of histones *in vitro* and provide the rationale for proposing that these aptamers have the potential to attenuate histone-mediated injury *in vivo.*

Efficacy of histone aptamer in a murine model of MODS

Histone administration causes neutrophil migration, endothelial injury and dysfunction, hemorrhage, and thrombosis and often results in death at levels as low as 50 mg/kg body weight. Intravenous injection of histones into mice leads to organ dysfunction and death (**Fig. 4**). Death occurred between 1 and 3 hrs in the mice treated with histones alone, but was inhibited by administration of aptamer (**Fig. 4A**). Injection of histones resulted in an increase in organ weight that was only partially reversed by the aptamer treatment (**Fig. 4B**). The increase in organ weight is likely a result of an increase in vascular congestion, multifocal neutrophilic aggregates in vessels, thrombi, and hemorrhage (**Fig. 4C and D**; the liver, lung and spleen shown **Supplementary Fig. 5**). Importantly, while no significant change in organ weight was observed with aptamer treatment, pathologic evidence of histone toxicity, as determined by H&E staining and immunostaining for presence of platelets and neutrophils in the various tissues, was inhibited by aptamer KU7 at a ratio of histone to aptamer of 2:1 and 4:1 (**Fig. 4C-D)**. As predicted, injection of histones into the circulation of mice also resulted in an increase in TLR activation via IL-6 (**Fig. 4E**). The increase in TLR activation was partially attenuated by aptamer treatment in the liver but not in lung or spleen, and is likely due to the retention of aptamer-histone complexes in these organs. Together, these data confirm that aptamers that bind to the histones implicated in MODS can attenuate histone-mediated injury *in vivo.*

The experimental protocol of the *in vivo* efficacy study described above (**Fig. 4**) is consistent with all previous studies performed in preclinical models of MODS with histone inhibitors[10, 52, 53],

such that the therapeutic treatment is administered prior to, or in conjunction with, the histones. To better represent the clinical scenario where the drug is administered after tissue injury, we evaluated the ability of anti-histone aptamers to *rescue* histone-induced toxicity as a function of time (**Fig. 5**). Anti-histone aptamers were added to EA.hy926 cells in culture at different time points following the addition of histones. Anti-histone aptamers prevented cytotoxicity in a time dependent manner when administered after the histones, demonstrating the ability to protect from histone-induced cell death 2 hrs after histone administration (**Fig. 5A**). The administration of KU7 rescued the increase in intracellular [Ca^{2+}] after histones had already induced an increase of [Ca^{2+}] (**Fig. 5B**). As shown in Figure 4A, intravenous injection of histones resulted in death of mice within 3 hrs, however, mice treated with anti-histone aptamer KU9 at 30 min following histone injection had markedly improved survival as compared to vehicle treated mice (**Fig. 5C; left panel**) and a reduction in lung weight **(Fig. 5C; right panel).**

Aptamers bind and neutralize NET toxicity

Recent data demonstrate the importance of NETs as an important source of extracellular histones in a variety of clinical disease including MODS, sepsis, rheumatologic diseases and thrombosis.[10, 54-56] We therefore assessed whether our anti-histone aptamers could prevent NET associated cell toxicity. Human neutrophils were isolated, stimulated with phorbol myristate acetate (PMA), and NETs were generated for immunofluorescence microscopy and cell toxicity assays (**Fig. 6**). DAPI stain demonstrates the formation of extracellular NETs (**Fig. 6A; top, left panel**) displaying histones (**Fig. 6A; top, right panel**). As shown in Figure 6A, aptamer KU7 binds to human neutrophils-derived NETs (**Fig. 6A, bottom, right panel**). ImageWhite color areas in the merged images demonstrate the close approximation of the aptamer KU7 with NETs (**Fig 6A; bottom, right panel**). Importantly, anti-histone aptamer KU7 also attenuated NET-induced cell death (**Fig. 6B**), confirming their potential as a viable therapeutic option for clinical conditions (e.g. sepsis) leading to MODS. Although previous reports of histone inhibitors

have demonstrated efficacy in the MODS *via* simultaneous administration of anti-histone therapy, this is the first report of an anti-histone therapy capable of *rescuing* the damaging cellular effects of extracellular histones *in vitro* and *in vivo.*

DISCUSSION

This is the first report of an aptamer-based therapeutic approach for MODS. In this study, we developed nuclease-resistant RNA aptamers that bind with high affinity and specificity to human histones H3 and H4 implicated in MODS. Importantly, the aptamers do not bind to other proteins in human serum and, thus, are expected to be safe for use in humans. We show that the aptamers inhibit histone-induced platelet aggregation (**Fig. 3A**), TLR activation (**Fig. 3B**) and endothelial cell death (**Fig. 3C**), and calcium influx (**Fig. 3D**) in human cells in culture. Importantly, these aptamers bind human NETs and neutralize their toxicity *in vitro* (**Fig. 6**). Finally, we demonstrate efficacy of one of the anti-histone aptamers (KU7) in a murine model of MODS (**Fig. 4 and 5**).

A key consideration when developing a drug that targets histones directly is that the drug must act exclusively in the extracellular space. Indeed, histone neutralizing drugs that obtain intracellular access could potentially disrupt DNA structure or function, and result in catastrophic side-effects. To this end, oligonucleotide aptamers are highly anionic and thus, membrane impermeable which would negate any concerns with regards to toxicity due to targeting chromatin. An additional safety feature engineered into our anti-histone aptamers was the minimization of potential interactions between the aptamers and serum proteins. This was achieved by performing a stringent negative selection step (against human IgG and BSA) at every round of selection. An additional benefit imparted by the negative selection step was the maximization of the fraction of the aptamer drug that binds histones in circulation, thereby reducing the therapeutic dose of the aptamer. While binding of oligonucleotide-based drugs to serum proteins is normally viewed as a benefit to improve the pharmacokinetic (PK) properties of the drug and prolong circulating times, previous therapeutic aptamers to specific serum proteins (e.g., thrombin and factor IX) which have shown efficacy in humans, were developed to minimize off-target interactions with non-target proteins in serum.[31, 57, 58]

Three distinct therapeutic approaches have been described to target extracellular histones. These include pharmacological agents to block histone release (e.g., PAD4 inhibitors and DNAse 1)[59, 60] or downstream signaling (e.g., TLR blocking mAb or C reactive protein – CRP) or agents that directly neutralize extracellular histones (e.g. anti-histone mAb, APC, and heparin).[8, 14, 55, 61, 62] Although these approaches have shown promise in animal models of MODS, further research is necessary to warrant their safe application in a clinical setting. Indeed, one of the common problems with many of these anti-histone approaches is their propensity for nonspecific, off-target effects resulting in systemic toxicity.

Oligonucleotide-based drugs have been under clinical development for the past thirty years, starting with anti-sense oligos (ASOs) and followed by aptamers and siRNAs. One of the key factors contributing to the approval of six oligonucleotide drugs over recent years has been the advent of nucleic acid chemistry to improve the safety and stability of these drugs. For example, the anti-vascular endothelial growth factor ($VEGF_{165}$) aptamer drug Macugen (formerly pegaptanib), which was approved by the FDA in 2004 to treat age-related macular degeneration of the retina, contains a phosphorothioate 3′-3′ deoxythymidine cap to promote nuclease stability, 2′-O-methylated purines and 2′-fluorinated pyrimidines. Finally, a 40 kDa molecular weight polyethylene glycol substituent was linked to the 5′ terminus of the aptamer to increase retention time in the eye.[64, 65] Another safety consideration when developing the pegaptanib aptamer was enhancing target specificity. The pegaptanib aptamer was selected to be highly specific for $VEGF_{165}$, the predominant VEGF isoform in the human eye, thereby reducing potential systemic effects and greatly boosting the safety profile of the drug. The anti-histone aptamers developed in this study, which are modified with 2′-fluoro chemistry, were shown to be extremely stable in human serum ($T_{1/2}$ KU7= 150 h and $T_{1/2}$ KU9= 48 h) (**Fig. 2B)** and safe *in*

vivo (**Fig. 4**). In addition, as discussed above, the anti-histone aptamers were engineered to selectively bind histones in serum.

One additional benefit of the modification of the 2′-position of the ribose is increased duplex stability (Tm). 2'F modification in particular polarize the bases more significantly and contribute to strengthening of WC base pairing. [67] For example, in the RNAi field the combined use of 2′-fluoro pyrimidines with 2′-O-methyl purines results in RNA duplexes with extreme stability in serum and improved *in vivo* performance. Chemically engineered oligonucleotides with 2′-chemistry have also been used as efficient and specific silencers of endogenous miRNAs in mice.[68, 69] This is attributed to the ability of these modified oligos to compete with endogenous miRNAs for binding to their target mRNAs.[70] Similarly, post-selection modification of the 2′-position of aptamers increases binding to the target[70-72] and possibly, favors binding of the anti-histone aptamers to both free histones and DNA-bound histones (nucleosomes) in serum (also see binding of aptamers to human neutrophil-derived NETs, Fig. 6A). Since free histones and DNA-bound histones are both pro-inflammatory,[17] a single drug capable of neutralizing both forms is optimal.

In summary, we describe a novel approach using nuclease stabilized RNA aptamers to neutralize the toxic effects of extracellular histones implicated in MODS. Our approach overcomes many of the limitations of other experimental anti-histone treatments and provides a promising avenue for clinical implementation of a robust therapeutic for MODS in combination with other interventions (anti-inflammatory and supportive care). Because extracellular histones have been implicated in the development of many different disease conditions, the anti-histone aptamer bio-drugs could potentially impact the treatment of numerous MODS-inducing clinical conditions including, acute lung injury, transfusion related acute lung injury, sepsis, trauma,

burns, stroke, cancer, autoimmune/inflammatory disorders and ischemia/reperfusion and drug-mediated tissue injury.

MATERIALS AND METHODS

Cell lines and cell culture reagents

Ea.Hy926 cells (ATCC®, Manassas, VA) were maintained in DMEM (GIBCO, Gaithersburg, MD) supplemented with 10% FBS (Atlanta Biologicals, Flowery Branch, GA) at 37 °C under 5% CO_2. The medium was changed every two to three days until confluent. During passaging, cells were trypsinized with Trypsin-EDTA (0.25%) (GIBCO, Gaithersburg, MD) and re-plated at a 1 to 4 ratio.

Selection protocol

The protocol for the generation of the initial (Round 0) RNA Library has been described elsewhere. Step 1: Generation of double-stranded DNA (dsDNA) template by elongation. *Elongation Solution 1* components: 9 µL of 100 mM tris-HCl pH 8.0 (Sigma-Aldrich, St. Louis, MO), 15 µL of 50 mM $MgCl_2$ (Sigma-Aldrich, St. Louis, MO), 1,000 picomoles (pmol) of Sel2N20 template oligo, (5′-TCGGGCGAGTCGTCTG-N20-CCGCATCGTCCTCCC-3′) (IDT, Coralville, IA), 2,000 pmol Sel2 5′ primer (5′-TAATACGACTCACTATAGGGAGGACGATGCGG-3′) (IDT, Coralville, IA), and UltraPure distilled H_2O (diH_2O) (ThermoFisher, Waltham, MA) to a final volume of 90 µL. The *Elongation Solution 1* was heated to 95 °C for 5 minutes (min) then 25 °C for 20 min. *Elongation Solution 2* components: 50 µL of 10× PCR buffer (Denville Scientific, Charlotte, NC), 10 µL of 10 mM dNTP mix (New England Biolabs, Ipswich, MA), 4 µL of Choice Taq (Denville Scientific, Charlotte, NC), and diH_2O to a final volume of 410 µL. The *Elongation Solution 2* was heated to 95 °C for 5 min then cooled to room temperature for 20 min. *Elongation Solutions 1* and *2* were combined and placed in a thermal cycler. Cycling conditions for elongation were as follows: 72 °C for 30 min; 25 °C for 10 min; and held at 4 °C. Step 2: To generate the Round 0 RNA library, the Round 0 dsDNA template was transcribed *in vitro* using the mutant Y639F T7 RNA polymerase as previously described. The *in vitro* transcription reaction conditions were as follows: a total reaction volume of 250 µL was composed of 250

pmol of the dsDNA template library, 25 µL of a 10× rNTP solution [10× rNTP solution: 10 mM 2′-OH purines (Roche, Indianapolis, IN ; GTP and ATP) and 30 mM 2′-Fluoro pyrimidines (TriLink BioTechnologies, LLC, San Diego, CA; 2′-Fluoro-2′-dCTP, 2′-Fluoro-2′-dUTP)] with 50 µL of a 5× Transcription Buffer [5× Transcription Buffer: 20% w/v Peg-8,000 (Sigma-Aldrich, St. Louis, MO), 200 mM Tris-HCL pH 8.0 (Life Technologies, Carlsbad, CA), 60 mM $MgCl_2$ (Sigma-Aldrich, St. Louis, MO), 5 mM spermidine HCl (Sigma-Aldrich, St. Louis, MO), 25 mM DTT (Sigma-Aldrich, St. Louis, MO), 2 µL of Inorganic pyrophosphatase (IPPI –ThermoFisher Scientific, Waltham, MA)] and diH_2O to 250 µL. The *in vitro* transcription reaction was incubated overnight at 37 °C. Removal of the dsDNA template was performed by addition of 1 µL (10 units) DNase I (Roche, Indianapolis IN) for 30 min at 37 °C followed by chloroform extraction. Step 3: The *in vitro* transcribed Round 0 RNA was purified using polyacrylamide gel electrophoresis (PAGE). The RNA was run on a denaturing PAGE gel [10% acrylamide (Bio-Rad, Hercules, CA); 8 M urea (RPI, Mount Prospect, IL)] for 30 min at 24 watts. The Round 0 RNA band was detected by UV shadowing, excised and eluted from the gel with TE low-EDTA buffer [0.1 mM EDTA (Sigma-Aldrich, St. Louis, MO), 10 mM TE pH 7.5 (Sigma-Aldrich, St. Louis, MO)] for 1 h at 37 °C in a rotator (Labnet, Edison, NJ). The eluted Round 0 RNA was run through a 0.2 µM Cellulose Acetate Centricon (Sigma-Aldrich, St. Louis, MO) to remove any residual gel fragments. A 10,000 Molecular Weight Cut-Off Amicon Ultra-4 Centrifugal Filter Unit (Millipore, Burlington, MA) was used to concentrate the RNA solution. RNA OD_{260} and 260/280 ratio were determined by Nanodrop 2,000 (ThermoFisher, Waltham, MA) to assess quantity and purity of Round 0 RNA library.

Histone aptamer SELEX protocol. For each round of selection, we performed a negative selection step (to remove nonspecific binding aptamers) and positive selection step (to enrich for histone binding aptamers). The Round 0 RNA library was first incubated with human IgG (negative selection) (Sigma-Aldrich, St. Louis, MO) in 1× binding buffer (BB) at 37 °C for [(1x

BB: 20 mM HEPES (Sigma-Aldrich, St. Louis, MO), 0.15 M NaCl (Sigma-Aldrich, St. Louis, MO), 2 mM $CaCl_2$ (Sigma-Aldrich, St. Louis, MO)]. Human IgG and human IgG binding aptamers were removed using a 0.2 µm nitrocellulose filter (GE, Chicago, IL). This was performed by incubating a 2 cm × 2 cm filter with the RNA solution for 20 min at 37 °C. Unbound RNA aptamers were transferred to a fresh tube containing (1,000 pmol) of either human histone H3 or H4 (New England Biolabs, Ipswich, MA) and were incubated at 37 °C for 10 min. The histone-bound RNA aptamers were isolated by capturing the histones and RNAs on a nitrocellulose filter as described above. Histone-bound aptamers were eluted from the nitrocellulose filter by extraction with phenol:chloroform:isoamyl alcohol extraction. Specifically, the nitrocellulose disk containing the histones and histone-bound aptamers was submerged in phenol:chloroform:isoamyl alcohol (Fisher Scientific, Hampton, NH) and vortexed for 1 min. The solution was separated into two phases by adding an equal volume of diH_2O, vortexed for 1 min, and centrifuging at 17,000 × *g* for 10 min. The aqueous layer (top layer containing the RNA aptamers) was collected and placed into an RNAse and DNAse-free 1.5 mL microcentrifuge tube (USA Scientific, Ocala, FL). An equal volume of chloroform (Fisher Scientific, Hampton, NH) was added to the aqueous layer to remove any trace of phenol, the solution was vortexed for 1 min, and centrifuged at 17,000 × *g* for 10 min. The aqueous layer (top layer containing the RNA aptamers) was collected and placed into a clean 1.5 mL microcentrifuge tube. The RNA aptamers were then ethanol precipitated by adding 5 µL of linear acrylamide (ThermoFisher, Waltham, MA), 1/10 volume of 10 M ammonium acetate (Fisher Scientific, Hampton, NH), and 2.5 volume of 100% ethanol (Pharmco-Aaper, Shelbyville, KY) followed by a 2 second (s) vortex and centrifugation at 17,000 × *g* for 15 min. The solution was incubated at -20 °C overnight, and then centrifuged for 15 min at 17,000 × g. The supernatant was removed, and the pellet washed with 1 mL of 95% ethanol. The solution was centrifuged at 4°C for 5 min at 17,000 × *g*, and the supernatant removed, and the RNA pellet air dried at room temperature. The RNA pellet was then resuspended in 25 µL of diH_2O. The RNA was then reverse-transcribed by combining 10

µL of 5× FS buffer (ThermoFisher Scientific, Waltham, MA), 1 µL 0.1 M DTT (Sigma-Aldrich, St. Louis, MO), 1 µL 100 µM Sel2 3'primer [5'-TCGGGCGAGTCGTCTG-3' (IDT, Coralville, IA)], 31 µL diH_2O and 5 µL of recovered RNA in a Polymerase Chain Reaction (PCR) tube (USA Scientific, Ocala, FL). Reaction conditions were as follows: 65 °C for 5 min, 22 °C for 5 min (annealing step), and room temperature for 10 min (cooling step). Then, 1 µL of 10 mM dNTP mix and 1 µL of Superscript III Reverse Transcriptase (ThermoFisher Scientific, Waltham, MA) was added to the mix followed by an incubation of 60 min at 55 °C, then 72 °C for 15 min and cooled to 4 °C. Twenty five microliters of the transcribed material was then added to 50 µL of 10× Taq Polymerase Buffer (Denville Scientific, Charlotte, NC), 20 µL of 10 mM dNTP mix, 5 µL of 100 µM Sel2 5′ primer, 5 µL of 100 µM Sel2 3′-primer, 25 units of Taq polymerase (Denville Scientific, Charlotte, NC), and brought up to 500 µL with diH_2O. The reaction was separated into five PCR tubes and ran at 95 °C for 2 min, 22 – 25 cycles of 95 °C for 30 s, 55 °C for 30 s, and 72 °C for 5 s, followed by 72 °C for 5 min, and then held at 4 °C. The amplified DNA (Round 1 DNA) was utilized as the template for the subsequent round of selection as described above to generate the Round 1 RNA pool. Selection conditions for each round of selection are provided in Supplemental Table 1.

Double-filter binding assay

Double-filter nitrocellulose binding assay was preformed to determine the binding affinity (K_D) of the aptamers for their target. Briefly, the transcribed RNA from rounds 0 (RD0) and 8 (RD8) of selection were dephosphorylated using Bacterial Alkaline Phosphatase (ThermoFisher, Waltham, MA). The dephosphorylating conditions were as follows: 100 pmol of RD0 or RD8 RNA was combined with 5 µL of 1 M tris-HCL pH 8.0, 1 µL BAP, and supplemented with diH_2O to reach 100 µL. The solution was then incubated at 55 °C for 60 min, followed by adding 10 µL of 10× *Dephosphorylation Stop Mixture* [(20 mM Tris-HCl, pH 8.0, 40 mM EDTA, 200 mM NaCl (RPI, Mount Prospect, IL), 1% SDS (RPI, Mount Prospect, IL) (w/v)]. 300 µL of low-EDTA buffer

was added to the reaction and then purified using the phenol:chloroform:isoamyl alcohol extraction described above.

The dephosphorylated RNA and synthetic aptamers (KU7 and KU9) were radiolabeled with gamma-^{32}P-ATP using T4 polynucleotide kinase (PNK) as follows: A total reaction volume of 20 µL was made up of 20 pmol of aptamer RNA, 2 µL PNK (New England Biolabs, Ipswich, MA), 2 µL PNK reaction buffer (New England Biolabs, Ipswich, MA), 2 µL gamma-^{32}P-ATP (PerkinElmer, Waltham, MA), and diH_2O. The mixture was then incubated at 37 °C for 30 min and 65 °C for 20 min to heat inactivate the PNK. 20 µL of 1× BB was added to the reaction followed by a centrifugation step through a G25 purification column (GE Healthcare, Little Chalfont, United Kingdom, IL) according to the manufacturer's instructions. Labeling efficiency was determined by a scintillation counter. All radiolabeled RNAs were diluted in 1× BB to 2,000 cpm/mL. Five microliters of 2,000 cpm/mL radiolabeled RNA were incubated at 37 °C for 5 min with 15 µL of either human histone H3.2 or H4 (positive selection targets) or human albumin (Sigma-Aldrich, St. Louis, MO) or serum (Sigma-Aldrich, St. Louis, MO) (negative control proteins) serially diluted in 1× BB. The binding reactions were loaded onto a dot blot apparatus (composed of nitrocellulose membrane on the top, nylon membrane (Sigma-Aldrich, St. Louis, MO) in the middle and Whatman paper (Sigma-Aldrich, St. Louis, MO) on the bottom). Treatment of the nitrocellulose membrane was as follows: pretreated with 0.5 M KOH (Sigma-Aldrich, St. Louis, MO) for 20 min, quick wash with diH_2O, and equilibrated in 0.1 M Tris HCl 7.5 for 45 min, washed with diH_2O, and transferred to 1× BB for 20 min before l (Sigma-Aldrich, St. Louis, MO). The nylon was also incubated in 1× BB for 20 min before being loaded on the manifold. Before loading the RNA/protein samples, the wells were washed with 100 µL of 1× BB. The amount of RNA bound (nitrocellulose) versus unbound (nylon) was determined by densitometry of imaged membrane on a Fuji Phosphor imager.

Illumina high-throughput sequencing and sample preparation

Preparation of RNA pools for Illumina sequencing. The RNA pools from all rounds of selection were reverse-transcribed using Superscript III Reverse Transcriptase and the Sel2 3′ primer. Briefly, the RNA from each selection round was heated for 60 min at 55 °C followed by 72 °C for 15 min. The DNA product was then PCR-amplified using Choice Taq DNA Polymerase with barcoded Illumina primers (**Supplementary Table 3**). The DNA product with the Illumina barcode was heated for 2 min at 95 °C, followed by 10 cycles of 95 °C for 30 s, 55 °C for 30 s, and 72 °C for 30 s with a final extension step at 72 °C for 5 min. The PCR product was then run on a 2% agarose gel and the appropriate bands (approximately 151 base pairs) were excised. The gel fragment was purified using the Qiagen Gel Extraction kit (Hilden, Germany) and quantified using a Nano Drop 2,000. Qualitative analysis of the samples was performed on an Agilent Model 2100 Bioanalyzer (Agilent, Santa Clara, CA). The samples were combined at equal molar amounts and submitted for Illumina sequencing (University of Iowa Genomic core, Iowa City, IA; Illumina Genome Analyzer II) as previously described.[76]

Illumina high-throughput sequencing data pre-processing. Illumina data were processed as previously described. Briefly, the Illumina base calls (sequence reads) were pre-processed and filtered to identify the Sel2N20 aptamer library variable region sequence. For each round of selection, all unique variable region sequences were enumerated with the repeat sequences being counted. The sequenced DNA code was converted to RNA and the 5' and 3' constant regions were added.

Surface Plasmon Resonance (SPR)

Immobilization of histones. pH scouting was performed with all proteins. Coating of histone H4 and BSA to the COOHV biosensor was performed at pH 4.7. Coating of calf thymus histone to the COOHV biosensor was performed at pH 6.0. To prevent non-specific binding to the vial and

sensor surface, a small concentration (~0.01%) of Tween-20 was added to these solutions. The proteins were immobilized following a standard amine coupling procedure where a mixture of EDC and NHS was injected to activate the surface carboxyl groups and protein was injected to react with and be coupled to the sensor surface. 1 M Tris pH 8 was injected last to deactivate remaining active carboxyl groups.

Kinetic assay. A 2-fold dilution series (ranging from 10 to 100 nM) was prepared for each aptamer in buffer. Each sample was injected over all three flow channels for 4 min at a flow rate of 30 µL/min and dissociation was monitored for 10 min. The sensor surface was regenerated after each analyte cycle by injecting 1 M NaCl for 1 min. Data were processed by subtracting the reference channel signal and buffer blank responses (double referencing method). A two-compartment kinetic (mass transport limited) model was fit to the data to determine rate constants of association (k_a) and dissociation (k_d). A local R_{max} was provided in the fit due to an apparent concentration-dependent surface activity.

Serum stability measurements

Chemically synthesized aptamers KU7 and KU9 were incubated at 37 °C under 5% CO_2 at a concentration of 5 µmol/L in 50% human serum. Incubation times ranged from 0 min to 28 days. At each time point, 10 pmol of aptamer (2 µL) was removed and added to 8 µL of 1× Tris base, Boric Acid, EDTA (TBE) (Fisher Scientific, Hampton, NH) and 2 µl of 2× Urea RNA loading dye [0.01 g Xylene Cyanol, 0.01 g bromophenol blue (Sigma-Aldrich, St. Louis, MO), 500 µl of 10 x TBE, and 10 mL of formamide (Amresco, Solon, OH)]. The samples were then heat-inactivated at 95 °C for 5 min and stored at -20 °C. All samples (10 µL/lane = 8 pmol aptamer RNA) were loaded into a denaturing PAGE gel (8M urea 10% acrylamide) and separated by electrophoresis at 10 watts for 30 min. The gel was stained with SYBR Gold (Invitrogen, Carlsbad, CA) at a 1:10,000 dilution in PBS for 30 min and visualized by UV light using a Chemidoc (Bio-Rad,

Hercules, CA). Briefly, the quantification area of the aptamers at each time point was set to the height and size of the band at the 0-min time point. The band intensity of each time point was then calculated and normalized to 0 min, which was set at 100%.

Platelet isolation

Washed human platelets were prepared as described previously. Briefly, 20 mL of healthy donor blood was collected in 3.2 % sodium citrate (9:1, v/v) vacutainer tubes (BD Scientific, San Jose, CA). The blood was pooled into 15 mL conical tubes (CellTreat, Pepperell, MA) and centrifuged at 100 × *g* for 15 min (without brakes) at room temperature. Platelet rich plasma (PRP) was collected into fresh tube and prostaglandin E1 (PGE1, final conc.1 µM) was added, and mixed gently by inverting tubes. PGE1-PRP was then centrifuged at 800 × *g* for 10 min to pellet the platelets. After centrifugation, platelet pellets were washed with modified Tyrode's buffer (134 mmol/L NaCl, 2.9 mmol/L KCl, 2.9 mmol/L $CaCl_2$, 0.34 mmol/L Na_2HPO_4, 12 mmol/L $NaHCO_3$, 20 mmol/L HEPES, 1.0 mmol/L $MgCl_2$, 5.0 mmol/L glucose, pH-7.35) containing 1 µM PGE1. After washing, the platelet pellets were re-suspended in modified Tyrode's buffer and counted on ADVIA 120 Hematology System (Siemens Healthineers, Malvern, PA).

Platelet aggregation assay

Washed platelets were prepared as above and re-suspended in Tyrode buffer to a final concentration of 2.5×10^8 platelets/mL. For the platelet aggregation studies, 400 µL of washed platelets were stirred at 1,200 rpm at 37 °C along with either collagen (1 µg/mL), histone H4 (10 µg/mL), selected RNA rounds, and/or KU7 or KU9) in a cuvette of an aggregometer (Chrono-log Model 560-VS) and light transmittance was recorded. Aggregation was measured as percent change in light transmission, where 100 % refers to transmittance through blank solution.

Neutrophil isolation

Human neutrophils were prepared as described previously [79].[79]. Briefly, 50 mL of healthy donor blood were collected in 3.2 % sodium citrate (9:1, v/v) vacutainer tubes (BD Scientific, San Jose, CA). The blood was mixed with equal volume of room temperature dextran/saline solution in 50 mL conical tubes (CellTreat, Pepperell, MA). The solution was then mixed by inverting 10 times and incubating upright for 20 minutes at room temperature. The upper layer (leukocyte-rich plasma) was carefully collected and transferred into a new 50 mL conical tube. The leukocyte-rich plasma solution was then centrifuged at 5 ºC for 10 min at 250 × g. The supernatant was discarded and the cells were immediately resuspended in 30 mL of 0.9% saline. A 10 mL ficoll-hypaque solution (Sigma- Aldrich, catalog number: 10771) was added beneath the cell suspension then centrifuged at 20 ºC for 30-40 min at 400 × g with no breaks. The top layer was aspirated leaving the neutrophil and red blood cell (RBC) pellet behind. The cell pellet was resuspended in 20 mL of ice-cold water for exactly 30 sec followed by 20 mL of cold 1.8% NaCl solution to restore isotonicity (0.9%). The neutrophil-containing solution was then centrifuge at 5 ºC for 6 mins at 250 × g. If the pellet was white, we resuspend in 5-10 mL of ice cold PBS and counted the cells. If the pellet was red we repeated the ice-cold water treatment as detailed above to remove RBC.

NETosis induction

NETs were generated as previously described [80]. Briefly, neutrophils were plated on 150cm150x20mm tissue culture dishes. After 30 min, when cells had adhered to the bottom of the dishes, they were stimulated for 4 hrs with 500 nM phorbol 12-myristate 13-acetate (PMA). Conditioned medium was gently aspirated and the neutrophil/NET monolayer was collected with ice-cold PBS-Ca^{2++}/Mg^{2++} and centrifuged for 10 min at 450 × g at 4°C to sediment cells. The cell-free but NET-rich supernatant was centrifuged for 10 min at 18,000 × g at 4°C and the pellet

containing NETs was suspended in Opti-MEM and DNA quantified by measuring absorbance at 260 nm using a nanodrop spectrophotometer.

Imaging of NETs

To visualize NET formation, neutrophils were seeded on 12 mm coverslips inserted into 12-well plates (300,000 cells/well). After cells had adhered, they were stimulated with PMA as described above and aptamer binding to NET-associated chromatin was visualized by immuno-fluorescence as described previously.[81] Briefly, after fixing with 4% paraformaldehyde and permeabilizing with 0.5% Triton X-100, coverslips were blocked with 5% normal goat serum overnight at 4 ºC. They were then sequentially incubated for 2.5 hours each with anti-histone H3 (Cayman #13784, 1:50) antibody and 2 µM KU7-647 aptamer diluted in blocking buffer. After washing with PBS, cells/NETs were incubated with goat anti-rabbit IgG-Alexa Fluor 488 (1:360) for 1 h and counterstained with 1.33 µg/mL DAPI. All incubations were performed in a humidified chamber at 37 ºC and were followed by three 5 min washes in PBS. Cells were mounted onto glass slides using Vectashield with DAPI. Images were captured using Leica LMD7000 confocal microscope under 40× oil/2.8× zoom magnification and processed using Fiji Imaging software.

Cytotoxicity assays

RNA aptamer efficacy with purified histones. EA.Hy926 cells were seeded in a 96-well flat bottom plate (CellTreat, Pepperell, MA) at a density of 8,000 cells/well in 100 µL of medium. After 24 h the medium was removed and replaced with 50 µL of Opti-MEM (GIBCO, Gaithersburg, MD) containing either calf thymus histones (Sigma-Aldrich, St. Louis, MO) and/or aptamer. After 24 h the medium was removed and MTS reagent (Abcam, Cambridge, MA) was

added for 1 h according to manufacturer's protocol and quantified using a Thermo Max Microplate Reader (Molecular Devices, Sunnyvale, CA) at 490 nm.

RNA aptamer efficacy with NETs. EA.Hy926 cells were seeded in a 96-well flat bottom plate (CellTreat, Pepperell, MA) at a density of 8,000 cells/well in 100 µL of medium. After 24 h the medium was removed and replaced with 50 µL of Opti-MEM (GIBCO, Gaithersburg, MD) containing either 8 µg of NET material (determined by DNA concentration) and/or 8 µg (10.66 µM) of aptamer. After 24 h the medium was removed and MTS reagent (Abcam, Cambridge, MA) was added for 1 h according to manufacturer's protocol and quantified using a Thermo Max Microplate Reader (Molecular Devices, Sunnyvale, CA) at 490 nm.

Time-course treatment. EA.Hy926 cells were seeded in a 96-well flat bottom plate (CellTreat, Pepperell, MA) at a density of 16,000 cells/well in 100 µL of medium. After 24 h the medium was removed and replaced with 40 µL of Opti-MEM (GIBCO, Gaithersburg, MD) containing 200 µg/mL calf thymus histones (Sigma-Aldrich, St. Louis, MO). Quadruple wells received 10 µL of either vehicle (negative control), heparin (positive control, 1:1), KU7 aptamer (1:2), or KU9 aptamer (1:2) at time points 0, 5, 10, 15, 30, 45, 60, 90, 120, and 180 min. After 3 h, all wells were washed with media, followed by incubation in MTS reagent (Abcam, Cambridge, MA) for 1 h according to manufacturer's protocol, and quantified using a Thermo Max Microplate Reader (Molecular Devices, Sunnyvale, CA) at 490 nm.

Intracellular calcium-influx measurements

Intracellular calcium concentration ($[Ca^{2+}]i$) was measured in single EA.hy926 cells using ratiometric calcium indicator fura 2-AM (fura-2-acetoxymethyl ester, Life Technologies, Carlsbad, CA). Cells grown on 35 mm glass-bottom plates (MatTek, Ashland, MA) were loaded with 1 µM fura 2-AM in calcium buffer (140 mM NaCl, 2.8 mM KCl, 2 mM $CaCl_2$, 2 mM $MgCl_2$,

10 mM glucose and 10 mM HEPES) for 15 min, washed and incubated in calcium buffer for another 15 min. Fura 2-AM-loaded cells were illuminated in calcium buffer by alternating 340/380-nm light delivered every 300 milliseconds by a DG-4 argon exciter (Sutter Instruments, Novato, CA) under the control of MetaFluor software, and fluorescence images were captured at an emission of 510 nm with a Photometrics Cool SNAP HQ charge coupled device camera (Roper Scientific, Tucson, AZ) based on a Nikon TE2000 fluorescent microscope. Calf thymus histones (50 µg/mL) without or with 3 min pre-incubation with RNA aptamer KU7 at various concentrations were added to loaded cells and calcium images were recorded for 10 min for each treatment condition. $[Ca^{2+}]i$ was reported as the ratio of fura 2 fluorescence emission at 340 and 380 nm (F340/F380) normalized to baseline. All procedures were performed at room temperature.

TLR activation studies

TLR activation as measured by IL-6 production. EA.Hy926 cells were seeded in a 96-well flat bottom plate at a density of 15,000 cells/well in 100 µL of medium. After 24 h the medium was removed and replaced with 100 µl of Opti-MEM containing either calf thymus histones and/or aptamers. After another 24 h, the supernatant was collected, processed and quantified according to manufacturer's protocol used in the human IL-6 Quantikine® ELISA kit (R&D Systems, Minneapolis, MN).

Animals

Eight to 12-week-old male BALB/cJ mice (Jackson Laboratory, Bar Harbor, ME) were used for this study. All procedures conformed to standards established in the Guide for Care and Use of Laboratory Animals (National Academy Press, Washington, D.C. 2011). The Institutional Animal Care and Use Committees of the University of Iowa, accredited by AAALAC, reviewed and

approved all protocols. All efforts were made to minimize the number of animals used and to avoid experiencing pain or distress.

Mouse model of multiple organ dysfunction (MODS)

RNA aptamer efficacy. Mice received a tail vein injection of calf thymus histones at 50 mg/kg and/or aptamer at 25 or 12.5 mg/kg or vehicle (100 µL per mouse). The mice were monitored for distress and were euthanized 6 h post-injection with isoflurane overdose if they survived histone toxicity.

RNA aptamer rescue studies. Mice received retro-orbital injection of calf thymus histones at 62.5 mg/kg or vehicle (100 µL per mouse). Thirty minutes after, the mice received a follow-up retro-orbital injection (opposite eye) of either vehicle or aptamer at 31.25mg/kg (100 µl per mouse). The mice were monitored for distress and were euthanized 6 h post-injection with isoflurane overdose if they survived histone toxicity.

Organ weights. Mouse weights were recorded prior to tail vein injections using a digital laboratory balance (Denver Instrument MXX-601, Bohemia, NY). Organs were harvested and weighed after euthanasia and normalized to the vehicle-treatment weight of each animal.

Histology. Histology was performed at the Comparative Pathology and Histology Research Laboratories (University of Iowa; http://www.medicine.uiowa.edu/pathology/research/dcp/). Tissues (lung, liver, and spleen) were excised and fixed in 4% paraformaldehyde (PFA) (Affymetrix, Santa Clara, CA) for at least 1 week at 4 °C. All fixed tissues were processed in a series of alcohol and xylene baths, paraffin-embedded, and 7 µm sections were stained with H&E. A veterinary pathologist (David K Meyerholz) examined all tissue sections. Dr. Meyerholz was blinded to the sample IDs. High-resolution digital images were acquired with a DP71

camera (Olympus) mounted on a BX51 microscope (Olympus) with MicroSuite Pathology Edition Software (Olympus).

Immunohistochemistry. Organs (lung, liver, and spleen) were dissected out immediately after death or euthanasia. A block of tissue (5 mm × 5 mm × 5 mm) from each organ was fixed in 4% PFA for 5 h and then cryo-protected overnight in 30% sucrose in phosphate buffered saline (PBS) at 4 °C. Frozen 20 µm coronal sections were cut with a cryostat and mounted on Colorfrost Plus microscope slides (Fisher Scientific, Hampton, NH). Procedures like those described in previous publications were used for different combinations of multiple-label immunofluorescent staining for histone H3, myeloperoxidase (MPO, a marker for activated neutrophils), CD41 (a marker for platelets) and IL-6, and fluorescent staining for cytoskeleton (phalloidin-Alexa Fluor 568) and nucleus (TO-PRO®-3). Briefly, sections were incubated in 10% donkey serum with a mixture of primary antibodies that were made in different species. The antibody for histone H3 was purchased from Cell Signaling (Danvers, MA, dilution 1:200), MPO from Abcam (Cambridge, MA, dilution 1: 200), CD41 from BD Biosciences (San Jose, CA, dilution 1:400), and IL-6 from Novus Biologicals (Littleton, CO, dilution 1:100). After washing with PBS, sections were incubated in a mixture of fluorophore-conjugated secondary antibodies (Alexa Fluor 488 conjugated donkey anti-rabbit IgG and/or Alexa Fluro 594 conjugated donkey anti-rat IgG, both from Jackson ImmunoResearch, Westgrove, PA; dilution 1:200) against species from which the primary antibodies were made. Stained sections were covered using cover-slips and Prolong Diamond Anti-Fade Reagents (Invitrogen, Carlsbad, CA) after the final washes with 1× PBS. Negative controls consisted of tissue processed in the absence of primary antibodies.

Confocal microscopy. Fluorescent immuno-stained slides were examined with a Zeiss LSM 710 confocal laser scanning microscope. Sections were scanned sequentially in different channels

to separate labels. Images from different channels were each assigned a pseudo-color and then were superimposed. Confocal images were obtained and processed with software provided with the Zeiss LSM 710.

Cytokine activation. Mouse organs (liver, lungs, and spleen) were excised and immediately flash frozen. The organs were ground using a mortar and pestle (RPI, Mount Prospect, IL) over dry ice, followed by total cellular RNA extraction using the RNeasy Mini Kit (Qiagen, Valencia, CA). The purity and concentration of isolated RNA was measured using a Nano-Drop 2000c spectrophotometer (ThermoFisher Scientific, Waltham, MA). The RNA was then reverse-transcribed into complementary DNA using SuperScript III Reverse Transcriptase (ThermoFisher Scientific, Waltham, MA). Real-time Polymerase Chain Reaction was used to quantify the mRNA expression levels of the immune-responsive gene *IL-6*. Briefly, 100 ng of cDNA was used per 20 µL reaction of Power SYBR Green (Applied Biosystems, Foster City, CA). All PCR cycle programs were as follows: 95 °C for 10 min, [95 °C for 15 s, 60 °C for 50 s] × 40 cycles, followed by a melting curve [95 °C for 15 s, 60 °C for 1 min, 95 °C for 1 s]. Each reaction was performed in triplicate, and relative gene expression data was calculated as fold change to β-actin (control) expression data. The mouse-specific primers used in this study were: *β-Actin* (Forward: CGG TTC CGA TGC CCT GAG GCT CTT; Reverse: CGT CAC ACT TCA TGA TGG AAT TGA), *IL-6* (Forward: GAG GAT ACC ACT CCC AAC AGA CC; Reverse: AAG TGC ATC ATC GTT GTT CAT ACA).

Statistical Analysis

Results are expressed as mean ± SEM. Statistical comparisons were performed by a two-tailed t-test, or one-way or two-way analysis of variance (ANOVA) with appropriate post-hoc analysis. A p value of < 0.05 was considered significant.

Figure 1

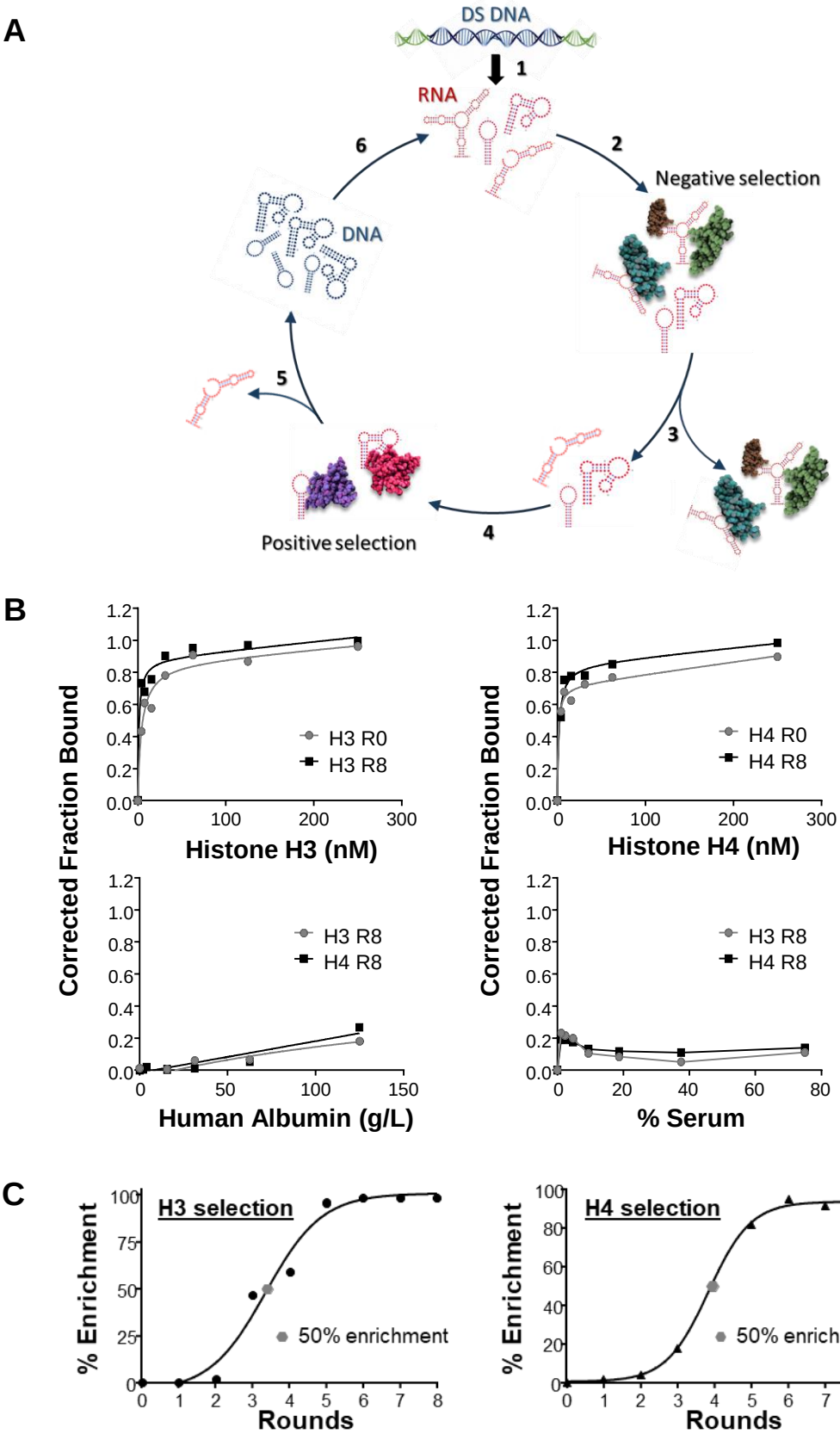
A
DS DNA
1
RNA
2
Negative selection
3
4
Positive selection
5
DNA
6
B
Corrected Fraction Bound
H3 R0
H3 R8
Histone H3 (nM)
H4 R0
H4 R8
Histone H4 (nM)
H3 R8
H4 R8
Human Albumin (g/L)
% Serum
C
H3 selection
% Enrichment
50% enrichment
Rounds
H4 selection

Figure 2

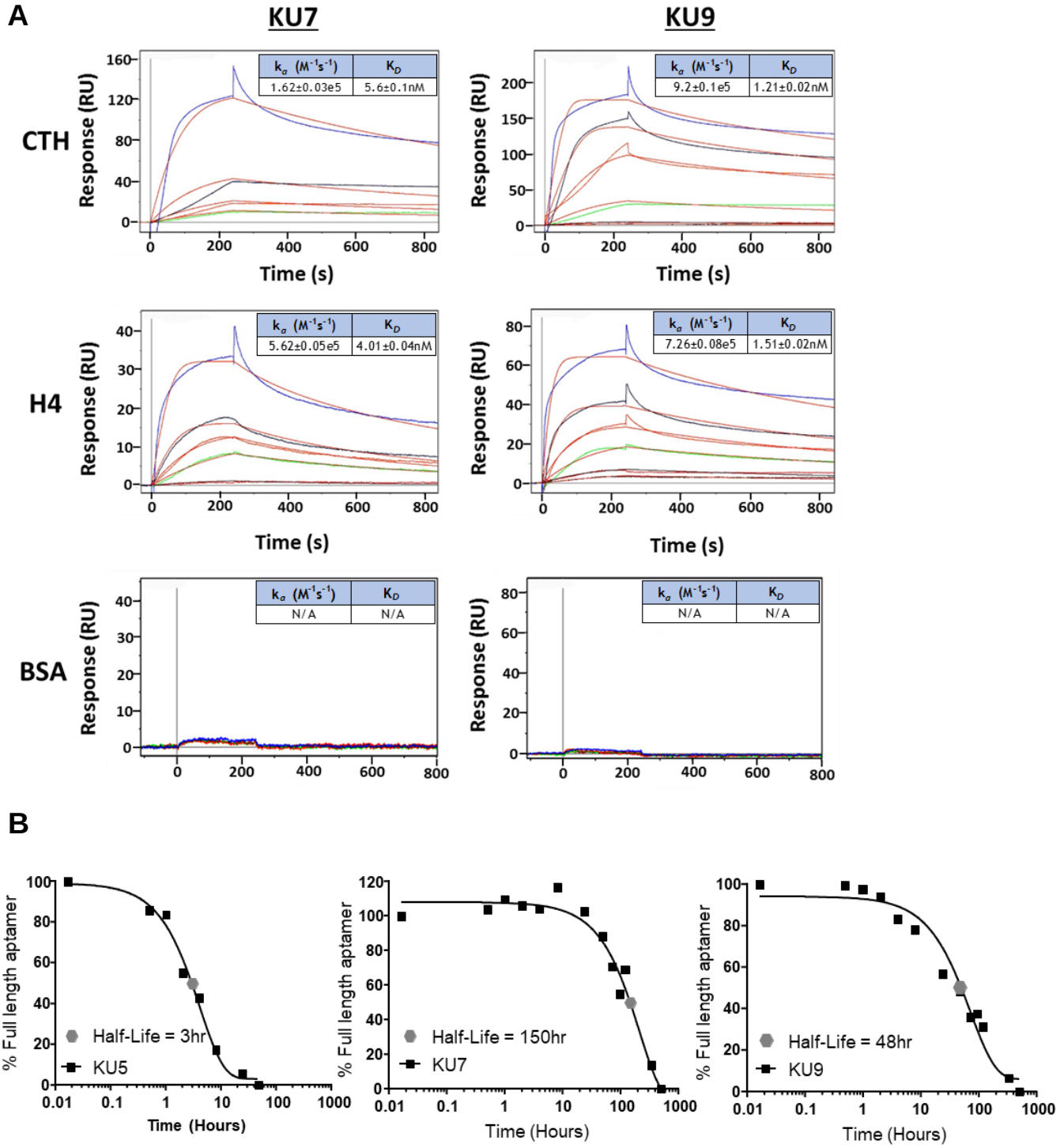
A
KU7
KU9
CTH
H4
BSA
Response (RU)
Time (s)
k_a ($M^{-1}s^{-1}$)
K_D
1.62±0.03e5
5.6±0.1nM
9.2±0.1e5
1.21±0.02nM
5.62±0.05e5
4.01±0.04nM
7.26±0.08e5
1.51±0.02nM
N/A
N/A
B
% Full length aptamer
Time (Hours)
Half-Life = 3hr
KU5
Half-Life = 150hr
KU7
Half-Life = 48hr
KU9

Figure 3

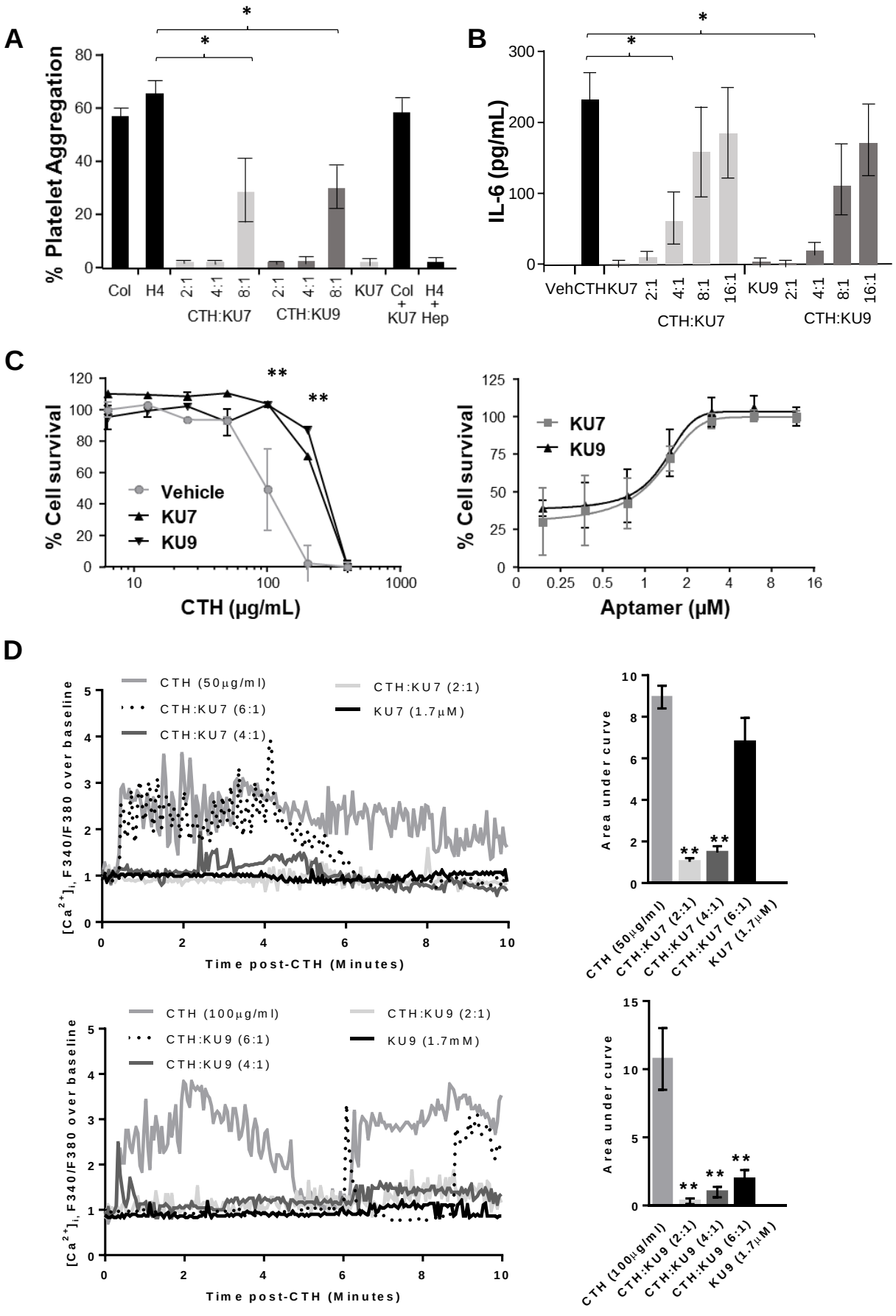
A
% Platelet Aggregation
Col
H4
2:1
4:1
8:1
CTH:KU7
CTH:KU9
KU7
Col + KU7
H4 + Hep
B
IL-6 (pg/mL)
Veh
CTH
KU7
KU9
16:1
C
% Cell survival
Vehicle
KU7
KU9
CTH (µg/mL)
Aptamer (µM)
D
CTH (50µg/ml)
CTH:KU7 (6:1)
CTH:KU7 (4:1)
CTH:KU7 (2:1)
KU7 (1.7µM)
[Ca2+]i, F340/F380 over baseline
Time post-CTH (Minutes)
Area under curve
CTH (100µg/ml)
CTH:KU9 (6:1)
CTH:KU9 (4:1)
CTH:KU9 (2:1)
KU9 (1.7mM)

Figure 4

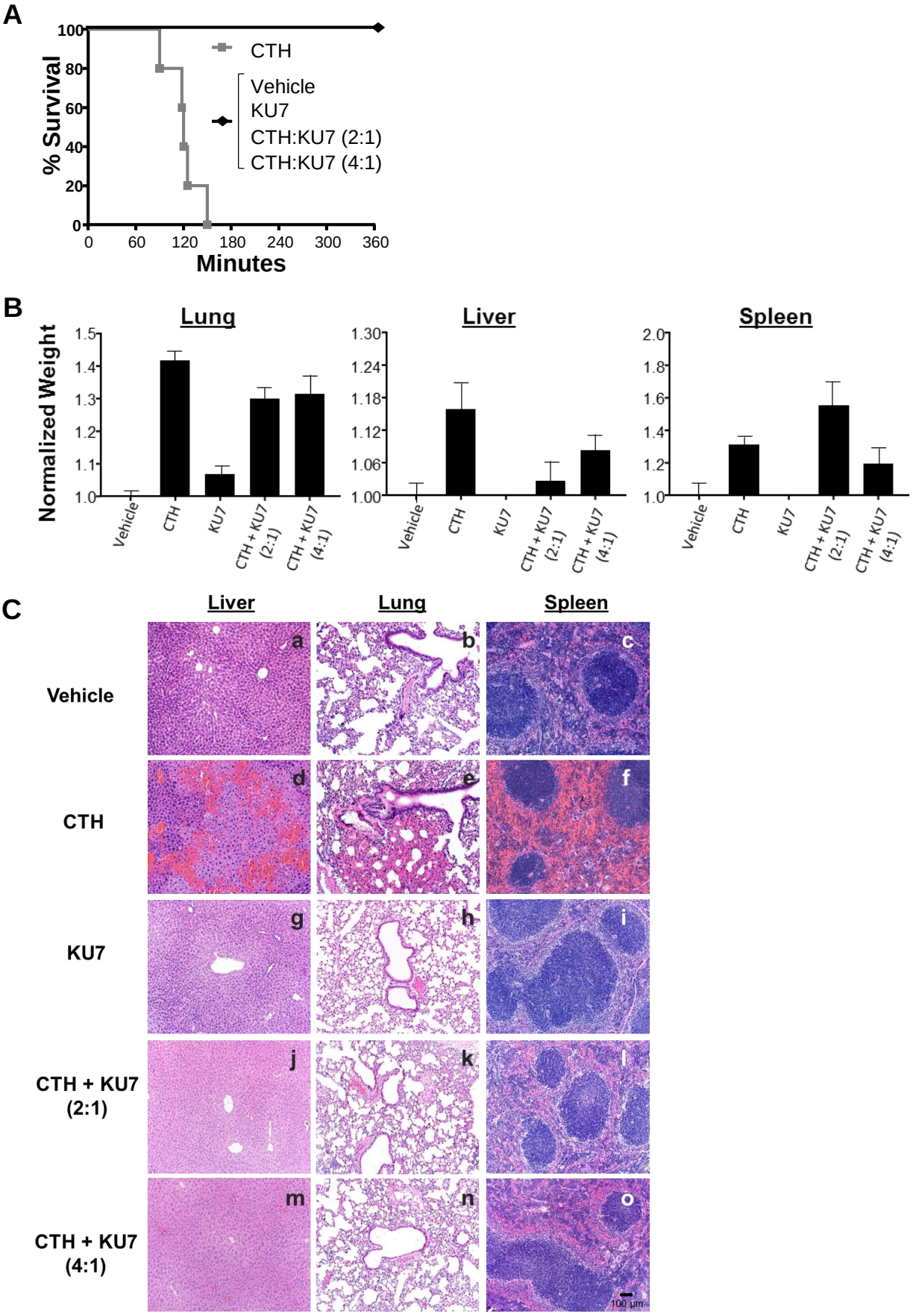
A
% Survival
Minutes
CTH
Vehicle
KU7
CTH:KU7 (2:1)
CTH:KU7 (4:1)
B
Normalized Weight
Lung
Liver
Spleen
Vehicle
CTH
KU7
CTH + KU7 (2:1)
CTH + KU7 (4:1)
C
Liver
Lung
Spleen
Vehicle
CTH
KU7
CTH + KU7 (2:1)
CTH + KU7 (4:1)
100 µm

Figure 4

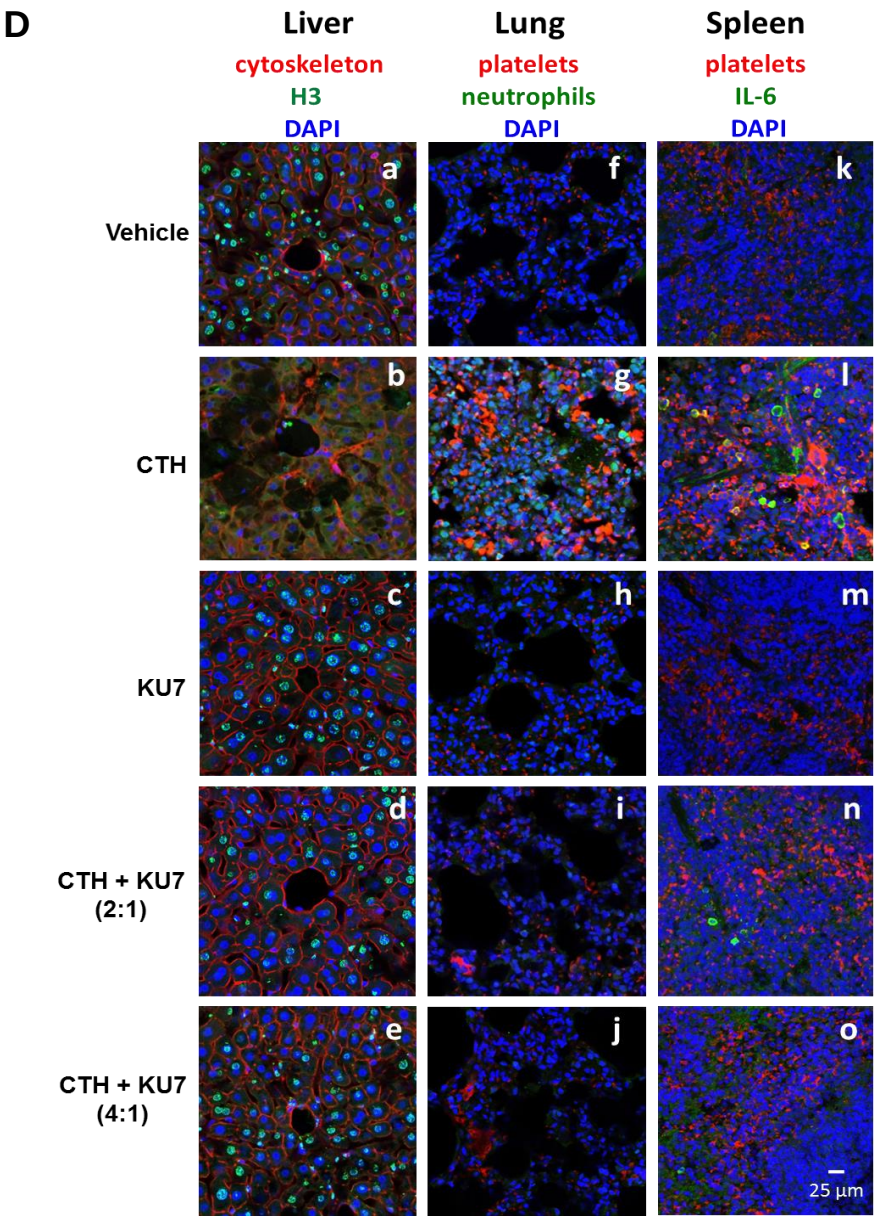
D
Liver
cytoskeleton
H3
DAPI
Lung
platelets
neutrophils
DAPI
Spleen
platelets
IL-6
DAPI
Vehicle
CTH
KU7
CTH + KU7 (2:1)
CTH + KU7 (4:1)
a
b
c
d
e
f
g
h
i
j
k
l
m
n
o
25 µm

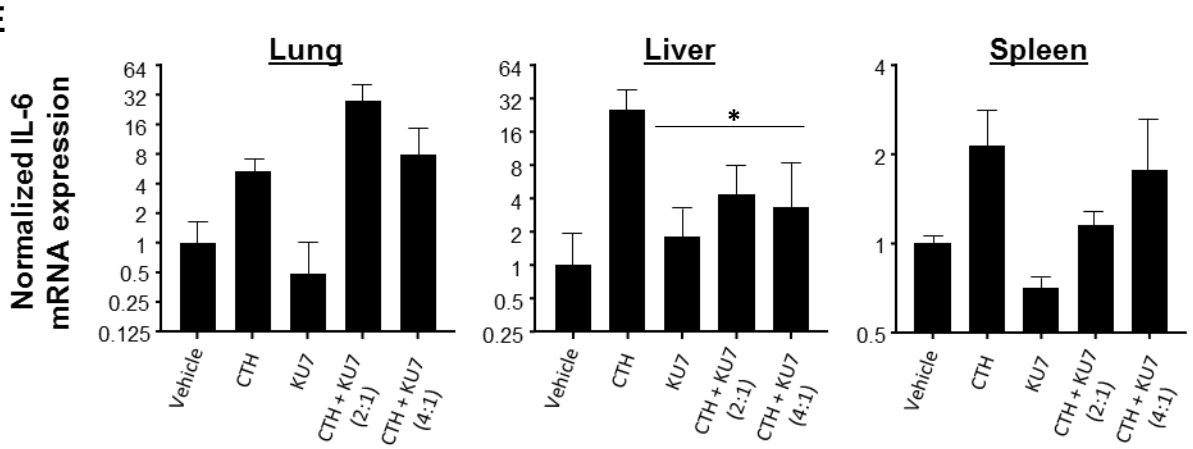
E
Normalized IL-6 mRNA expression
Lung
Liver
Spleen
64
32
16
8
4
2
1
0.5
0.25
0.125
*
Vehicle
CTH
KU7
CTH + KU7 (2:1)
CTH + KU7 (4:1)

Figure 5

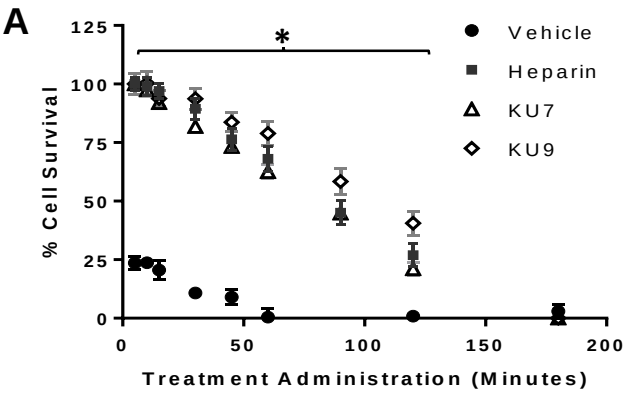
A
125
100
75
50
25
0
% Cell Survival
*
Vehicle
Heparin
KU7
KU9
0
50
100
150
200
Treatment Administration (Minutes)

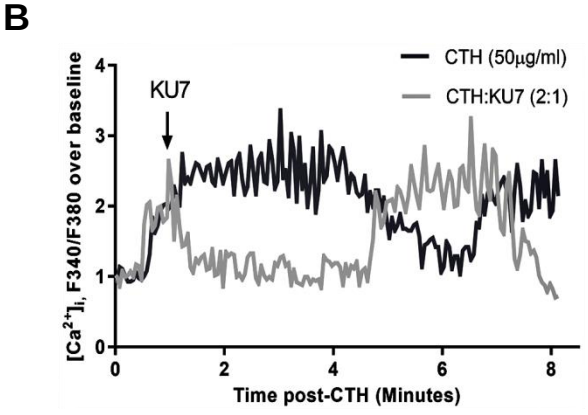
B
CTH (50µg/ml)
CTH:KU7 (2:1)
KU7
[Ca2+]i, F340/F380 over baseline
4
3
2
1
0
0
2
4
6
8
Time post-CTH (Minutes)

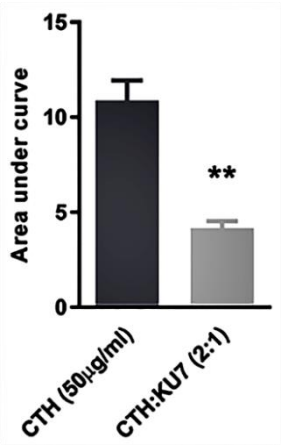
Area under curve
15
10
5
0
**
CTH (50µg/ml)
CTH:KU7 (2:1)

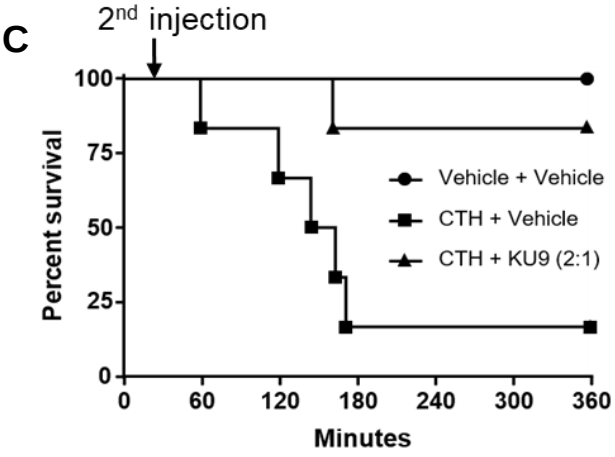
C
2nd injection
Percent survival
100
75
50
25
0
Vehicle + Vehicle
CTH + Vehicle
CTH + KU9 (2:1)
0
60
120
180
240
300
360
Minutes

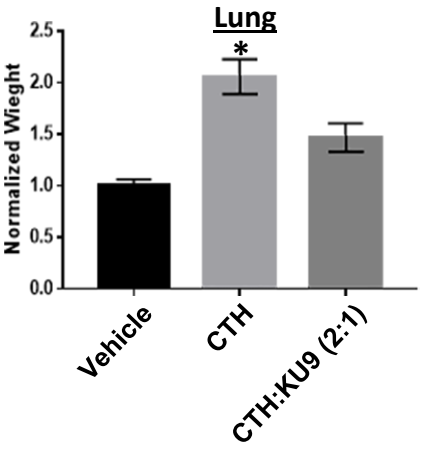
Lung
Normalized Wieght
2.5
2.0
1.5
1.0
0.5
0.0
*
Vehicle
CTH
CTH:KU9 (2:1)

Figure 6

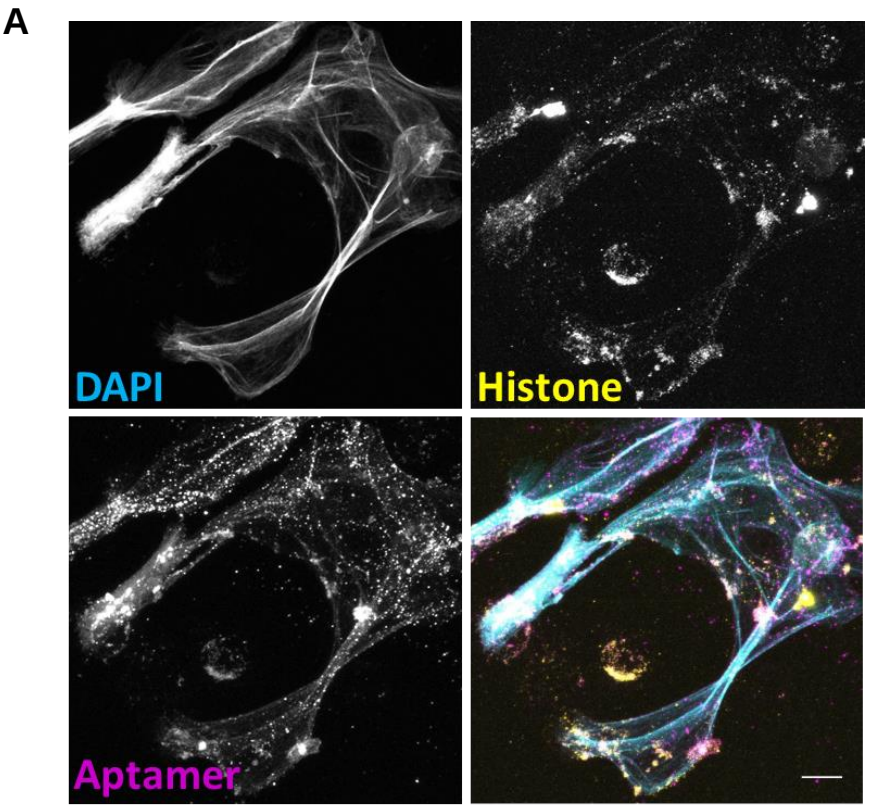
A
DAPI
Histone
Aptamer

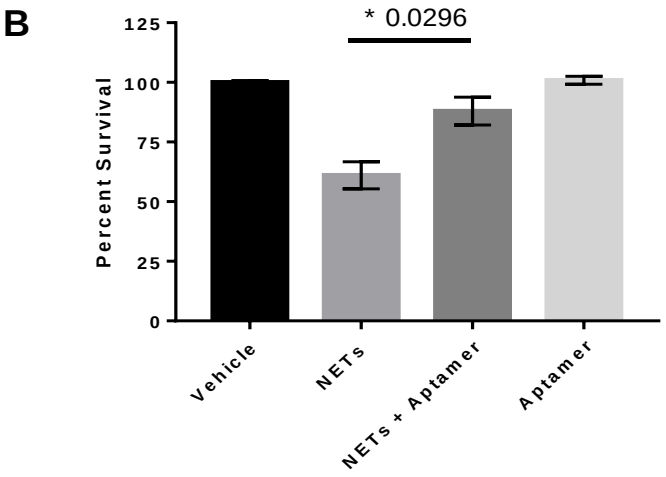
B
* 0.0296
Percent Survival
125
100
75
50
25
0
Vehicle
NETs
NETs + Aptamer
Aptamer

Data Availability

The datasets generated during and/or analyzed during the current study are available from the corresponding author on request.

REFERENCES

1. Wafaisade, A. et al. Epidemiology and risk factors of sepsis after multiple trauma: An analysis of 29,829 patients from the Trauma Registry of the German Society for Trauma Surgery*. *Critical care medicine* **39**, 621-628 (2011).
2. Frohlich, M. et al. Epidemiology and risk factors of multiple-organ failure after multiple trauma: an analysis of 31,154 patients from the TraumaRegister DGU. *J Trauma Acute Care Surg* **76**, 921-927; discussion 927-928 (2014).
3. Xu, J. et al. Extracellular histones are major mediators of death in sepsis. *Nat Med* **15**, 1318-1321 (2009).
4. Wildhagen, K.C. et al. Nonanticoagulant heparin prevents histone-mediated cytotoxicity in vitro and improves survival in sepsis. *Blood* **123**, 1098-1101 (2014).
5. Fuchs, T.A., Bhandari, A.A. & Wagner, D.D. Histones induce rapid and profound thrombocytopenia in mice. *Blood* **118**, 3708-3714 (2011).
6. Semeraro, F. et al. Extracellular histones promote thrombin generation through platelet-dependent mechanisms: involvement of platelet TLR2 and TLR4. *Blood* **118**, 1952-1961 (2011).
7. Chen, R., Kang, R., Fan, X.G. & Tang, D. Release and activity of histone in diseases. *Cell Death Dis* **5**, e1370 (2014).
8. Abrams, S.T. et al. Circulating histones are mediators of trauma-associated lung injury. *American journal of respiratory and critical care medicine* **187**, 160-169 (2013).
9. Murray, M.J. & Coursin, D.B. Multiple organ dysfunction syndrome. *Yale J Biol Med* **66**, 501-510 (1993).
10. Xu, J. et al. Extracellular histones are major mediators of death in sepsis. *Nature medicine* **15**, 1318 (2009).
11. Alhamdi, Y. et al. Circulating Histones Are Major Mediators of Cardiac Injury in Patients With Sepsis. *Crit Care Med* **43**, 2094-2103 (2015).
12. Biterge, B. & Schneider, R. Histone variants: key players of chromatin. *Cell Tissue Res* **356**, 457-466 (2014).
13. Semeraro, F. et al. Extracellular histones promote thrombin generation through platelet-dependent mechanisms: involvement of platelet TLR2 and TLR4. *Blood* **118**, 1952-1961 (2011).
14. Xu, J., Zhang, X., Monestier, M., Esmon, N.L. & Esmon, C.T. Extracellular histones are mediators of death through TLR2 and TLR4 in mouse fatal liver injury. *J Immunol* **187**, 2626-2631 (2011).
15. Yang, X., Li, L., Liu, J., Lv, B. & Chen, F. Extracellular histones induce tissue factor expression in vascular endothelial cells via TLR and activation of NF-kappaB and AP-1. *Thromb Res* **137**, 211-218 (2016).
16. Hoeksema, M., van Eijk, M., Haagsman, H.P. & Hartshorn, K.L. Histones as mediators of host defense, inflammation and thrombosis. *Future Microbiol* **11**, 441-453 (2016).
17. Allam, R., Kumar, S.V., Darisipudi, M.N. & Anders, H.-J. Extracellular histones in tissue injury and inflammation. *Journal of Molecular Medicine* **92**, 465-472 (2014).
18. Lv, X. et al. Extracellular histones are clinically relevant mediators in the pathogenesis of acute respiratory distress syndrome. *Respiratory research* **18**, 165 (2017).
19. Thålin, C. et al. Citrullinated histone H3 as a novel prognostic blood marker in patients with advanced cancer. *PloS one* **13**, e0191231 (2018).
20. Li, X. et al. Patients with HBV-related acute-on-chronic liver failure have increased concentrations of extracellular histones aggravating cellular damage and systemic inflammation. *Journal of viral hepatitis* **24**, 59-67 (2017).
21. Ekaney, M.L. et al. Impact of plasma histones in human sepsis and their contribution to cellular injury and inflammation. *Crit Care* **18**, 543 (2014).

22. Johansson, P.I., Windelov, N.A., Rasmussen, L.S., Sorensen, A.M. & Ostrowski, S.R. Blood levels of histone-complexed DNA fragments are associated with coagulopathy, inflammation and endothelial damage early after trauma. *J Emerg Trauma Shock* **6**, 171-175 (2013).
23. Kawai, C. et al. Circulating Extracellular Histones Are Clinically Relevant Mediators of Multiple Organ Injury. *Am J Pathol* **186**, 829-843 (2016).
24. Huang, H. et al. Histones activate the NLRP3 inflammasome in Kupffer cells during sterile inflammatory liver injury. *J Immunol* **191**, 2665-2679 (2013).
25. Li, X., Egorina, E., Bertelsen, E.L., Dahlen, H. & Hannestad, K. Antinucleosome autoantibodies bind directly to cell lines in vitro and via the FcgammaRIIB receptor to B lymphocytes in vivo: a role for immune complexes in interactions between antinucleosome IgG2a and B cells of BXSB lupus mice. *Scand J Immunol* **60**, 121-133 (2004).
26. Losman, M.J., Fasy, T.M., Novick, K.E. & Monestier, M. Relationships among antinuclear antibodies from autoimmune MRL mice reacting with histone H2A-H2B dimers and DNA. *Int Immunol* **5**, 513-523 (1993).
27. Opal, S.M., Dellinger, R.P., Vincent, J.L., Masur, H. & Angus, D.C. The next generation of sepsis clinical trial designs: what is next after the demise of recombinant human activated protein C?*. *Crit Care Med* **42**, 1714-1721 (2014).
28. Afifi, S. et al. Role of Histone Deacetylase Inhibitors in Relapsed Refractory Multiple Myeloma: A Focus on Vorinostat and Panobinostat. *Pharmacotherapy* **35**, 1173-1188 (2015).
29. Bongartz, T. et al. Anti-TNF antibody therapy in rheumatoid arthritis and the risk of serious infections and malignancies: systematic review and meta-analysis of rare harmful effects in randomized controlled trials. *JAMA* **295**, 2275-2285 (2006).
30. Shields, L.B. et al. Adverse effects associated with high-dose recombinant human bone morphogenetic protein-2 use in anterior cervical spine fusion. *Spine (Phila Pa 1976)* **31**, 542-547 (2006).
31. Keefe, A.D., Pai, S. & Ellington, A. Aptamers as therapeutics. *Nat Rev Drug Discov* **9**, 537-550 (2010).
32. Dassie, J.P. & Giangrande, P.H. Current progress on aptamer-targeted oligonucleotide therapeutics. *Ther Deliv* **4**, 1527-1546 (2013).
33. Thiel, K.W. & Giangrande, P.H. Therapeutic applications of DNA and RNA aptamers. *Oligonucleotides* **19**, 209-222 (2009).
34. Sundaram, P., Kurniawan, H., Byrne, M.E. & Wower, J. Therapeutic RNA aptamers in clinical trials. *Eur J Pharm Sci* **48**, 259-271 (2013).
35. Esposito, C.L. et al. A neutralizing RNA aptamer against EGFR causes selective apoptotic cell death. *PLoS One* **6**, e24071 (2011).
36. Povsic, T.J. et al. A Phase 2, randomized, partially blinded, active-controlled study assessing the efficacy and safety of variable anticoagulation reversal using the REG1 system in patients with acute coronary syndromes: results of the RADAR trial. *Eur Heart J* **34**, 2481-2489 (2013).
37. Vavalle, J.P. & Cohen, M.G. The REG1 anticoagulation system: a novel actively controlled factor IX inhibitor using RNA aptamer technology for treatment of acute coronary syndrome. *Future Cardiol* **8**, 371-382 (2012).
38. Chan, M.Y. et al. Phase 1b randomized study of antidote-controlled modulation of factor IXa activity in patients with stable coronary artery disease. *Circulation* **117**, 2865-2874 (2008).
39. Chan, M.Y. et al. A randomized, repeat-dose, pharmacodynamic and safety study of an antidote-controlled factor IXa inhibitor. *J Thromb Haemost* **6**, 789-796 (2008).

40. Povsic, T.J. et al. Pegnivacogin results in near complete FIX inhibition in acute coronary syndrome patients: RADAR pharmacokinetic and pharmacodynamic substudy. *Eur Heart J* **32**, 2412-2419 (2011).
41. Tuerk, C. & Gold, L. Systematic evolution of ligands by exponential enrichment: RNA ligands to bacteriophage T4 DNA polymerase. *Science* **249**, 505-510 (1990).
42. Ellington, A.D. & Szostak, J.W. In vitro selection of RNA molecules that bind specific ligands. *Nature* **346**, 818-822 (1990).
43. Thiel WH, B.T., Thiel KW, Dassie JP, Rockey WM, Howell CA; Liu XY, Dupuy AJ, Huang L, Owczarzy R, Behlke MA, McNamara JO II, Giangrande PH Nucleotide bias observed with a short SELEX RNA aptamer library. *Oligonucleotides* (2011).
44. Zuker, M. Mfold web server for nucleic acid folding and hybridization prediction. *Nucleic acids research* **31**, 3406-3415 (2003).
45. Semeraro, N., Ammollo, C.T., Semeraro, F. & Colucci, M. Coagulopathy of Acute Sepsis. *Semin Thromb Hemost* **41**, 650-658 (2015).
46. Freeman, C.G. et al. The accumulation of circulating histones on heparan sulphate in the capillary glycocalyx of the lungs. *Biomaterials* **34**, 5670-5676 (2013).
47. Abrams, S.T. et al. Circulating histones are mediators of trauma-associated lung injury. *Am J Respir Crit Care Med* **187**, 160-169 (2013).
48. Gillrie, M.R. et al. Plasmodium falciparum histones induce endothelial proinflammatory response and barrier dysfunction. *Am J Pathol* **180**, 1028-1039 (2012).
49. Kleine, T.J., Lewis, P.N. & Lewis, S.A. Histone-induced damage of a mammalian epithelium: the role of protein and membrane structure. *Am J Physiol* **273**, C1925-1936 (1997).
50. Kleine, T.J., Gladfelter, A., Lewis, P.N. & Lewis, S.A. Histone-induced damage of a mammalian epithelium: the conductive effect. *Am J Physiol* **268**, C1114-1125 (1995).
51. Abrams, S.T. et al. Human CRP defends against the toxicity of circulating histones. *J Immunol* **191**, 2495-2502 (2013).
52. Fuchs, T.A., Bhandari, A.A. & Wagner, D.D. Histones induce rapid and profound thrombocytopenia in mice. *Blood* **118**, 3708-3714 (2011).
53. Nakahara, M. et al. Recombinant thrombomodulin protects mice against histone-induced lethal thromboembolism. *PloS one* **8**, e75961 (2013).
54. Sollberger, G., Tilley, D.O. & Zychlinsky, A. Neutrophil extracellular traps: the biology of chromatin externalization. *Developmental cell* **44**, 542-553 (2018).
55. Saffarzadeh, M. et al. Neutrophil extracellular traps directly induce epithelial and endothelial cell death: a predominant role of histones. *PloS one* **7**, e32366 (2012).
56. McDonald, B. et al. Platelets and neutrophil extracellular traps collaborate to promote intravascular coagulation during sepsis in mice. *Blood*, blood-2016-2009-741298 (2017).
57. Rusconi, C.P. et al. RNA aptamers as reversible antagonists of coagulation factor IXa. *Nature* **419**, 90-94 (2002).
58. Rusconi, C.P., Yeh, A., Lyerly, H.K., Lawson, J.H. & Sullenger, B.A. Blocking the initiation of coagulation by RNA aptamers to factor VIIa. *Thromb Haemost* **84**, 841-848 (2000).
59. Huang, H. et al. Damage-associated molecular pattern-activated neutrophil extracellular trap exacerbates sterile inflammatory liver injury. *Hepatology* **62**, 600-614 (2015).
60. Caudrillier, A. et al. Platelets induce neutrophil extracellular traps in transfusion-related acute lung injury. *J Clin Invest* **122**, 2661-2671 (2012).
61. Allam, R. et al. Histones from Dying Renal Cells Aggravate Kidney Injury via TLR2 and TLR4. *Journal of the American Society of Nephrology* **23**, 1375-1388 (2012).
62. Bosmann, M. et al. Extracellular histones are essential effectors of C5aR-and C5L2-mediated tissue damage and inflammation in acute lung injury. *The FASEB Journal* **27**, 5010-5021 (2013).

63. Stein, C.A. & Castanotto, D. FDA-Approved Oligonucleotide Therapies in 2017. *Mol Ther* **25**, 1069-1075 (2017).
64. Ng, E.W. et al. Pegaptanib, a targeted anti-VEGF aptamer for ocular vascular disease. *Nat Rev Drug Discov* **5**, 123-132 (2006).
65. Ng, E.W. & Adamis, A.P. Anti-VEGF aptamer (pegaptanib) therapy for ocular vascular diseases. *Ann N Y Acad Sci* **1082**, 151-171 (2006).
66. Behlke, M.A. Chemical modification of siRNAs for in vivo use. *Oligonucleotides* **18**, 305-319 (2008).
67. Pallan, P.S. et al. Unexpected origins of the enhanced pairing affinity of 2′-fluoro-modified RNA. *Nucleic acids research* **39**, 3482-3495 (2010).
68. Krutzfeldt, J. et al. Specificity, duplex degradation and subcellular localization of antagomirs. *Nucleic Acids Res* **35**, 2885-2892 (2007).
69. Krutzfeldt, J. et al. Silencing of microRNAs in vivo with 'antagomirs'. *Nature* **438**, 685-689 (2005).
70. Mittelberger, F. et al. RAID3--An interleukin-6 receptor-binding aptamer with post-selective modification-resistant affinity. *RNA Biol* **12**, 1043-1053 (2015).
71. Da Rocha Gomes, S. et al. (99m)Tc-MAG3-aptamer for imaging human tumors associated with high level of matrix metalloprotease-9. *Bioconjug Chem* **23**, 2192-2200 (2012).
72. Meyer, C. et al. Stabilized Interleukin-6 receptor binding RNA aptamers. *RNA Biol* **11**, 57-65 (2014).
73. Urak, K.T. et al. In vitro RNA SELEX for the generation of chemically-optimized therapeutic RNA drugs. *Methods* **103**, 167-174 (2016).
74. Sousa, R. & Padilla, R. A mutant T7 RNA polymerase as a DNA polymerase. *EMBO J* **14**, 4609-4621 (1995).
75. Wong, I. & Lohman, T.M. A double-filter method for nitrocellulose-filter binding: application to protein-nucleic acid interactions. *Proc Natl Acad Sci U S A* **90**, 5428-5432 (1993).
76. Thiel, W.H. et al. Rapid identification of cell-specific, internalizing RNA aptamers with bioinformatics analyses of a cell-based aptamer selection. *PLoS One* **7**, e43836 (2012).
77. Thiel, W.H. Galaxy Workflows for Web-based Bioinformatics Analysis of Aptamer High-throughput Sequencing Data. *Molecular Therapy - Nucleic Acids* **5**, e345 (2016).
78. Dayal, S. et al. Enhanced susceptibility to arterial thrombosis in a murine model of hyperhomocysteinemia. *Blood* **108**, 2237-2243 (2006).
79. Clark, R.A. & Nauseef, W.M. Isolation and functional analysis of neutrophils. *Current Protocols in Immunology* **19**, 7.23. 21-27.23. 17 (1996).
80. Najmeh, S., Cools-Lartigue, J., Giannias, B., Spicer, J. & Ferri, L.E. Simplified Human Neutrophil Extracellular Traps (NETs) Isolation and Handling. *Journal of visualized experiments: JoVE* (2015).
81. Brinkmann, V., Laube, B., Abed, U.A., Goosmann, C. & Zychlinsky, A. Neutrophil extracellular traps: how to generate and visualize them. *Journal of visualized experiments: JoVE* (2010).
82. Lin, L., Taktakishvili, O. & Talman, W. Colocalization of neurokinin-1, N-methyl-D-aspartate, and AMPA receptors on neurons of the rat nucleus tractus solitarii. *Neuroscience* **154**, 690-700 (2008).
83. Lin, L.-H., Dragon, D.N., Jin, J. & Talman, W.T. Targeting neurons of rat nucleus tractus solitarii with the gene transfer vector adeno-associated virus type 2 to up-regulate neuronal nitric oxide synthase. *Cellular and molecular neurobiology* **31**, 847-859 (2011).
84. Thiel, K.W. et al. Delivery of chemo-sensitizing siRNAs to HER2+-breast cancer cells using RNA aptamers. *Nucleic acids research* **40**, 6319-6337 (2012).

ACKNOWLEDGMENTS

The authors would like to acknowledge the use of the University of Iowa Pathology Core, a core resource supported by the Vice President for Research & Economic Development, the Holden Comprehensive Cancer Center, and the Carver College of Medicine. We would like to thank the labs of Drs. Adam Dupuy, George Wiener, and the Iowa City VA Microscopy Core for the use of equipment (Biorad Imager, plate reader, and confocal microscope).

AUTHOR CONTRIBUTIONS

Conceptualization: FJM and PHG; Methodology: FJM, PHG, SD, MEW, JAS and LHL; Data Acquisition, Curation and Analysis: KTU, GNB, LHL, JPD, SS, YC, VKS, BL, JAS, SM, JKT, FJM and PHG; Resources: FJM and PHG; Writing – original draft: KTU, GNB and LHL; Writing – review and editing: JKT, FJM, PHG, SS and LHL; Supervision: FJM and PHG.

Funding Sources

KTU was supported by the American Heart Association (AHA) pre-doctoral fellowship (17PRE33410335). This work was supported by grants to PHG and FJM from Department of Defense Congressionally Directed Medical Research Programs (PR150627 and PR150627P1), University of Iowa Carver College of Medicine (CCOM) (Carver Collaborative Pilot Grant Award 2015) and University of Iowa Award from The Office of the Vice President for Research and Economic Development (OVPRED 2015). FJM is also supported by the Office of Research and Development, Department of Veterans Affairs (2I01BX001729). This study was also supported in part by National Institutes of Health grants AG049784 to SD.

Figure Legends

Figure 1. Identification of histone-specific RNA aptamers using SELEX. A) Schematic of the *in vitro* Systematic Evolution of Ligands by Exponential Enrichment (SELEX) procedure. Step 1. Double-stranded DNA (DS DNA) template library (Sel2N20) is *in vitro* transcribed in the presence of 2′ Fluoro pyrimidines and 2' OH purines to generate the 2′ Fluoro-modified Round 0 RNA library (RNA). Step 2. The Round 0 RNA library was incubated with human albumin and human IgG to remove RNAs that bind to human serum proteins (Negative selection). Step 3. RNA-bound to serum proteins was discarded. Step 4. RNA not bound to serum proteins was incubated with human histones H3 and H4, respectively. Step 5. Histone-bound aptamers were collected and reverse-transcribed into DNA. Step 6. Round 1 DNA was then transcribed into RNA for the subsequent round of selection. A total of eight rounds of selection were performed for each histone selection (see **Supplementary Table 1**). **B)** Binding of Round 0 (R0) and Round 8 (R8) RNA to recombinant human histone H3 (top, left panel) and H4 (top, right panel) proteins. Binding of R8 RNA to human albumin (bottom, left panel) and human serum (bottom, right panel). **C)** Percent sequence enrichment (% Enrichment) at each round of selection (black circle). 50% sequence enrichment point (grey circle) is indicated for each selection.

Figure 2. Binding characterization and stability measurements of individual histone RNA aptamer sequences. **A)** Binding kinetic rate constants (k_a and K_D) determined for aptamers KU7 (left panels) and KU9 (right panels) binding to CTH (top panels), H4 (middle panels), and BSA (bottom panels). Aptamers concentrations tested: 100 nM (blue), 50 nM (black), 25 nM (red), 12.5 nM (green), 10 nM (magenta). **B)** Serum stability measurements for aptamers KU7 and KU9 (5 µM) in 50% human serum. $T_{1/2}$ KU7 = 150 hrs. $T_{1/2}$ KU9 = 48 hrs.

Figure 3. *In vitro* efficacy of RNA aptamers. A) Human platelet aggregation measurements using platelets derived from 3 independent healthy donors (n = 3). Collagen (Col), histone H4

(H4), histone aptamers (KU7 and KU9), heparin (Hep). *P <0.05 vs H4 **B)** TLR activation: IL-6 ELISA detection of IL-6 protein levels (as a measurement of TLR activation) in supernatants of EA.Hy926 cells treated with media alone (Veh), calf thymus histones (CTH), histone aptamers (KU7 and KU9) alone or in combination. * P <0.05 vs CTH **C)** Cytotoxicity measurements: Aptamer inhibition of histone-mediated cytotoxicity of endothelial cells determined by MTS assay. (Left panel) EA.hy926 cells treated with 1.2 µM of aptamers (KU7 or KU9) and varying amounts (0 to 1,000 µg/mL) of calf thymus histones (CTH). (Right panel) EA.hy926 cells treated with 180 µg/mL of CTH and increasing amounts (0 to 16 µM) of aptamers (KU7 or KU9). N = 4 biological replicates. **P <0.01 *vs*. vehicle (100 µg/ml). **D)** Dynamic changes of intracellular calcium levels in fura 2-AM loaded EA.hy926 cells using fluorescence microscopy. (Left panel) Representative intracellular calcium elevation traces (F340/F380) of EA.hy926 treated with CTH (50 µg/mL) alone, aptamer KU7 alone (25 µg/mL, top panels), aptamer KU9 alone (25 µg/mL, bottom panels), or CTH (50 µg/mL) in the presence of varying aptamer amounts (Molar ratio of CTH to aptamer indicated). (Right panel) Summary of data from multiple EA.hy926 cells (n = 19 – 69 cells per bar). **p <0.01 *vs*. CTH.

Figure 4. Efficacy of histone aptamer in murine model of MODS. A) Survival curves of mice injected IV with CTH in the presence or absence of aptamer treatment. Gray square = CTH alone group. Black diamond = 1× BB (vehicle), aptamer alone (KU7) or CTH plus aptamer (CTH + KU7) groups, at two different concentrations. Molar ratio of CTH to aptamer indicated. **B)** Bar graph representing normalized organ weight of the liver, lung, and spleen from the treatment groups compared to the vehicle. All organ weights were normalized to pre-treatment body weight. **C)** Histology of the liver, lung, and spleen of vehicle (a-c), CTH (d-f), KU7 (g-i), CTH + KU7 (2:1) (j-l), and CTH + KU7 (4:1) (m-o) treated mice. Vascular congestion, thrombi and hemorrhaging are indicated by yellow arrows. Scale bar = 100 µm**. D)** Immunostaining of mouse liver (a-e), lung (f-j) and spleen (k-o). TO-PRO®3 (nucleus, pseudo blue stain), cytoskeleton and

platelets (pseudo red stain), histone H3, neutrophils and IL-6 (pseudo green stain) (see Supplementary Fig. 4 for quantitative analysis of immunostaining data). Scale bar = 25 µm. **E)** Normalized IL-6 mRNA expression levels in the liver, lung, and spleen of mice. Normalized IL-6 mRNA expression was determined using the following equation: 2^(Δ-ΔCT). ΔCT= beta actin - IL-6, Δ-ΔCT = Vehicle ΔCT – Treatment ΔCT. Error bars represent the lower limit (LL) and upper limit (UL) of the standard deviation from the Δ-ΔCT [2^(LL Δ-ΔCT) and 2^(UL Δ-ΔCT)]. *p <0.05 *vs*. CTH (50 mg/kg).

Figure 5. Efficacy of anti-histone aptamers when administered after histones. A) Aptamer inhibition of histone-mediated cytotoxicity of endothelial cells determined by MTS assay. EA.hy926 cells treated with 200 µg/mL of calf thymus histones followed by administration of either vehicle (negative control), heparin (positive control, 1:1), KU7 aptamer (1:2), or KU9 aptamer (1:2) at time points 0, 5, 10, 15, 30, 45, 60, 90, 120, and 180 min. n = 3 biological replicates. *p <0.0025 *vs*. vehicle. **B)** Dynamic changes of intracellular calcium levels in fura 2-AM loaded EA.hy926 cells using fluorescence microscopy. (Left panel) Representative intracellular calcium elevation traces (F340/F380) of EA.hy926 treated with CTH (50 µg/mL) followed by addition of vehicle or aptamer KU7 (Molar ratio of CTH to aptamer 2:1) added 1 minute after CTH. (Right panel) Summary of data from multiple EA.hy926 cells (n = 23 – 27 cells per bar). *p <0.05 *vs*. CTH. **C)** Efficacy of anti-histone aptamers in murine model of MODS. Survival curves of mice injected IV with vehicle, or CTH (62.5 mg/kg), followed the 30 min by IV injection of vehicle or aptamer KU9 (31.25 mg/kg). n = 6 biological replicates. *p <0.05 vs. CTH + vehicle. Lung weight of the treatment groups compared to the vehicle. All lung weights were normalized to pre-treatment body weight. n = 6 biological replicates. *p <0.05 *vs*. CTH + vehicle (right panel).

Figure 6. Aptamers bind to human neutrophil-derived NETs and inhibit NET-induced cytotoxicity. **A)** Confocal microscopy of human neutrophil-derived NETs. Single images are shown in grey scale. DAPI (top, left); Histones (top, right); aptamer KU7 (bottom, left); merged images show cyan=DAPI labeling of DNA, yellow = histones, magenta = aptamer KU7-647 (bottom, left). White areas in the merged image represent close-proximity of DNA, histone, and aptamer. Representative images, captured with 40× oil and 2.8× zoom, are shown. Scale is equivalent to 10 µm. **B)** Cytotoxicity measurements: Aptamer inhibition of NETs-mediated cytotoxicity of endothelial cells determined by MTS assay. EA.hy926 cells treated with 8 µg/well of NETs material (based on DNA concentration) and/or 8 µg/well (10.66 µM) of aptamer (KU7). Data are shown as Mean ± SEM of 9 wells/treatment and are representative of 3 different donors (*$p < 05$).

Supplementary Materials

Supplementary Methods

Platelet Aggregation assay

Washed platelets were prepared as described in the Methods section. Platelets were re-suspended in Tyrode buffer to a final concentration of 2.5×10^8 platelets/mL. For the platelet aggregation studies, 400 µl of washed platelets were stirred at 1,200 rpm at 37 °C along with either collagen (1 µg/mL), histone H4 (10 µg/mL), selected RNA rounds (15 µg/mL) in a cuvette of an aggregometer (Chrono-log Model 560-VS) and light transmittance was recorded. Aggregation was measured as percent change in light transmission, where 100 % refers to transmittance through blank solution.

TLR activation studies

EA.Hy926 cells were seeded in a 96-well flat bottom plate at a density of 15,000 cells/well in 100 µl of media. After 24 h the medium was removed and replaced with 100 µl of Opti-MEM containing either calf thymus histones (CTH) at varying concentrations or LPS (50 µg/mL) with/out Aptamers KU7 and KU9 (50 µg/mL). After 24 h, the supernatant was collected, processed and quantified according to manufacturer's protocol in the human interleukine-6 (IL-6) Quantikine® ELISA kit (R&D Systems, Minneapolis, MN).

Double-filter binding assay

Double-filter nitrocellulose binding assay was preformed to determine the binding affinity (K_D) of the aptamers for their target [1]. Synthetic aptamers (KU7 and KU9) were radiolabeled with gamma-^{32}P-ATP using T4 polynucleotide kinase (PNK) as follows: A total reaction volume of 20 µL was made up of 20 pmol of aptamer RNA, 2 µL PNK (New England Biolabs, Ipswich, MA), 2 µL PNK reaction buffer (New England Biolabs, Ipswich, MA), 2 µL gamma-^{32}P-ATP (PerkinElmer, Waltham, MA), and diH_2O. The mixture was then incubated at 37 °C for 30 min and 65 °C for 20 min to heat inactivate the PNK. 20 µL of 1× BB was added to the reaction followed by a centrifugation step through a G25 purification

column (GE Healthcare, Little Chalfont, United Kingdom, IL) according to manufactures instructions. Labeling efficiency was determined by a scintillation counter. All radiolabeled RNAs were diluted in 1× BB to 2,000 cpm/mL. 5 µL of 2,000 cpm/mL radiolabeled RNA was incubated at 37 °C for 5, 50, and 100 mins respectively with 15 µL of either human histone H4 serially diluted in 1× BB. The binding reactions were loaded onto a dot blot apparatus (composed of nitrocellulose membrane on the top, nylon membrane (Sigma-Aldrich, St. Louis, MO) in the middle and Whatman paper (Sigma-Aldrich, St. Louis, MO) on the bottom). Treatment of the nitrocellulose membrane was as follows: pretreated with 0.5 M KOH (Sigma-Aldrich, St. Louis, MO) for 20 min, quick wash with diH_2O, and equilibrated in 0.1 M Tris HCl 7.5 for 45 min, washed with diH_2O, and transferred to 1× BB for 20 min before l (Sigma-Aldrich, St. Louis, MO). The nylon was also incubated in 1× BB for 20 min before being loaded on the manifold. Before loading the RNA/protein samples, the wells were washed with 100 µL of 1× BB. The amount of RNA bound (nitrocellulose) versus unbound (nylon) was determined by densitometry of imaged membrane on a Fuji Phosphor imager.

Supplementary Figure 1

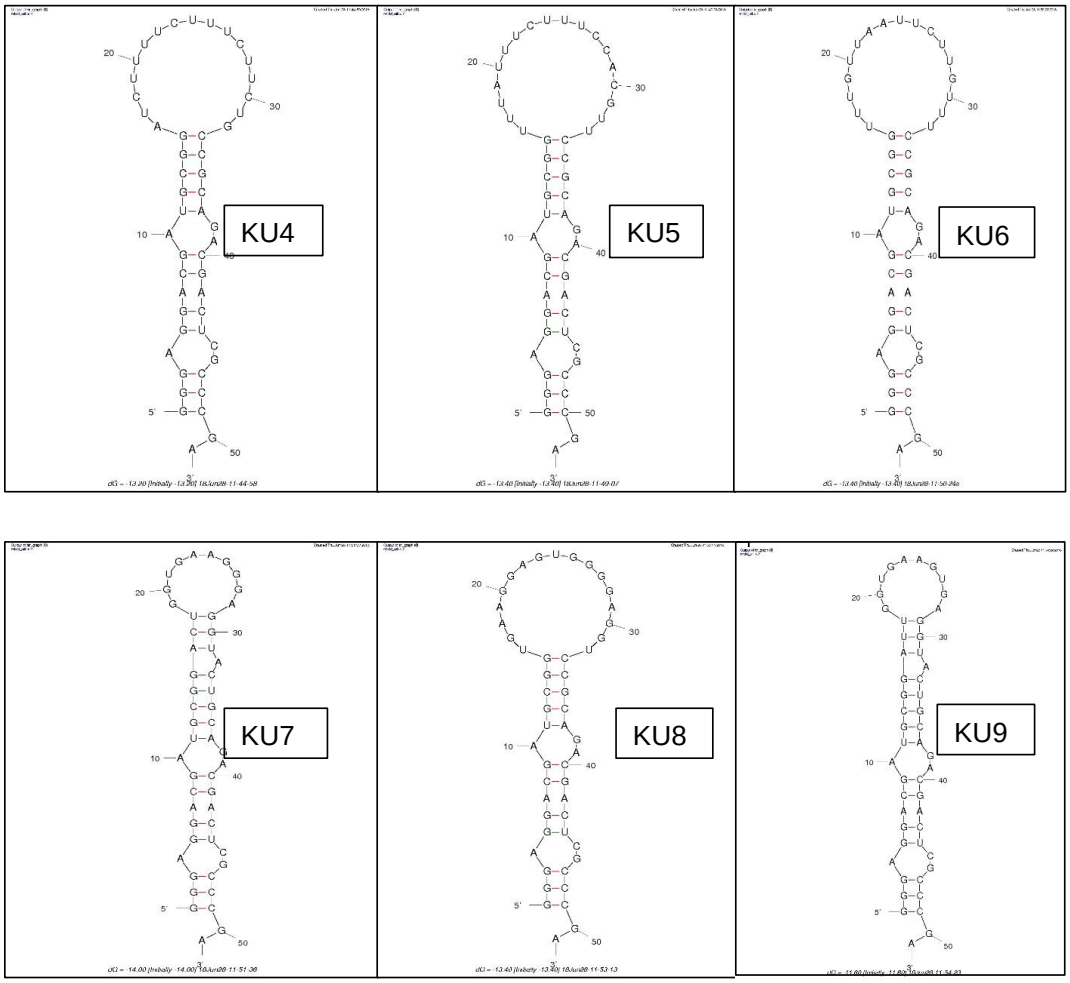

Supplementary Figure 1. Theoretical secondary RNA structures for the top 6 histone aptamers.

Secondary RNA structures for histone aptamers KU4 – KU9 ~~)~~ predicted using Mfold.

Supplementary Figure 2

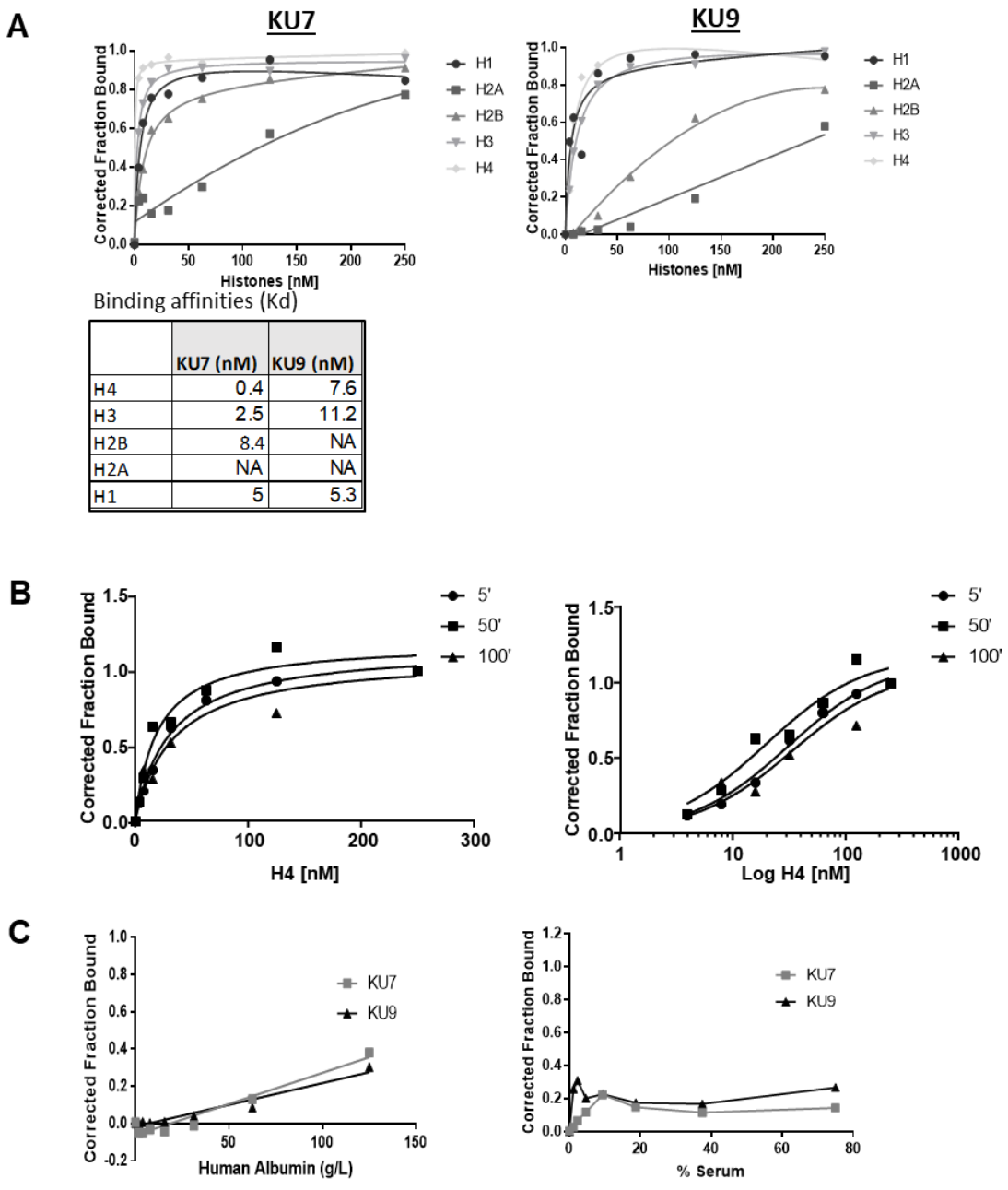

	KU7 (nM)	KU9 (nM)
H4	0.4	7.6
H3	2.5	11.2
H2B	8.4	NA
H2A	NA	NA
H1	5	5.3

Supplementary Figure 2. Sensitivity and specificity for selected RNA aptamers. **A)** Binding of KU7 (left panel) and KU9 (right panel) to recombinant histones H1, H2A, H2B, H3 and H4. Binding constants are listed in table (bottom). **B)** Binding of KU7 to H4 histones (middle, left and right panel) at 5, 50 and 100 mins to determine equilibrium binding time. **C)** Binding of selected RNA aptamers KU7 and KU9 human serum albumin (lower, left panel) and to serum (lower, right panel)

Supplementary Figure 3

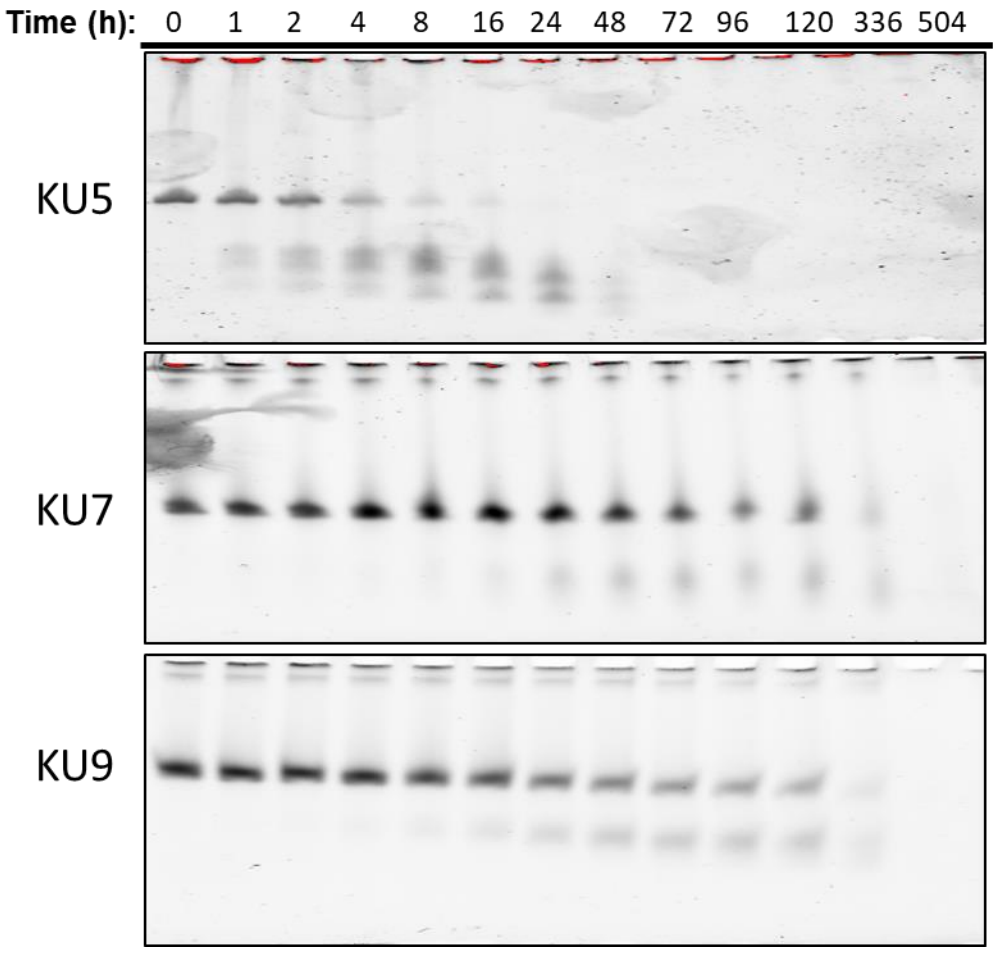

Supplementary Figure 3. Stability measurements of individual histone RNA aptamer sequences

Full-sized 8M urea gels of the aptamers highlighting the degradation or stability of each aptamer.

Supplementary Figure 4

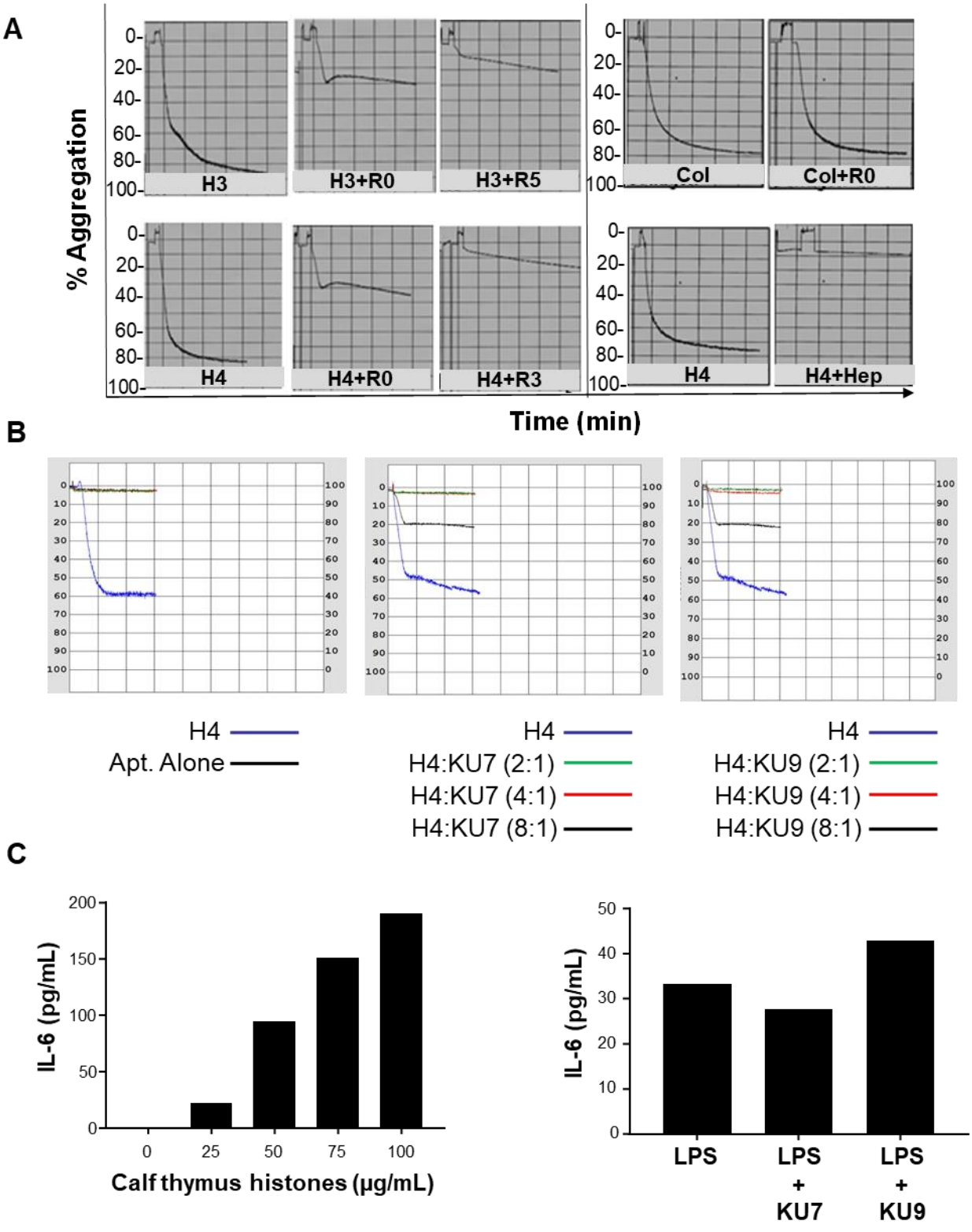

Supplementary Figure 4. *In vitro* efficacy of RNA aptamers. A) Human platelet aggregation measurements using platelets derived from healthy donor blood. Collagen **(**Col), human histones (H3 and H4), Round 0 RNA (R0), Round 3 RNA (R3), Round 5 RNA (R5), heparin (Hep). **B)** Human platelet aggregation measurements using platelets derived from 3 independent healthy donors (n = 3). Histone H4 (H4), histone aptamer (Apt). (Left panel) Platelets were treated with 10 µg/mL of histone H4 alone (blue) or 10 µg/mL aptamers alone (black). Platelets were treated with 10 µg/mL of histone H4 alone (blue) or histone plus varying amounts of RNA aptamer KU7 (middle panel) or KU9 (right panel). Molecular weight of H4 to aptamer is indicated in legend. **C)** TLR activation. (Left panel) IL-6 protein levels (as a measurement of TLR activation) in supernatants of EA.Hy926 cells treated with various amounts (0 to 100 µg/mL of CTH using an IL-6 ELISA. (Right panel) IL-6 protein levels (as a measurement of TLR activation) in supernatants of EA.Hy926 cells treated with 50 µg/mL of LPS, or LPS plus 50 µg/mL aptamers KU7 or KU9.

Supplementary Figure 5

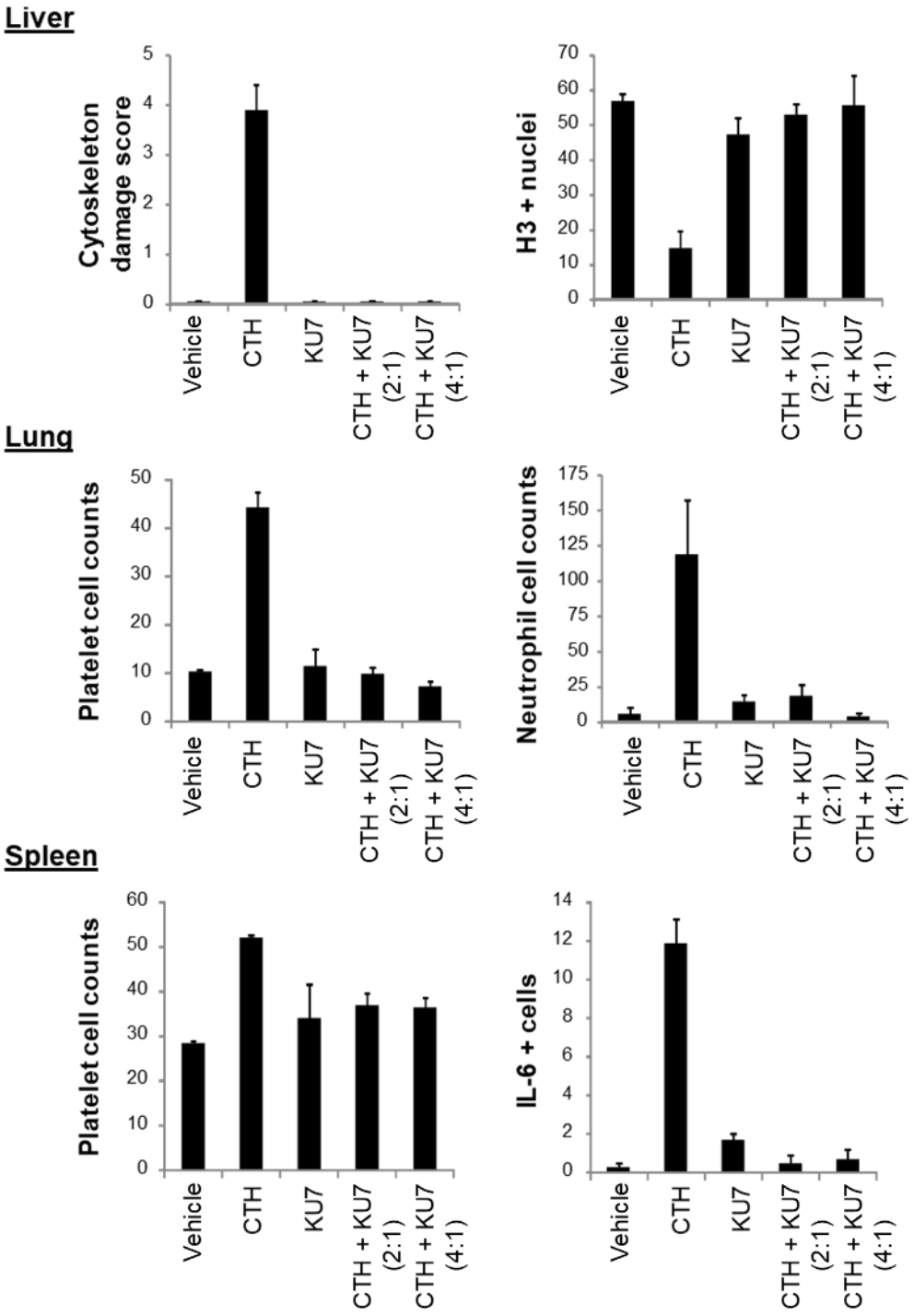

Supplementary Figure 5. Efficacy of histone aptamer bio-drug in murine model of MODS. Quantitative analyses of immunostaining of mouse liver (top panels), lung (middle panels) and spleen (bottom panels) tissues. Bars represent mean values of 2-4 mice (each mouse estimated from 4-5 independent confocal images taken at 20× magnification with 2× zoom, using the image analysis program, NIH ImageJ). Cytoskeleton damage score (liver) was assigned a score from 0 to 5 (no damage = 0, most severe = 5). Platelet cell counts (lung and spleen) represent mean optical density measurements. Error bars = standard deviation of 2-4 mice (each mouse estimated from 4-5 independent confocal images).

Supplementary Table 1. Histone selection protocol

	Round	Ratio of Protein:RNA	RNA (pmol)	Protein (pmol)	[Protein] (nM)	Binding Reaction Volume (mL)	Binding Time	[NaCl] (mM)	Pre-Clear conditions	Pre-Clear Time	Washes (10mL)
Positive Selection (Histones) and Negative Selection (hIgG and BSA)	1	1:10	1000	100	10	10	10 min in solution 10 min with disk	150	hIgG	20 min in solution 20 min with disk	3 x 5 min
	2	1:10	1000	100	10	10	5 min in solution 5 min with disk	150	hIgG	20 min in solution 20 min with disk	3 x 10 min
	3	1:20	1000	50	5	10	5 min in solution 5 min with disk	150	hIgG	20 min in solution 20 min with disk	3 x 10 min
	4	1:40	2000	50	5	10	5 min in solution 5 min with disk	150	hIgG + BSA	10 min in solution 10 min with disk	3 x 10 min
	5	1:40	2000	25	5	10	5 min in solution 5 min with disk	150	hIgG + BSA	10 min in solution 3 x 10 min with disk	3 x 15 min
	6	1:80	2000	25	5	5	5 min in solution 5 min with disk	150	hIgG + BSA	10 min in solution 10 min with disk	3 x 30 min
Negative Selection (hIgG and BSA)	7	-	-	-	-	-	-	150	hIgG + BSA	10 min in solution 3 x 10 min with disk	-
	8	-	-	-	-	-	-	150	hIgG + BSA	10 min in solution 3 x 10 min with disk	-

Supplementary Table 2. Affinity measurements

	Histone H3	Histone H4	CTH	Human Albumin	Human Serum
Round 0	4.221	1.963	-		
Round 8	1.306	1.038	-	N/A	N/A
KU7	0.3117	0.68	4.109	N/A	N/A
KU9	5.239	0.8575	12.46	N/A	N/A

Supplementary Table 3. Top aptamer sequences from histone selection

Original name	name	sequence	Fold enrichment (R3:5)	Fold enrichment (6:8)
0081_H4	KU4	GGGAGGACGAUGCGGAUCUUUUCUUUCUUCUGCCGCAGACGACUCGCCCGA	9.704	0.47
0065_H4	KU5	GGGAGGACGAUGCGGUUUAUUUCUUUCCACGUUCCGCAGACGACUCGCCCGA	9.699	0.47
0120_H4	KU6	GGGAGGACGAUGCGGUUUGUUAAUUCUUGUUUCCGCAGACGACUCGCCCGA	9.22	0.23
0145_H32	KU7	GGGAGGACGAUGCGGACUGGUGAAGGGAGGUACUGCAGACGACUCGCCCGA	6.91	2.22
0236_H32	KU8	GGGAGGACGAUGCGGUGAAGGAGUGGGGAGGUCCGCAGACGACUCGCCCGA	6.74	1.3
0243_H32	KU9	GGGAGGACGAUGCGGAUUGGUGAAGUGAGGUACUGCAGACGACUCGCCCGA	6.58	0.6

Supplementary Table 4. Next-generation sequencing (NGS) primers

Illumina primers with Barcode	sequence
BC01	AAT GAT ACG GCG ACC ACC GAG ATC TAC ACT CTT TCC CTA CAC GAC GCT CTT CCG ATC TAA GAA GGG AGG ACG ATG CGG
BC02	AAT GAT ACG GCG ACC ACC GAG ATC TAC ACT CTT TCC CTA CAC GAC GCT CTT CCG ATC TGG CAA GAA GGG AGG ACG ATG CGG
BC03	AAT GAT ACG GCG ACC ACC GAG ATC TAC ACT CTT TCC CTA CAC GAC GCT CTT CCG ATC TCC TAA GAA GGG AGG ACG ATG CGG
BC04	AAT GAT ACG GCG ACC ACC GAG ATC TAC ACT CTT TCC CTA CAC GAC GCT CTT CCG ATC TCG AGA GAA GGG AGG ACG ATG CGG
BC05	AAT GAT ACG GCG ACC ACC GAG ATC TAC ACT CTT TCC CTA CAC GAC GCT CTT CCG ATC TGT GGA GAA GGG AGG ACG ATG CGG
BC06	AAT GAT ACG GCG ACC ACC GAG ATC TAC ACT CTT TCC CTA CAC GAC GCT CTT CCG ATC TTA CGA GAA GGG AGG ACG ATG CGG
BC07	AAT GAT ACG GCG ACC ACC GAG ATC TAC ACT CTT TCC CTA CAC GAC GCT CTT CCG ATC TAT CCA GAA GGG AGG ACG ATG CGG

RNA inhibitors of extracellular histones to prevent multiple organ dysfunction syndrome

Francis J Miller, MD[1,2], Kevin T Urak[3], Giselle N Blanco[3], Li-Hsien Lin[3], Beilei Lei, PhD[1], and Paloma H Giangrande, PhD[3]

[1]Duke University, Durham, NC
[2]Veterans Administration Medical Center, Durham, NC
[3]University of Iowa, Iowa City, IA

Background: Severe tissue injury, including major trauma, sepsis, burns, radiation, inhalation of toxic substances, or radiation, will often result in the development of multiple organ dysfunction syndrome (MODS) or acute respiratory distress syndrome (ARDS). MODS/ARDS is primarily managed with supportive care, as there is no treatment to prevent or reverse its development, and the associated morbidity and mortality is high. Following cellular injury, nuclear proteins, of which histones are the most abundant, are released by dying cells. In the extracellular space, histones act as cytotoxic damage-associated molecular pattern proteins by activating platelets to cause thrombi formation; toll-like receptors resulting in cytokine production; and with cellular membranes triggering calcium influx and cell death. These effects of circulating histones result in remote cellular injury and a positive feedback loop of additional histone release. We hypothesized that RNA aptamers could selectively bind extracellular histones and abrogate histone-mediated injury. RNA aptamers are chemically-stabilized nucleic acid bio-drugs that bind with high affinity and specificity to their targets. As a therapeutic, aptamers possess several key advantages over other biologics: (1) they are self-refolding, single-chain, and redox-insensitive. Unlike proteins, they do not aggregate, and they tolerate pH and temperatures that proteins do not, making them ideal for field administration. (2) They have high selectivity for their target, eliminating potential for off-target effects. (3) They are easy to synthesize and their production does not depend on bacteria, cell cultures or animals. (4) Cross-species reactive aptamers can be easily engineered, thus expediting testing of the same reagent in preclinical animal models and human clinical trials.
Methods: Systematic evolution of ligands by exponential enrichment technology was used to select for RNA aptamers that bind to the histones primarily responsible for MODS/ARDS (H3 and H4), but not to other serum proteins. The RNA aptamers were evaluated for efficacy against histone-mediated toxicity *in vitro* using cultured human cells. *In vivo* efficacy was examined in a mouse model of MODS consisting of intravenous injection of histones into the tail vein. The dose of histones used were similar to that measured in serum of patients with MODS due to trauma or sepsis.
Results: First, we developed nuclease-resistant, 2′ fluoro-modified RNA aptamers with high affinity (K_D = nanomolar) for histones H3 and H4. These anti-histone aptamers inhibited histone-induced platelet aggregation in a dose-dependent manner. In contrast, the aptamers did not inhibit platelet aggregation induced by collagen. The aptamers also inhibited histone-induced toll-like receptor activation in cultured endothelial cells, as measured by IL-6 production. Extracellular histones induce cytotoxicity through their interaction with the plasma membrane, leading to calcium influx, cell swelling, and cytolysis. Aptamers significantly inhibited the histone-induced increase of intracellular

calcium as measured by the calcium indicator fura 2-AM. We confirmed that administration of histones to human endothelial and epithelial cell lines caused dose-dependent cell death. RNA aptamers had a dose-dependent protective effect in neutralizing histone-induced cytotoxicity. Next, we tested the efficacy of the RNA aptamer in a mouse model of MODS/ARDS. Tail vein injection of histones resulted in dose-dependent organ dysfunction and death in mice. Histologic staining of lung and liver revealed tissue edema, inflammatory cell infiltration, microthrombi, and hemorrhage. The administration of RNA aptamers at the same time or 30 minutes after histones prevented death and reduced the histopathologic findings of tissue injury. *Conclusion:* These data confirm that RNA aptamers, selected to bind to extracellular histones, can attenuate histone-mediated injury in human platelets and endothelial cells *in vitro* and protect from morbidity in a mouse model of MODS. Given the many etiologies of severe tissue injury, these aptamers could have a significant impact on the treatment of numerous clinical conditions associated with MODS/ARDS.

Detection of extracellular histones in serum using RNA aptamers

Shambhavi Shubham[1], Li-Hsien Lin[1], Piedad del Carmen Gomez Contreras[1], Kevin T Urak[1,7], Giselle Blanco[1], Felicia Ruffin [10], Fowler VG Jr [10], Julia Klesney Tait[1], Francis J Miller[3], Paloma H Giangrande,[1,2,4,5,6,7,8,9]

Internal Medicine, University of Iowa, Iowa City, IA, USA, Abboud Cardiovascular Research Center, University of Iowa, Iowa City, IA, USA, Departments of Internal Medicine and Pharmacology and Cancer Biology, Duke University, Durham, NC, USA, Holden Comprehensive Cancer Center, University of Iowa, Iowa City, IA, USA, Radiation Oncology, University of Iowa, Iowa City, IA, USA, Environmental Health Sciences Research Center (EHSRC), University of Iowa, Iowa City, IA, USA
Molecular & Cellular Biology Program, University of Iowa, Iowa City, IA, USA
Division of Infectious Diseases and International Health, Department of Medicine, Duke University School of Medicine, Durham, NC

ABSTRACT:

Sepsis remains a major health problem resulting in an extremely high rate of morbidity and mortality worldwide, partly due to delayed diagnosis during early disease. Currently, sepsis is diagnosed *via* bacterial culturing of blood samples over several days prolonging time to diagnosis, or PCR-based molecular methods, which often lack sensitivity and specificity. The use of nucleic acid aptamer biosensors that bind sepsis biomarkers in the circulation with high affinity and specificity, could provide robust and rapid sepsis diagnosis. Previously, we used the systematic evolution of ligands by exponential enrichment technique to develop chemically-modified RNA aptamers to extracellular histones implicated in sepsis (histones H3 and H4). Here, we show that these aptamers can detect low levels (< 10 µg/mL) of circulating histones in septic patient samples. The aptamer-based detection assay was orders of magnitude more sensitive at detecting circulating histones in serum compared to current antibody-based methods. Importantly, with the aptamer-based detection assay, we establish a well-defined correlation between sepsis severity and serum levels of circulating histones. Given the potential impact of early identification of sepsis on patient outcome, these aptamers could provide culture and amplification-free tests that can be used in combination with current bacterial detection methods for rapid clinical sepsis diagnosis.

Shambhavi Shubham, PhD
University of Iowa
375 Newton Road, 5241 MERF
Iowa City, IA
shamshu27@gmail.com

RNA Inhibitors of Nuclear Proteins Implicated in Multiple Organ Dysfunction Syndrome

Kevin Urak

Molecular Medicine Seminar 2018

Canonical function of histones

Infection

Trauma

Poor life choices

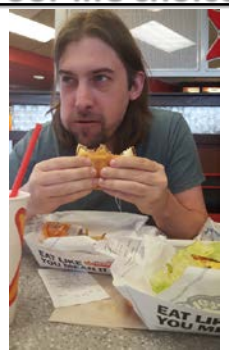

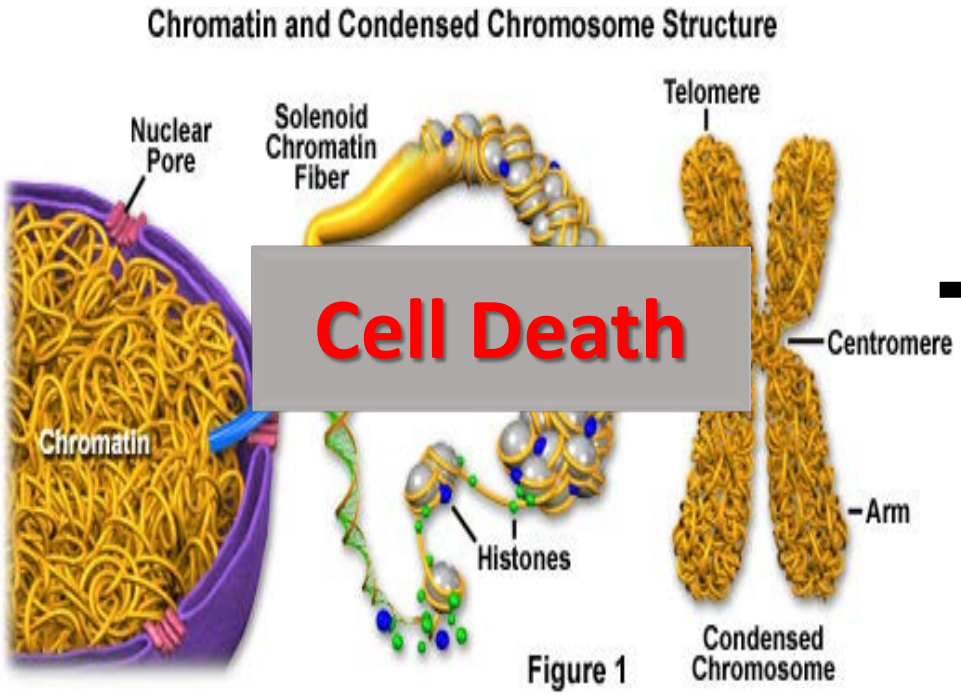

Cell Death

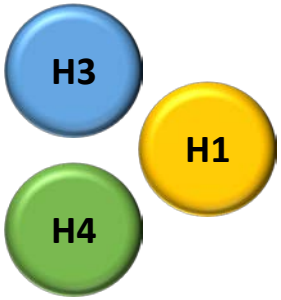

Problems with extracellular histones

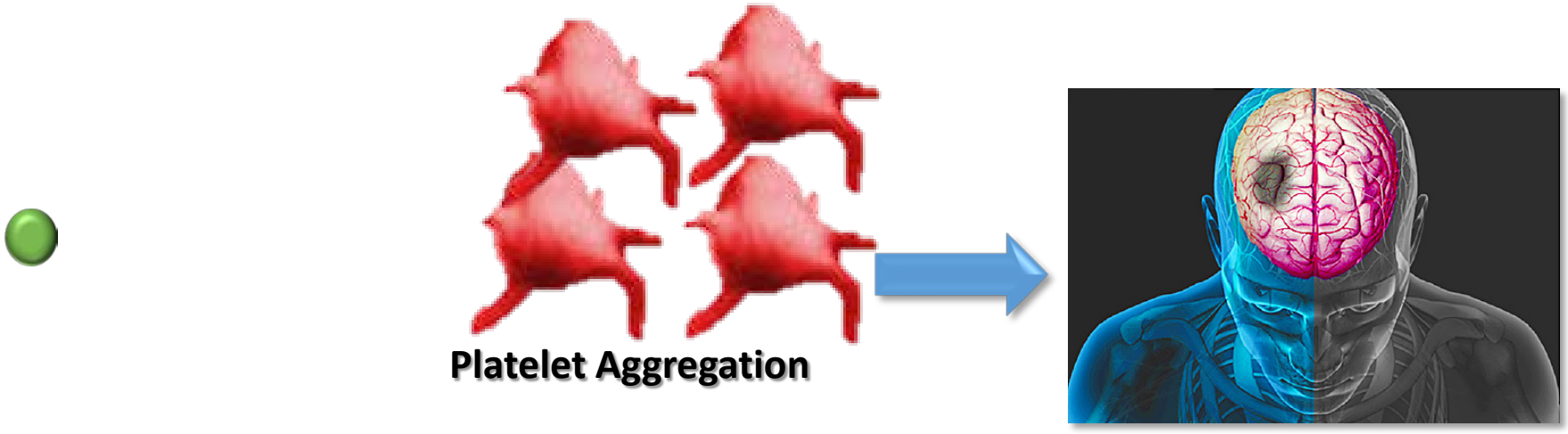

Extracellular histones are major mediators of death in sepsis
Xu et al. Nature Medicine 15, 1318 - 1321 (2009)

Role of extracellular histones in the cardiomyopathy of sepsis
Kalbitz et al. The FASEB Journal *vol. 29 no. 5 2185-2193*

Extracellular histones promote thrombin generation through platelet-dependent mechanisms: involvement of platelet TLR2 and TLR4
Semeraro et al. Blood 2011 118:1952-1961

Histones induce rapid and profound thrombocytopenia in mice
Fuchs et al. Blood 2011 118:3708-3714

Extracellular histones neutralizing agents

We will test the *hypothesis* that neutralization of extracellular histones with RNA aptamers can prevent the morbidity and mortality associated with critical illnesses

Sepsis & Trauma

Extracellular Histones

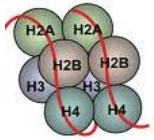

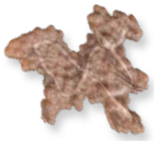

RNA aptamer

Identification of histone aptamers

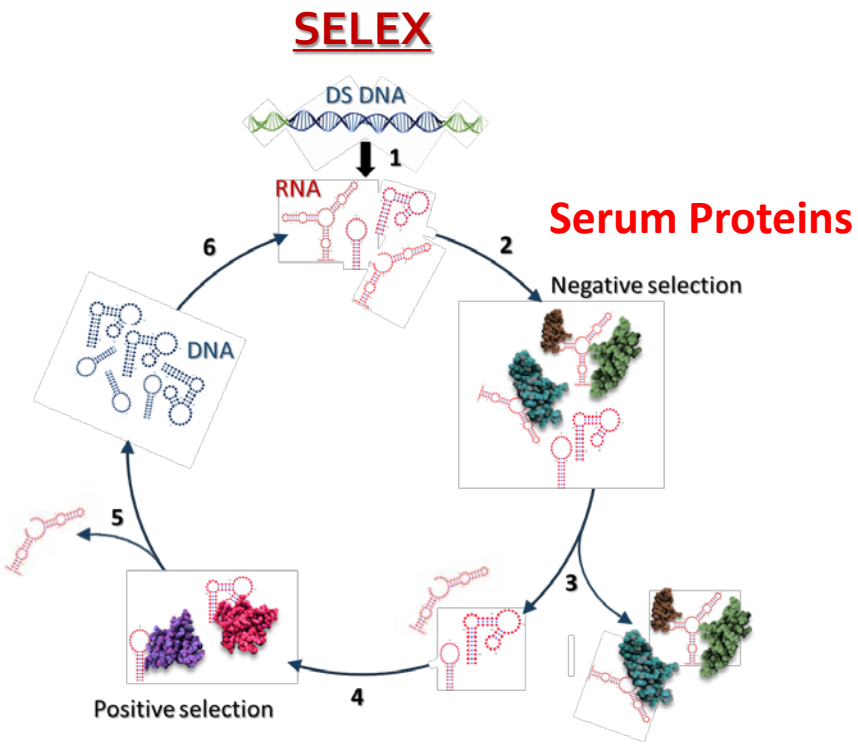

Histone H3 & H4

Histone aptamer selection specificity

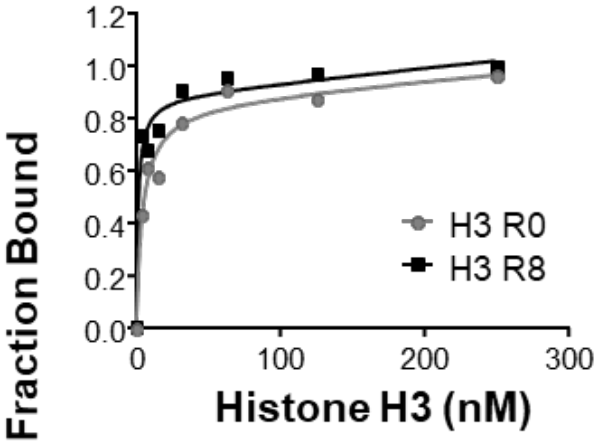

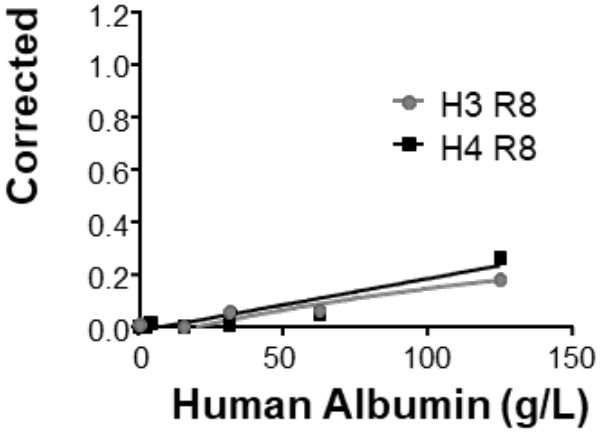

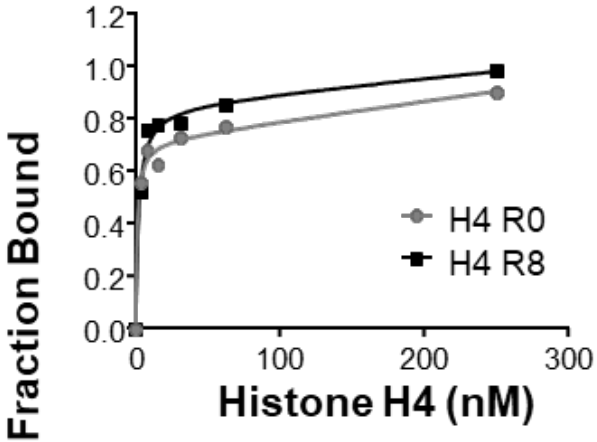

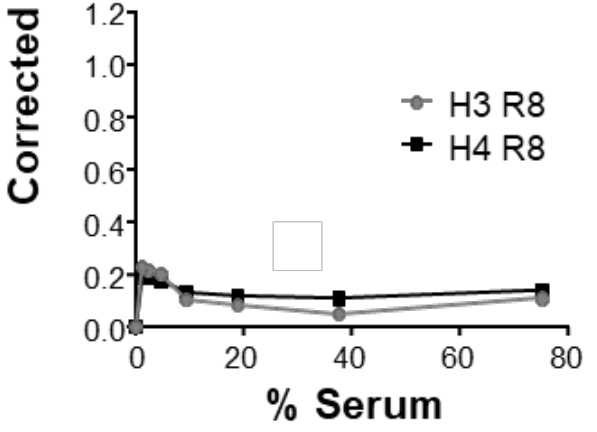

Identification of histone aptamers

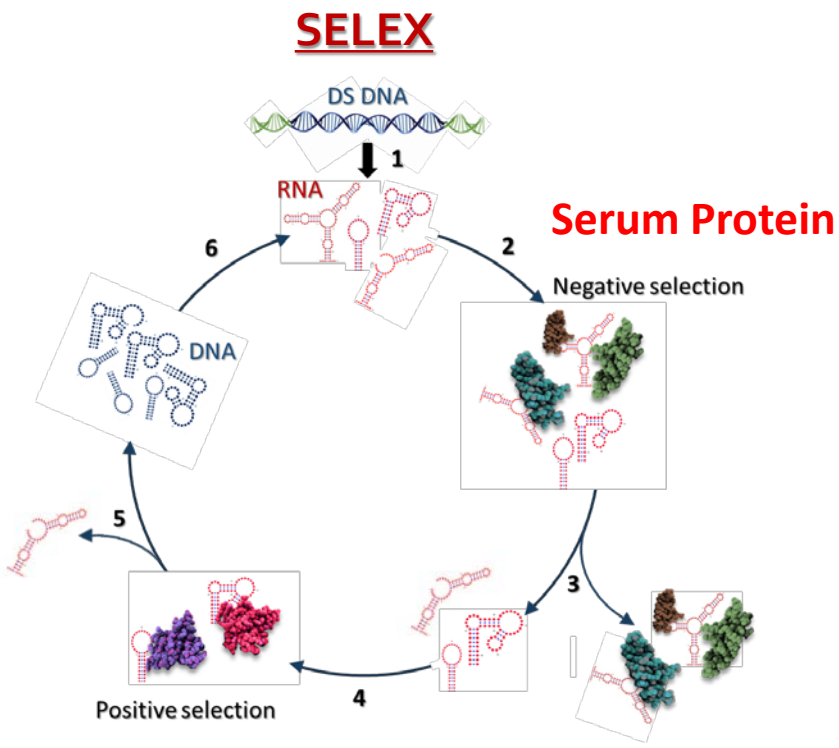

Histone H3 & H4

Histone aptamer stability

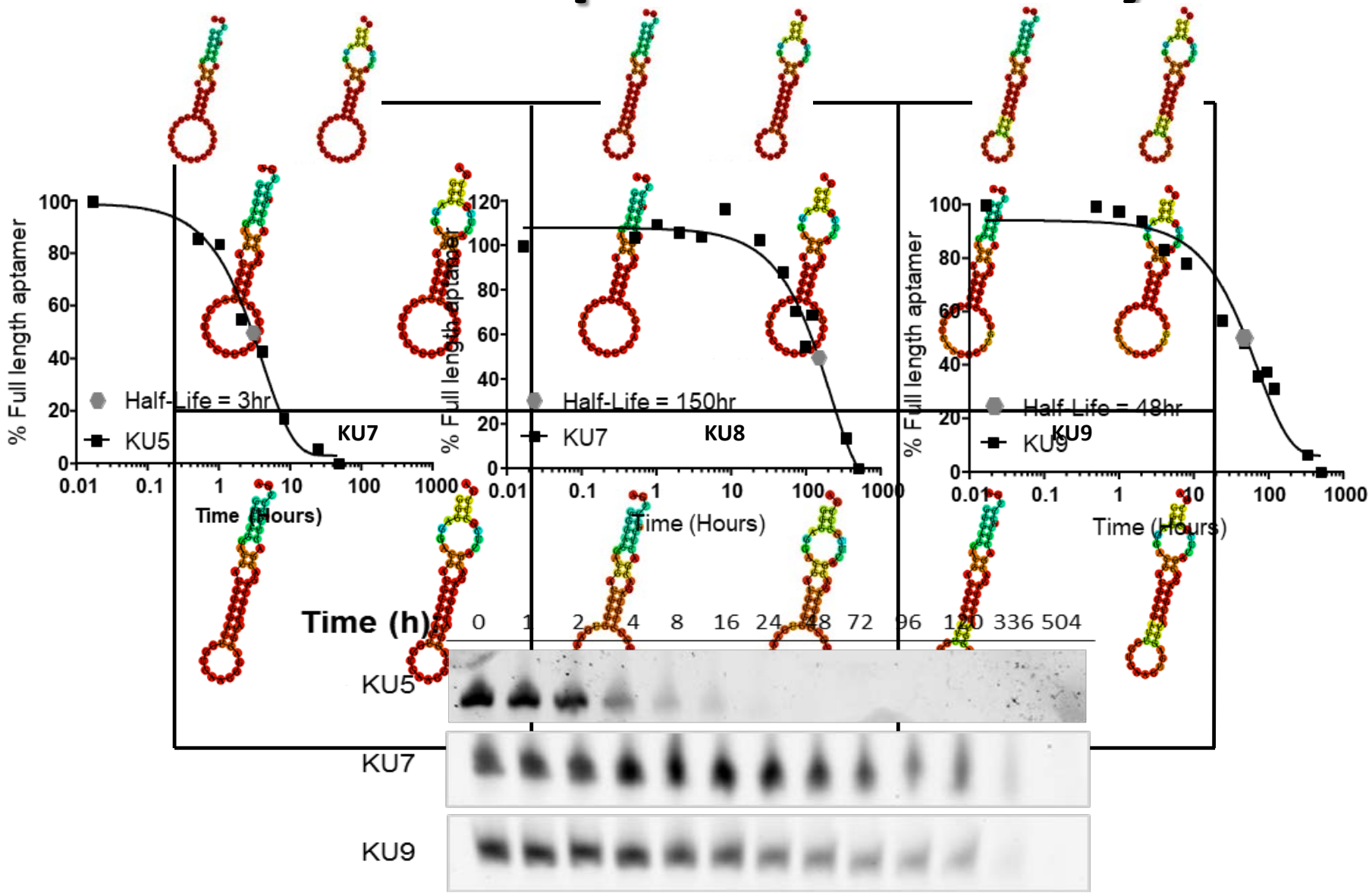

Histone aptamer specificity

Surface Plasmon Resonance

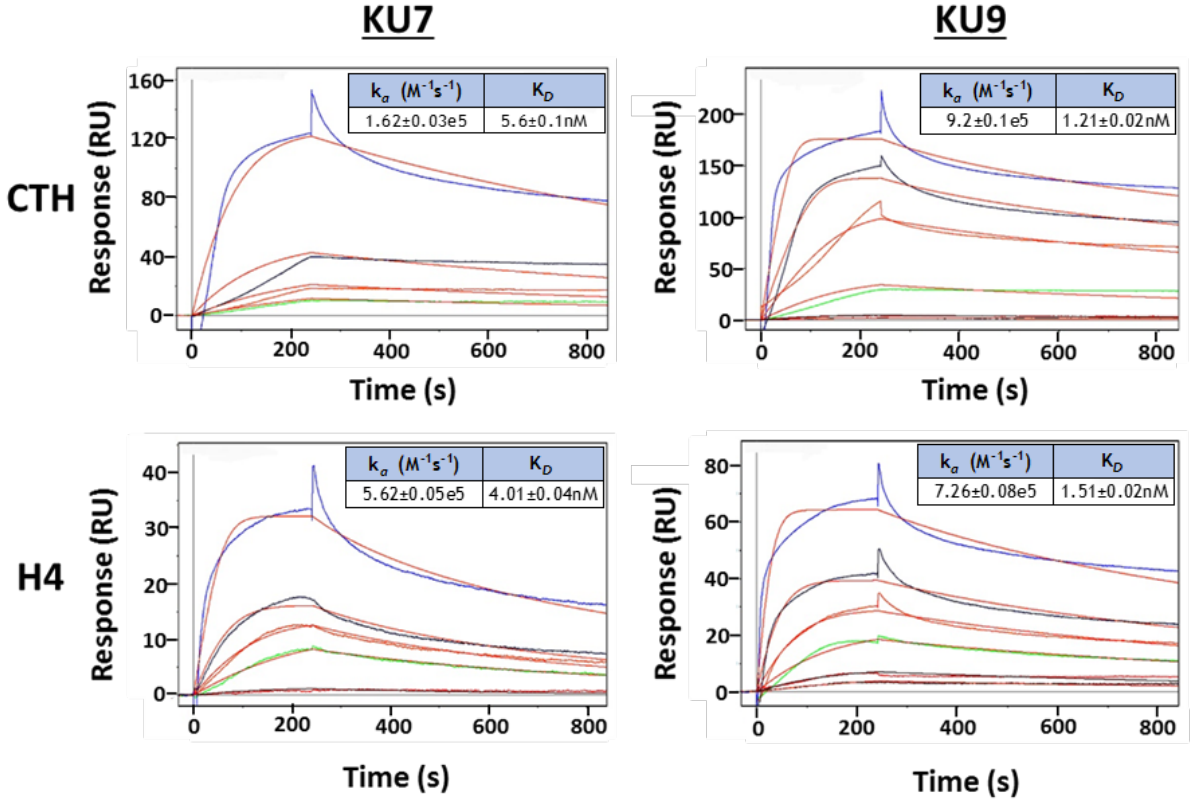

Aptamers inhibit histone-mediated Calcium Influx

Fura-2

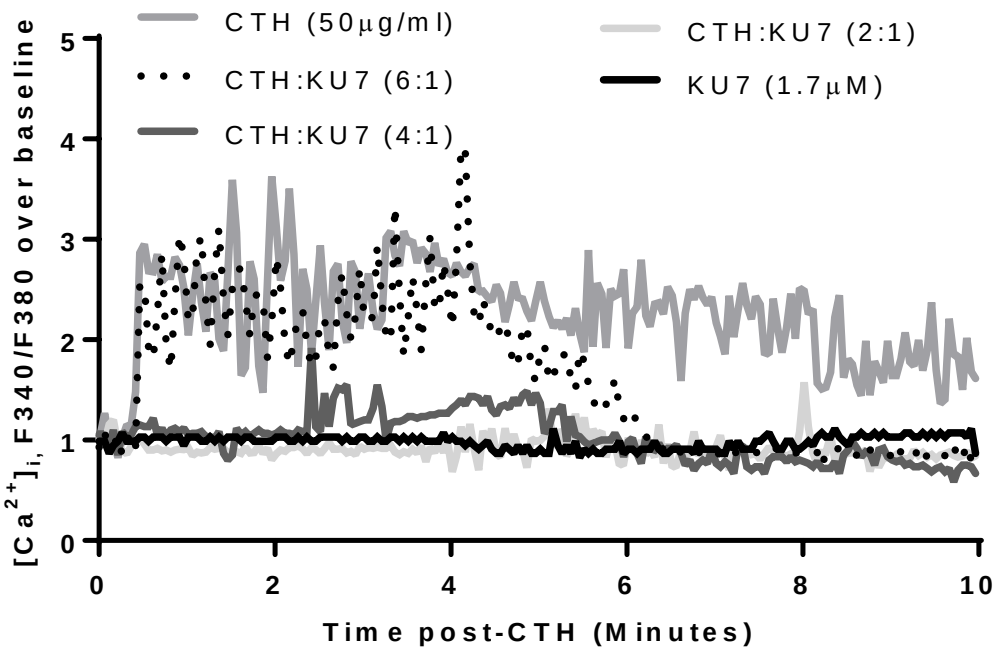

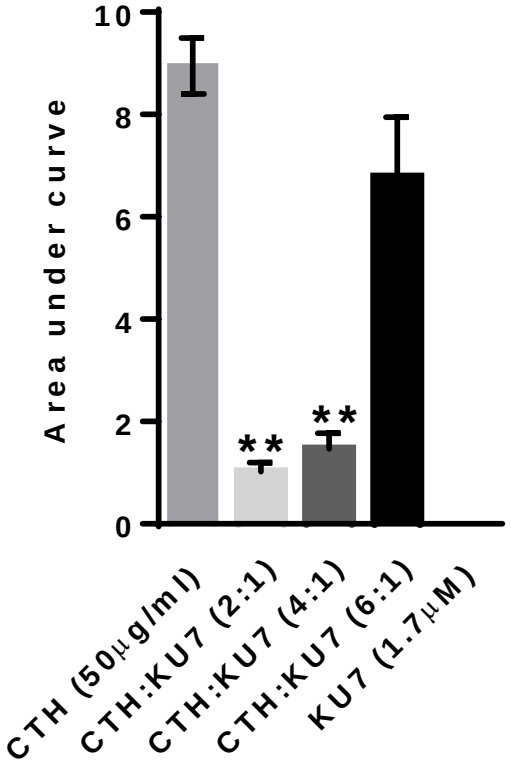

Aptamers inhibit histone-mediated Il-6 production

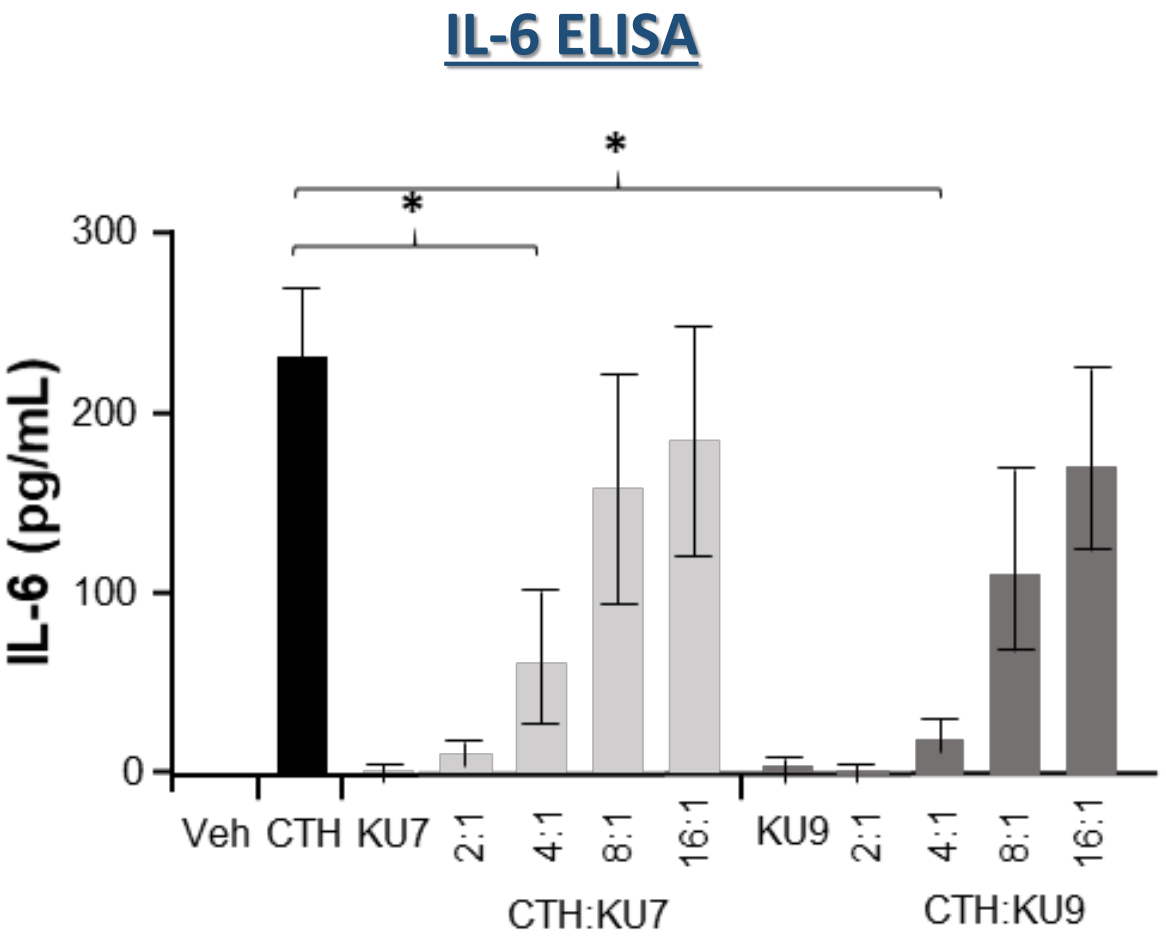

Aptamers inhibit histone-mediated platelet aggregation

Light transmission aggregometry

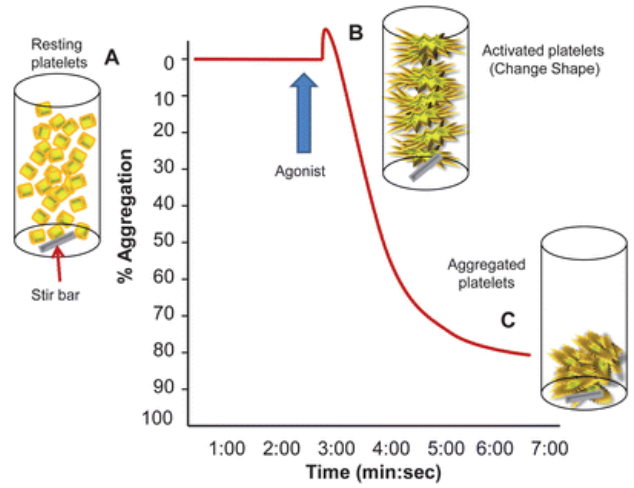

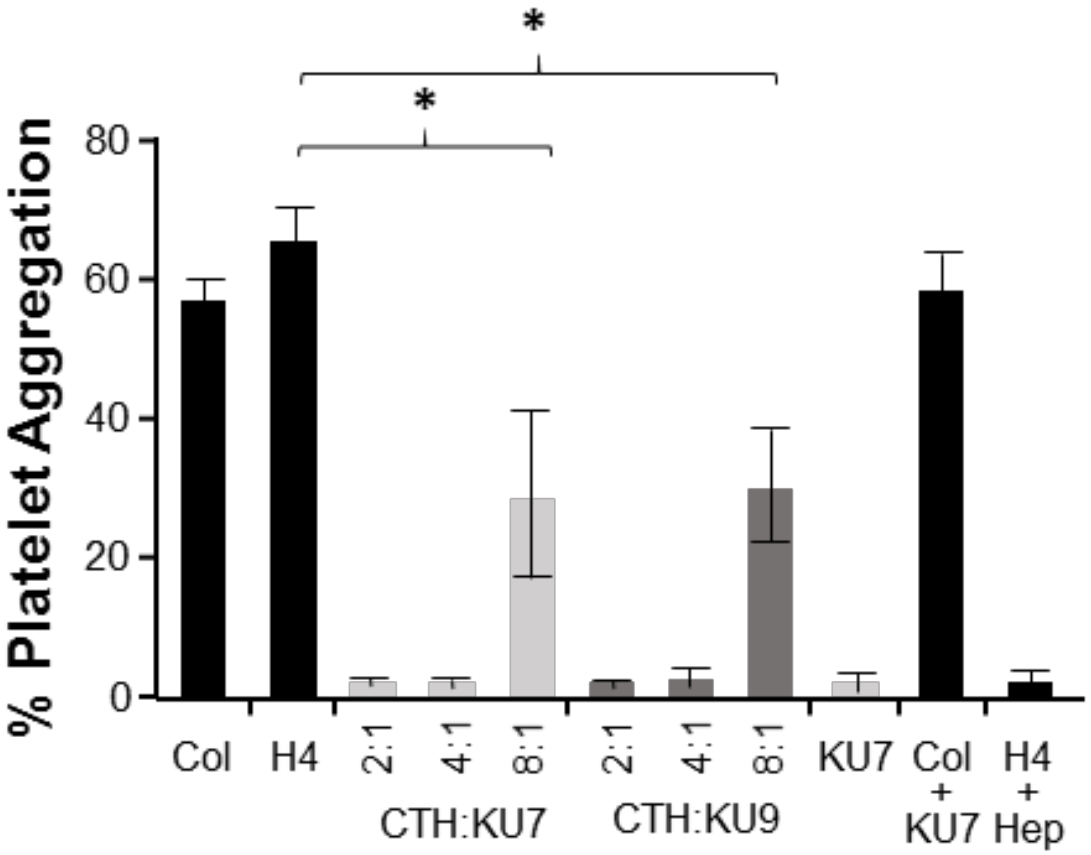

Aptamers inhibit histone-mediated cell toxicity

MTS assay

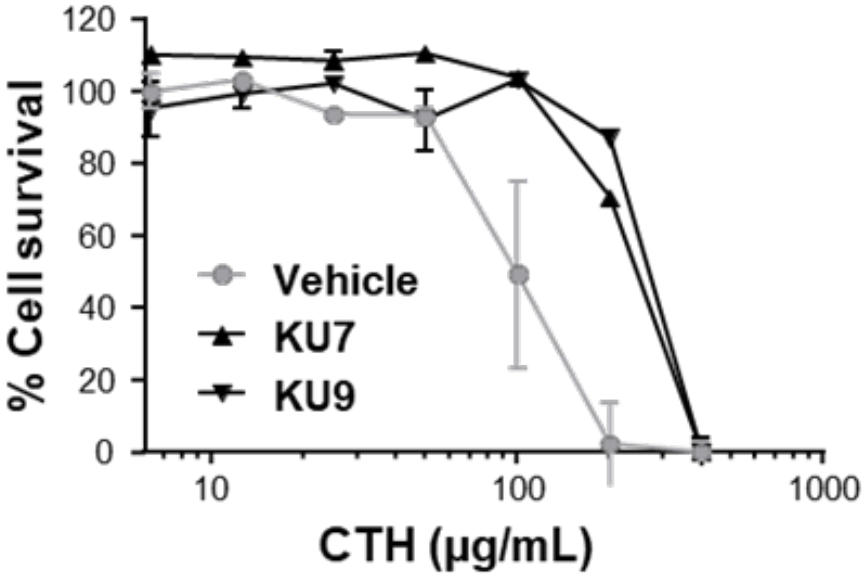

Efficacy of histone aptamers in murine MODS model

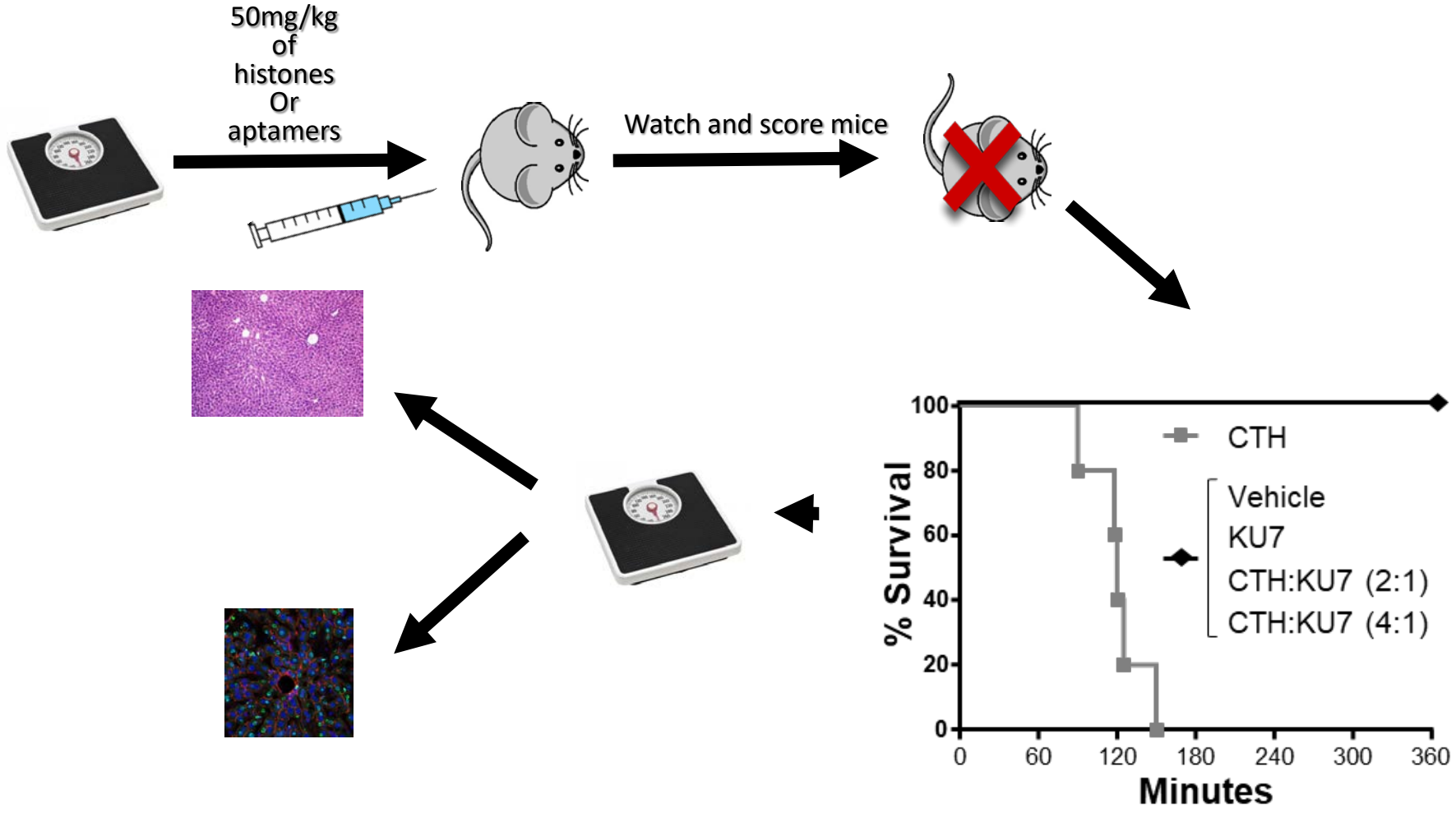

Efficacy of histone aptamers in murine MODS model

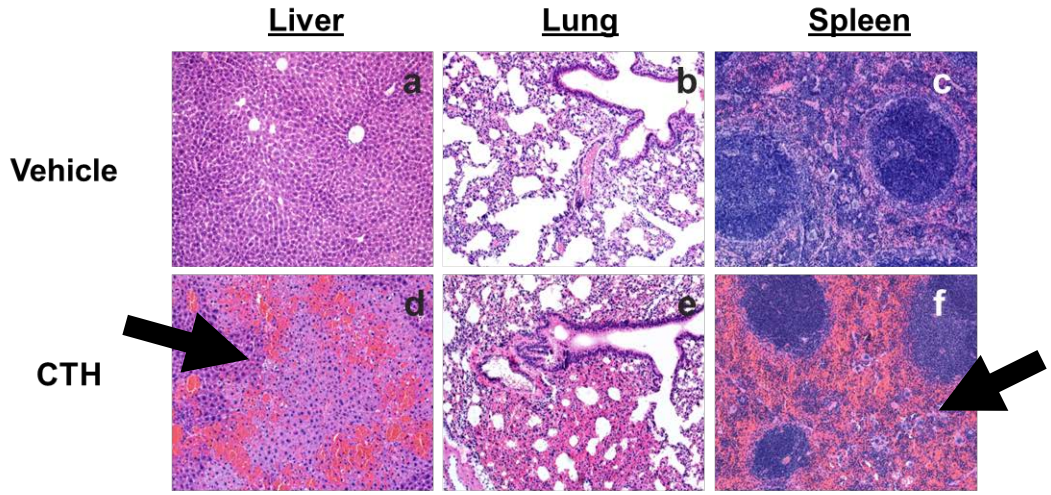

Efficacy of histone aptamers in murine MODS model

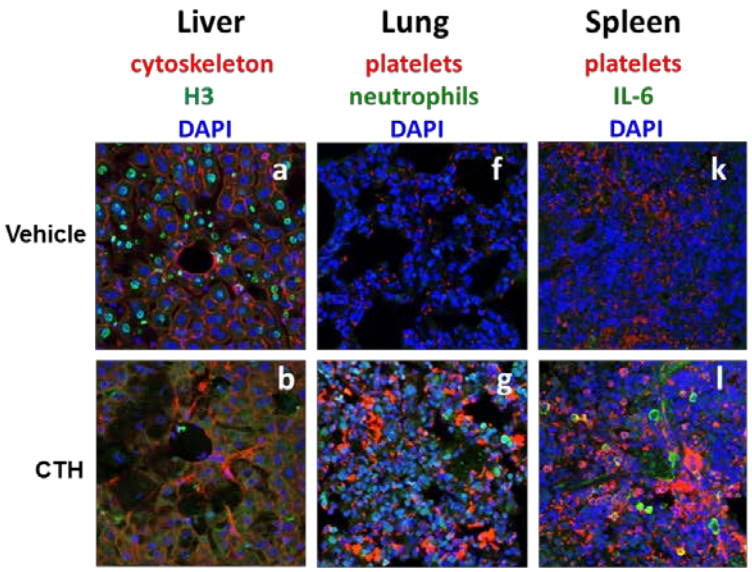

Conclusions

Development of histone aptamers protects from histone-mediated:

- Cell toxicity
- Calcium influx
- Platelet aggregation
- IL-6 production
- Organ dysfunction
- Death

Aptamers inhibit histone-mediated cell toxicity in a time dependent manner

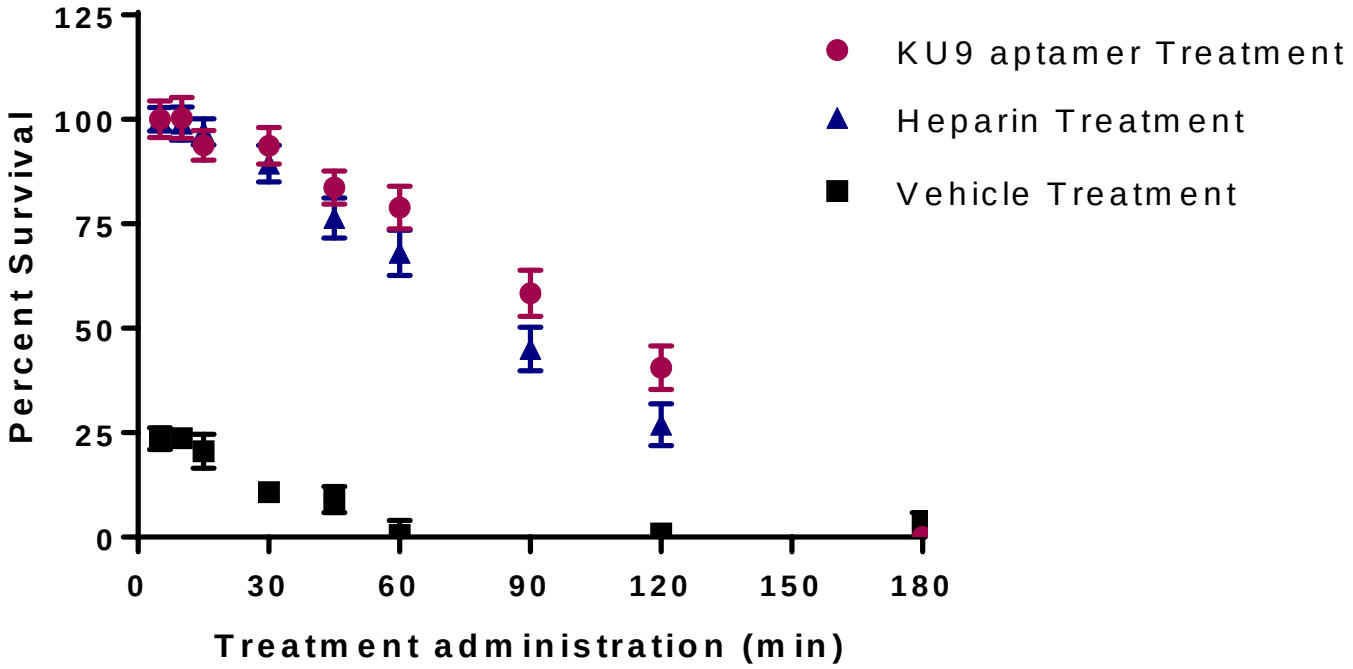

Toxicology screen for aptamers safety

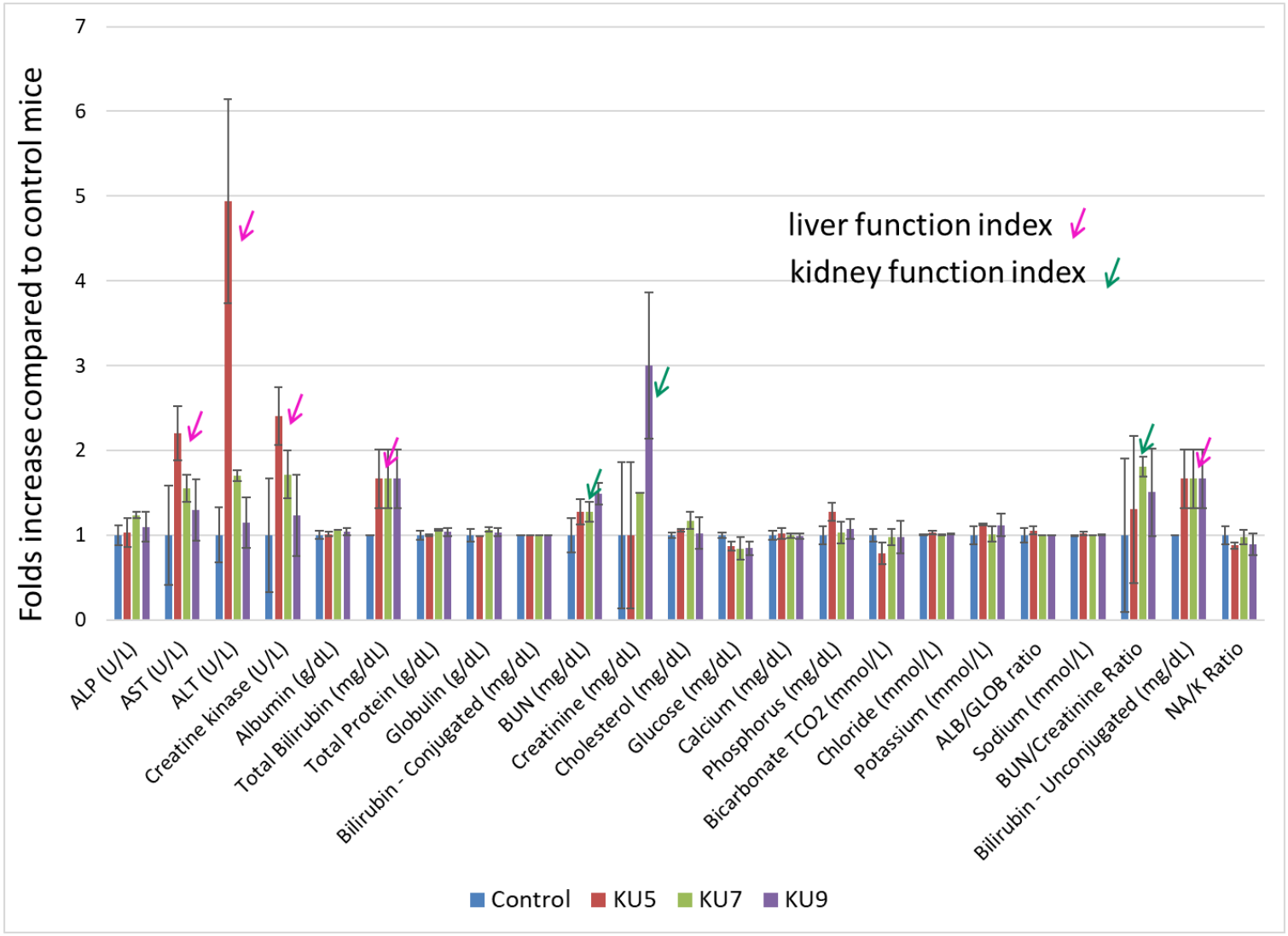

Extracellular histones are present in CLP mice

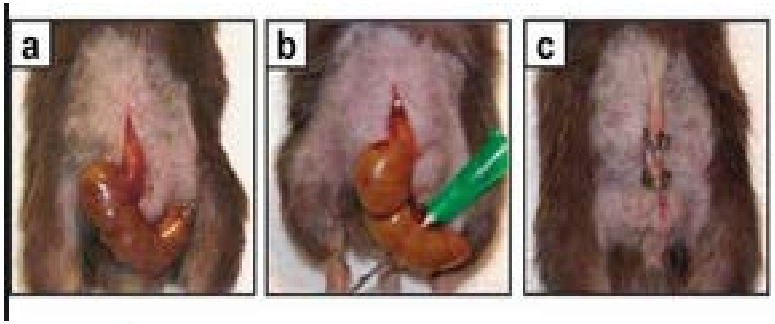

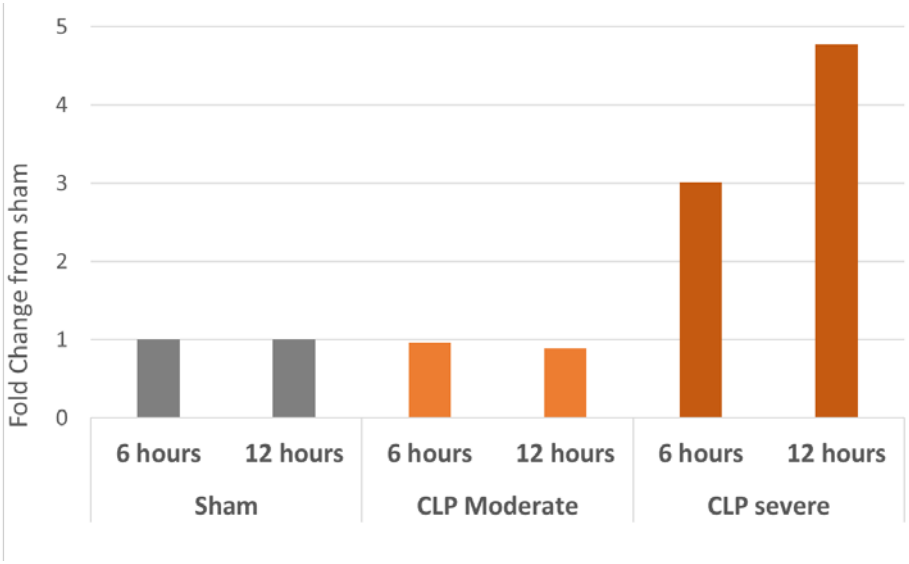

Future Directions

- Relevant animal models
- Collect human samples to determine histone levels
- Safety
- Pharmacokinetics

THANK YOU!

Giangrande Lab

Giselle Blanco
Justin Dassie
David Dickey
Luiza Hernandez
Craig Howell
Sven Kruspe
Li-Hsien Lin
Xiu Ying (Lisa) Liu
William Rockey
Kristina Wyatt Thiel
William Thiel
Gregory Thomas
Ofonime Udofot
Ryan Whitaker

U Iowa

Vladimir Badovinac
Kent Choi
Julia Klesney-Tait
Patrick McGonagill
David Meyerholz
Sanjana Dayal
Francis Miller

IDT Inc.

Mark Behlke

TriLink

Anton McCaffrey
Richard Hogrefe

Thesis Committee

James McNamara
Kathrine Musselman
Adam Dupey
Mary Wilson

MCB program

Fredrick Domann
Paulette Villhauer

ELSA U. PARDEE FOUNDATION

THE UNIVERSITY OF IOWA
PRESIDENTIAL BIOLOGICAL SCHOLAR PROGRAM

Questions?

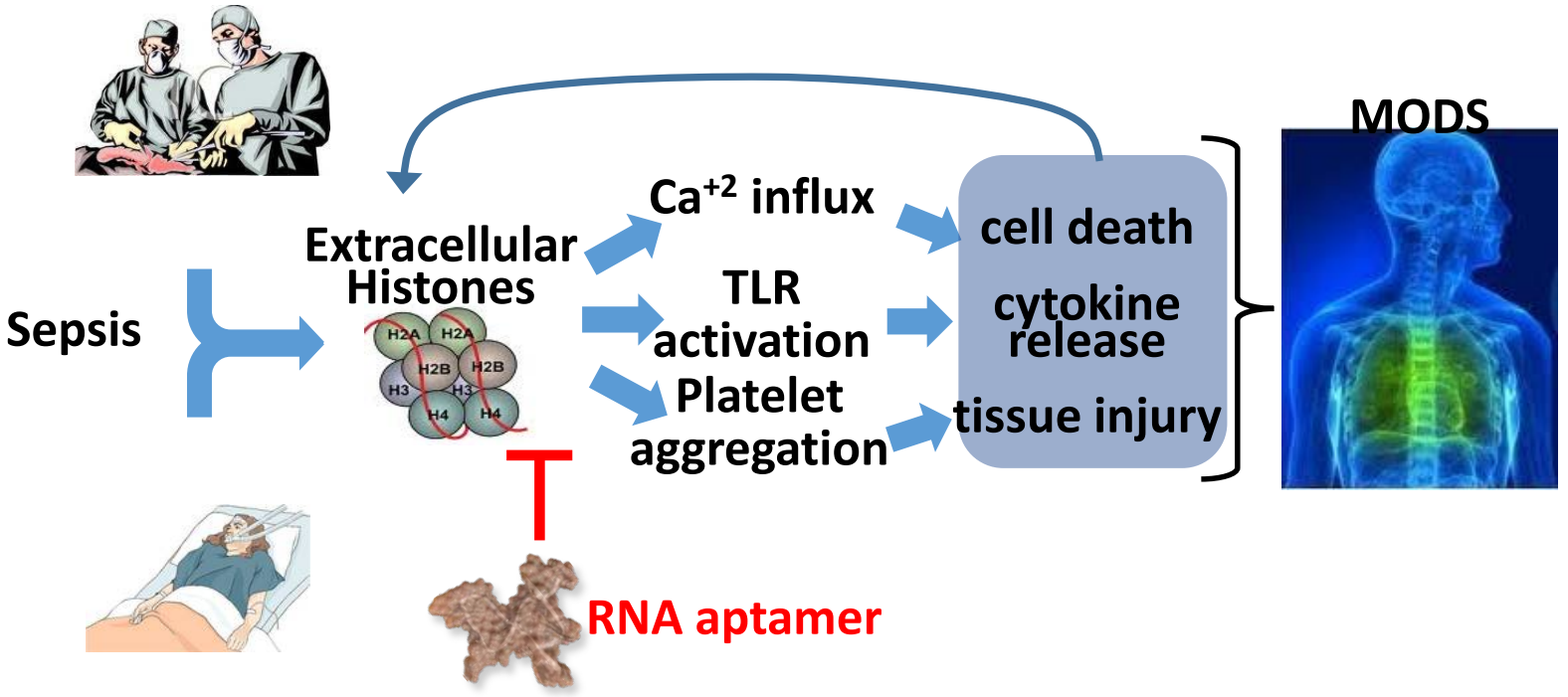
Sepsis
Extracellular Histones
H2A
H2A
H2B
H2B
H3
H3
H4
H4
Ca+2 influx
TLR activation
Platelet aggregation
cell death
cytokine release
tissue injury
MODS
RNA aptamer

RNA Inhibitors of Nuclear Proteins Implicated in Multiple Organ Dysfunction Syndrome

Kevin Urak

Grand Rounds 2018

Canonical function of histones

Infection

Trauma

Poor life choices

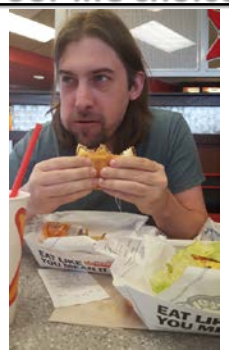

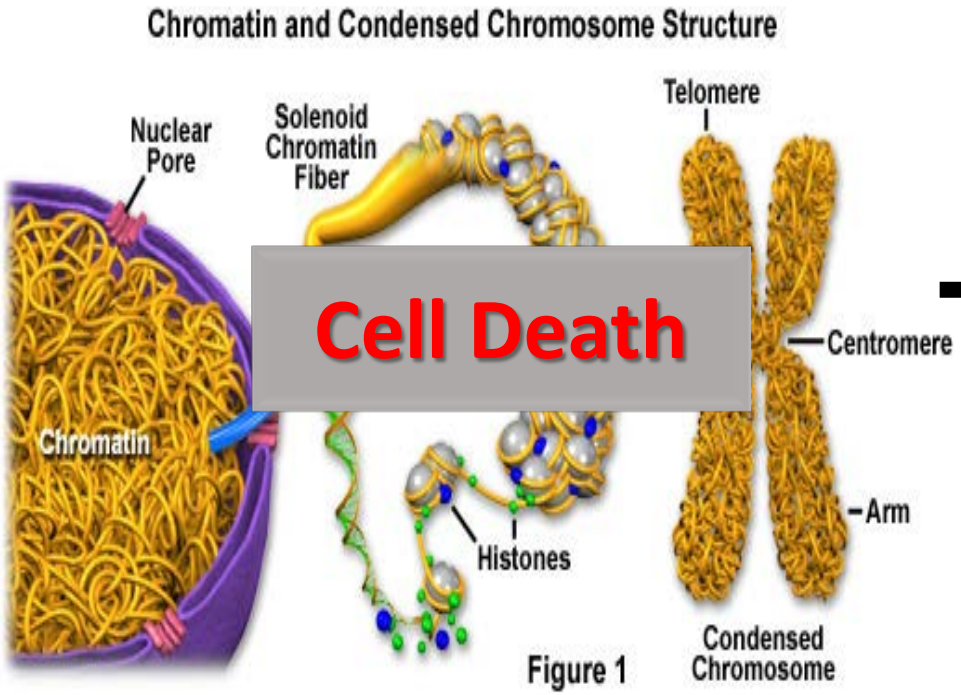

Cell Death

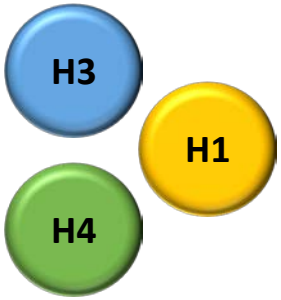

Problems with extracellular histones

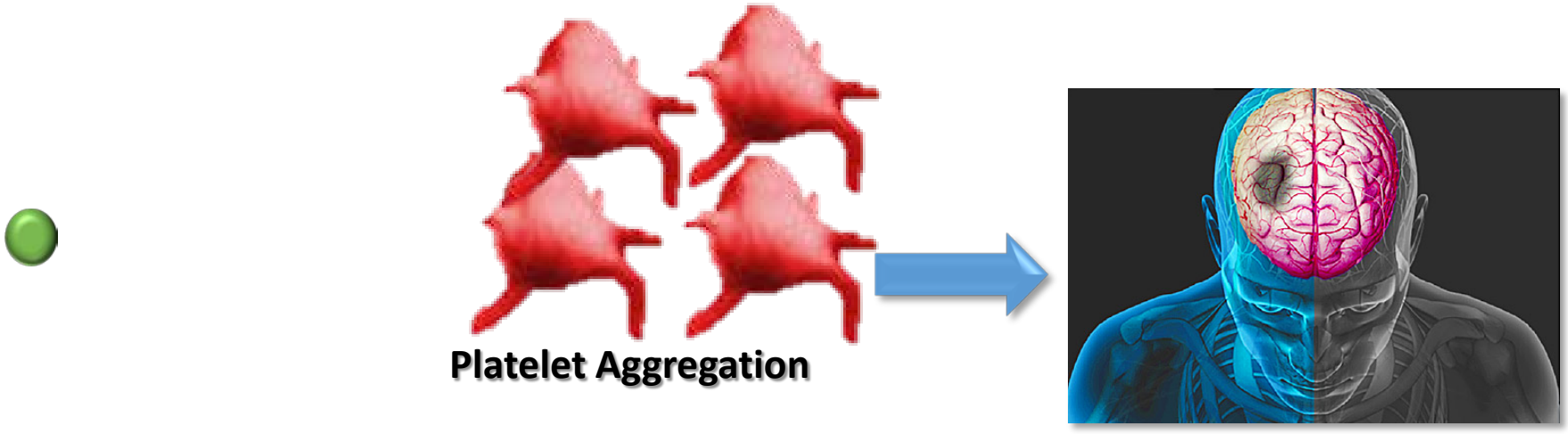

Extracellular histones are major mediators of death in sepsis
Xu et al. Nature Medicine 15, 1318 - 1321 (2009)

Role of extracellular histones in the cardiomyopathy of sepsis
Kalbitz et al. The FASEB Journal *vol. 29 no. 5 2185-2193*

Extracellular histones promote thrombin generation through platelet-dependent mechanisms: involvement of platelet TLR2 and TLR4
Semeraro et al. Blood 2011 118:1952-1961

Histones induce rapid and profound thrombocytopenia in mice
Fuchs et al. Blood 2011 118:3708-3714

Extracellular histones neutralizing agents

We will test the *hypothesis* that neutralization of extracellular histones with RNA aptamers can prevent the morbidity and mortality associated with critical illnesses

Sepsis & Trauma

Extracellular Histones

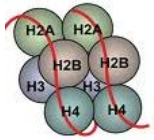

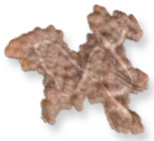

RNA aptamer

Identification of histone aptamers

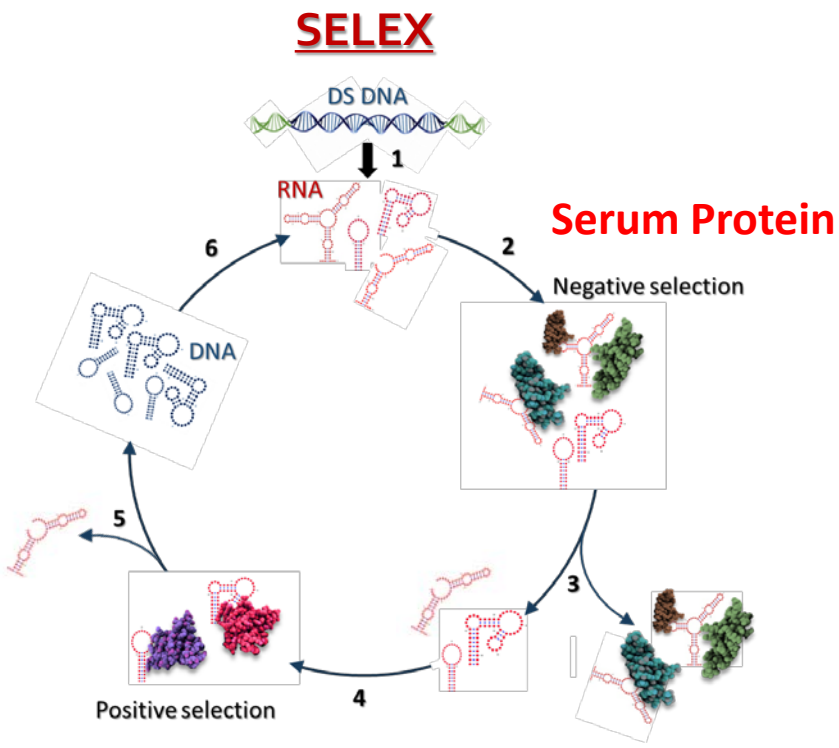

Histone H3 & H4

Histone aptamer specificity

Surface Plasmon Resonance

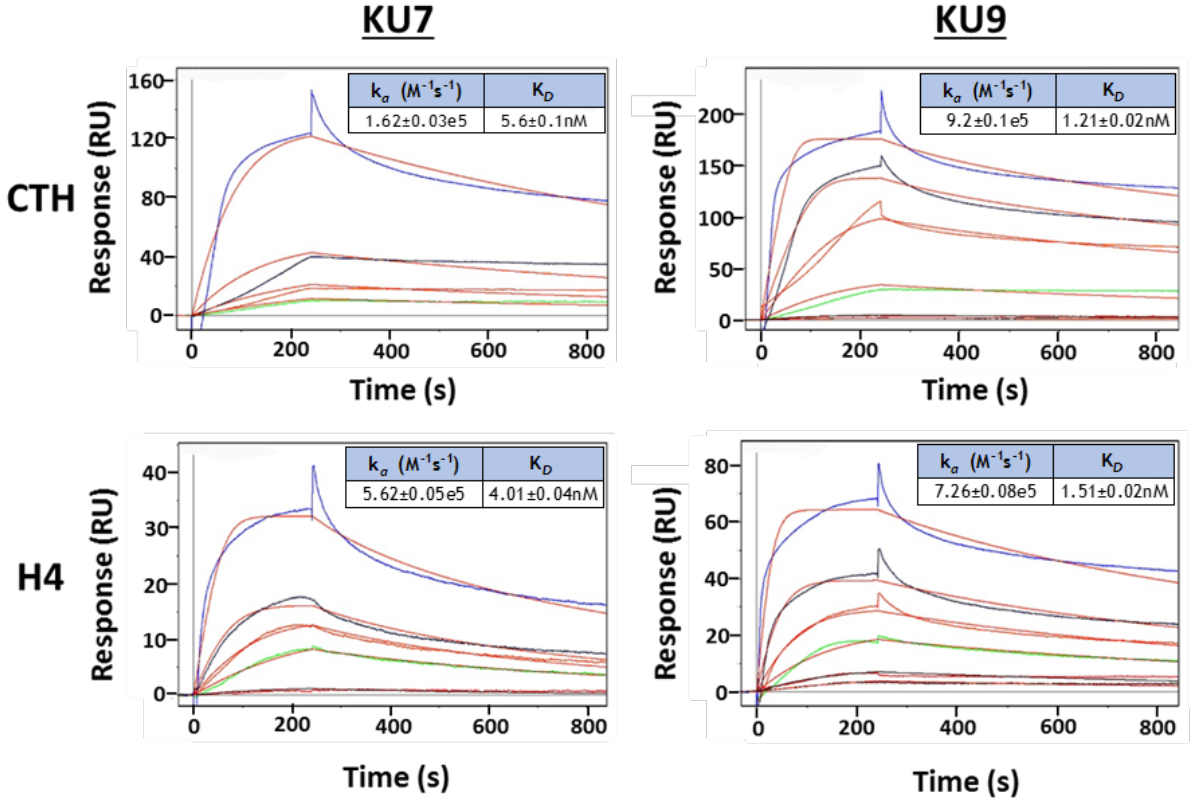

Aptamers inhibit histone-mediated Calcium Influx

Fura-2

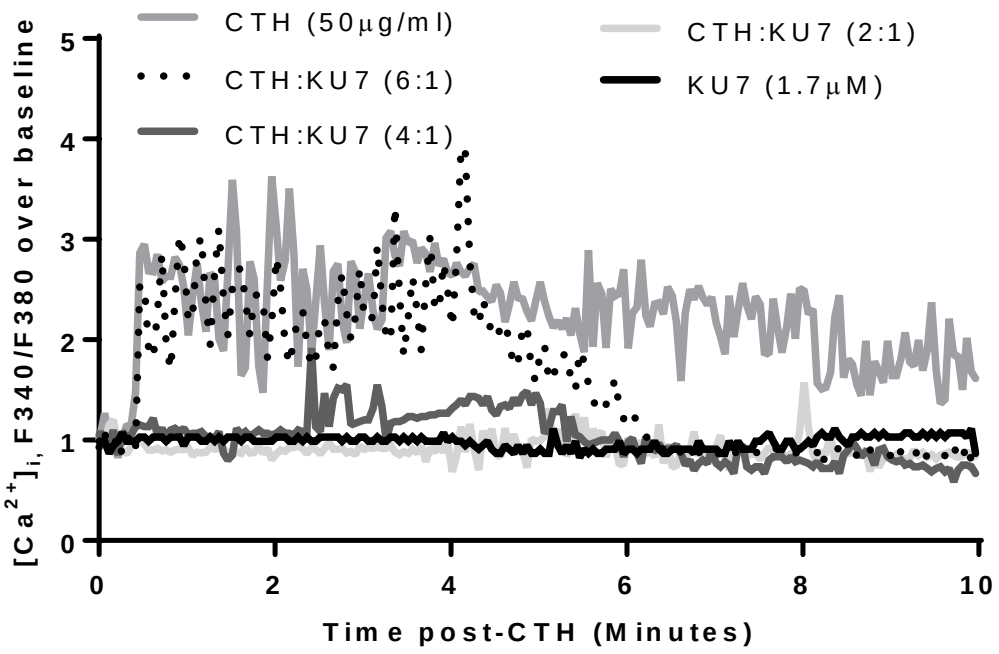

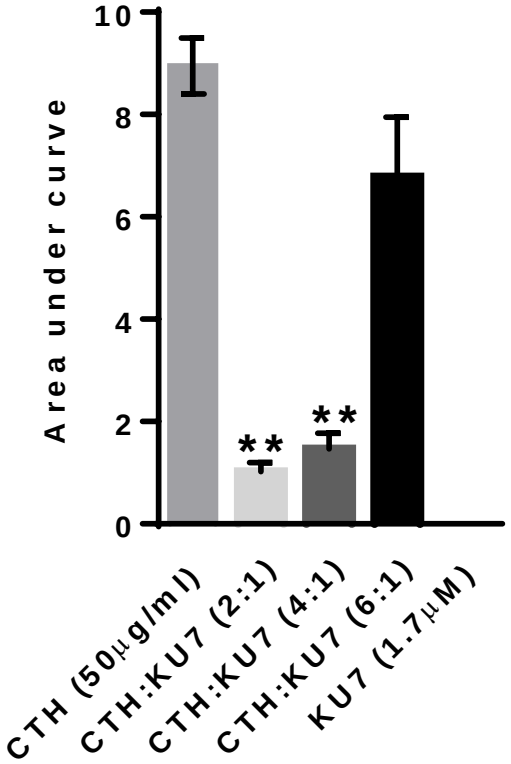

Aptamers inhibit histone-mediated Il-6 production

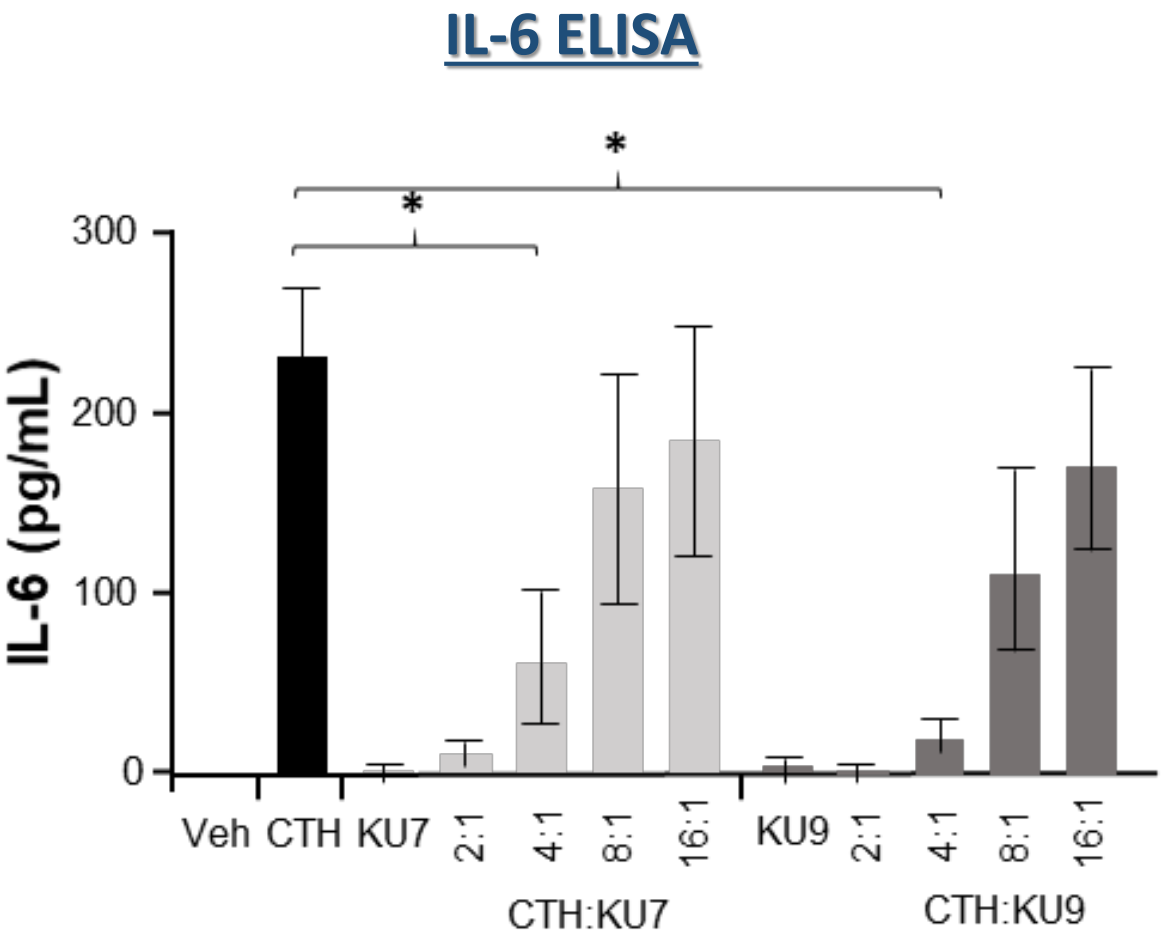

Aptamers inhibit histone-mediated platelet aggregation

Light transmission aggregometry

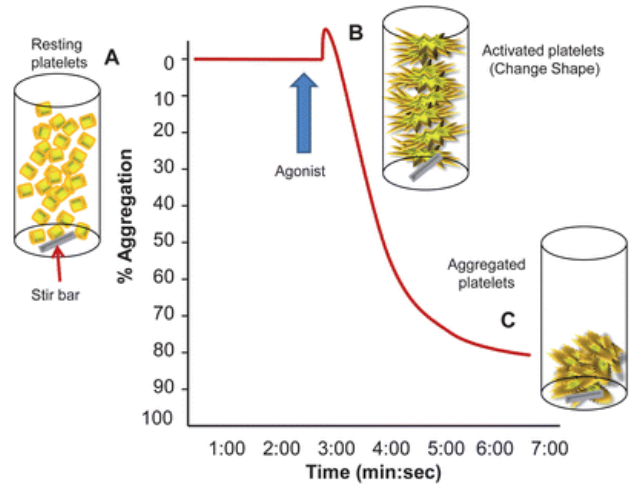

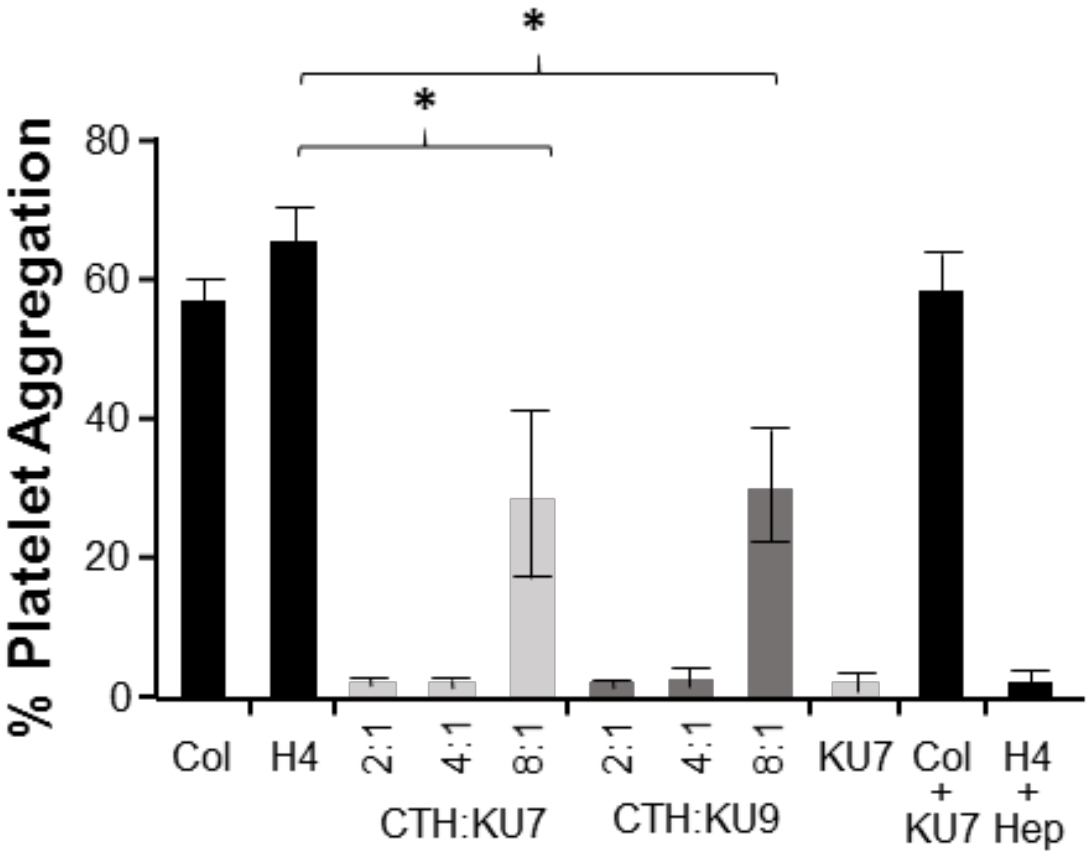

Aptamers inhibit histone-mediated cell toxicity

MTS assay

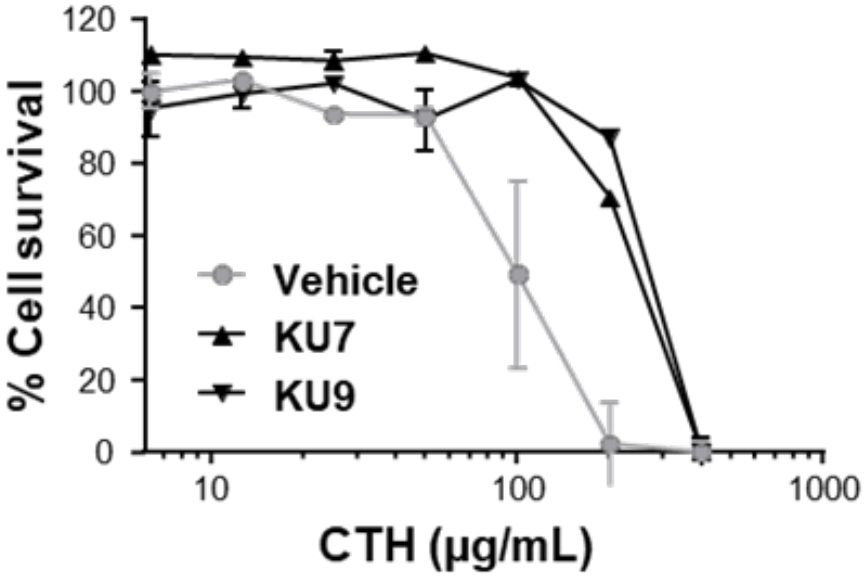

Efficacy of histone aptamers in murine MODS model

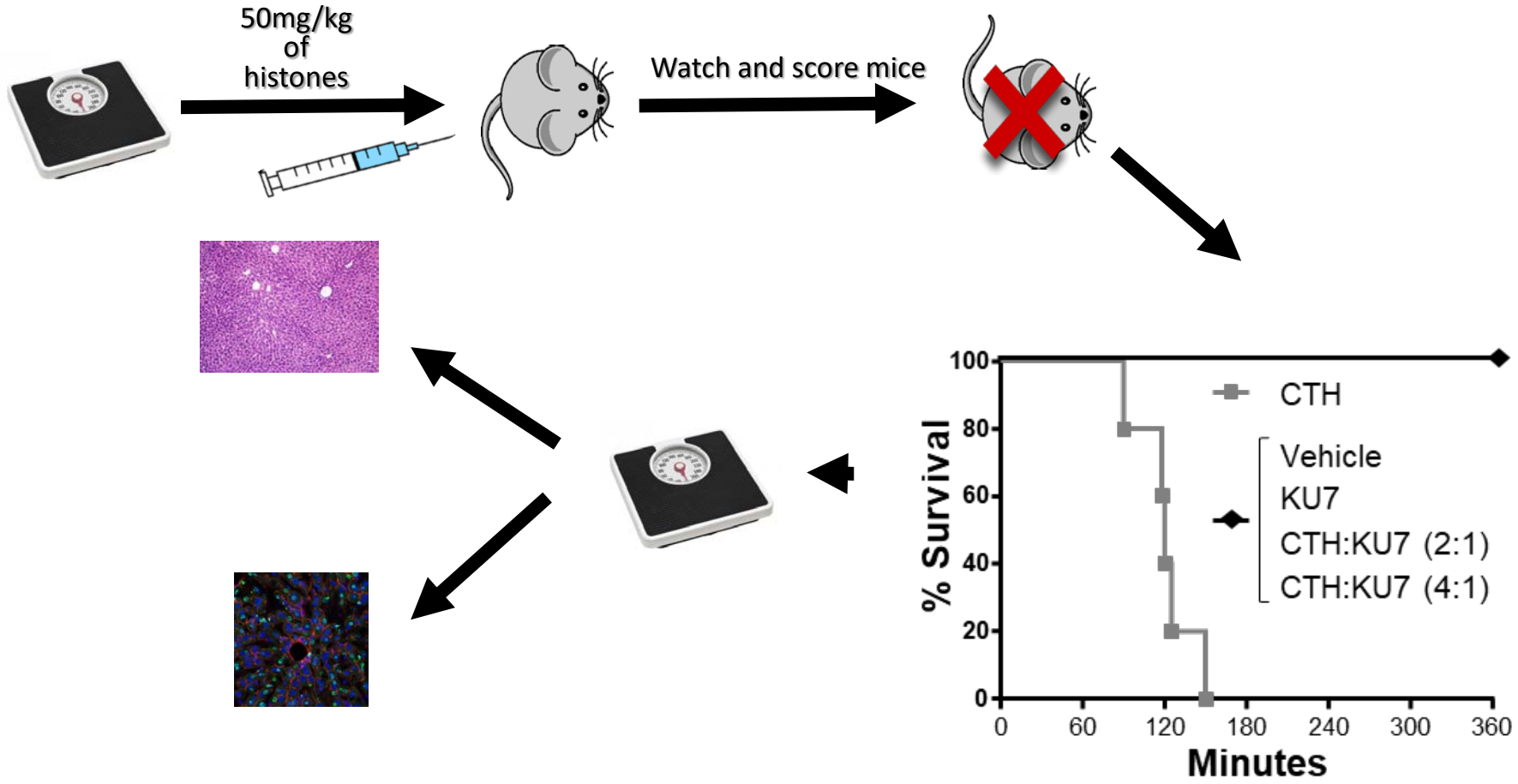

Efficacy of histone aptamers in murine MODS model

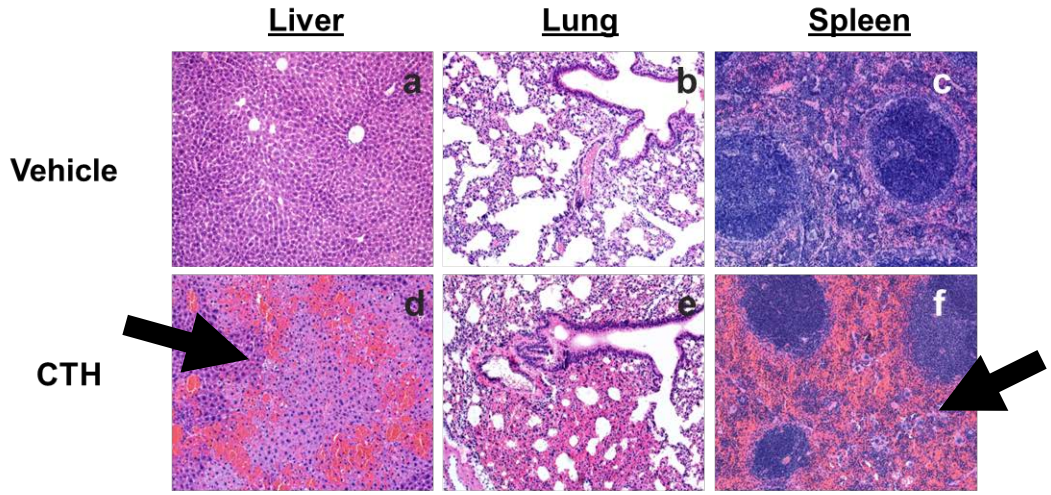

Efficacy of histone aptamers in murine MODS model

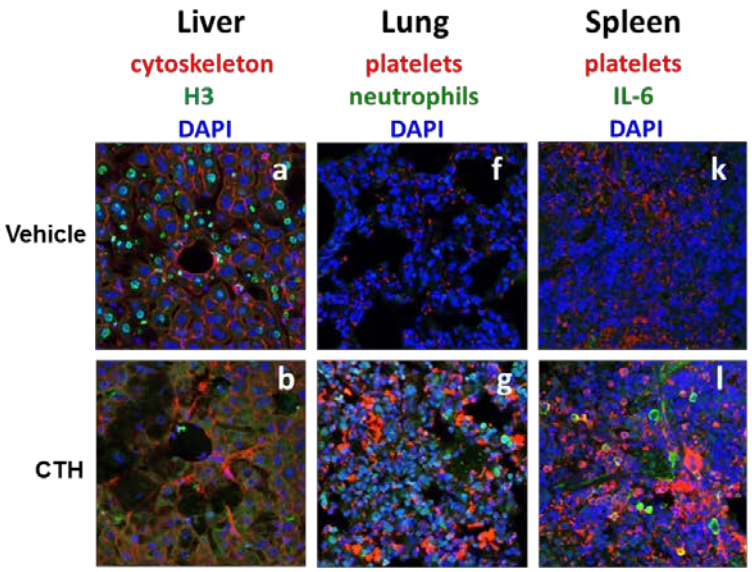

Future Directions

- Relevant animal models
- Collect human samples to determine histone levels
- Safety
- Pharmacokinetics

THANK YOU!

Giangrande Lab

Giselle Blanco
Justin Dassie
David Dickey
Luiza Hernandez
Craig Howell
Sven Kruspe
Li-Hsien Lin
Xiu Ying (Lisa) Liu
William Rockey
Kristina Wyatt Thiel
William Thiel
Gregory Thomas
Ofonime Udofot
Ryan Whitaker

U Iowa

Vladimir Badovinac
Kent Choi
Julia Klesney-Tait
Patrick McGonagill
David Meyerholz
Sanjana Dayal
Francis Miller

IDT Inc.

Mark Behlke

TriLink

Anton McCaffrey
Richard Hogrefe

Thesis Committee

James McNamara
Kathrine Musselman
Adam Dupey
Mary Wilson

MCB program

Fredrick Domann
Paulette Villhauer

ELSA U. PARDEE FOUNDATION

THE UNIVERSITY OF IOWA
PRESIDENTIAL BIOLOGICAL SCHOLAR PROGRAM

Questions?

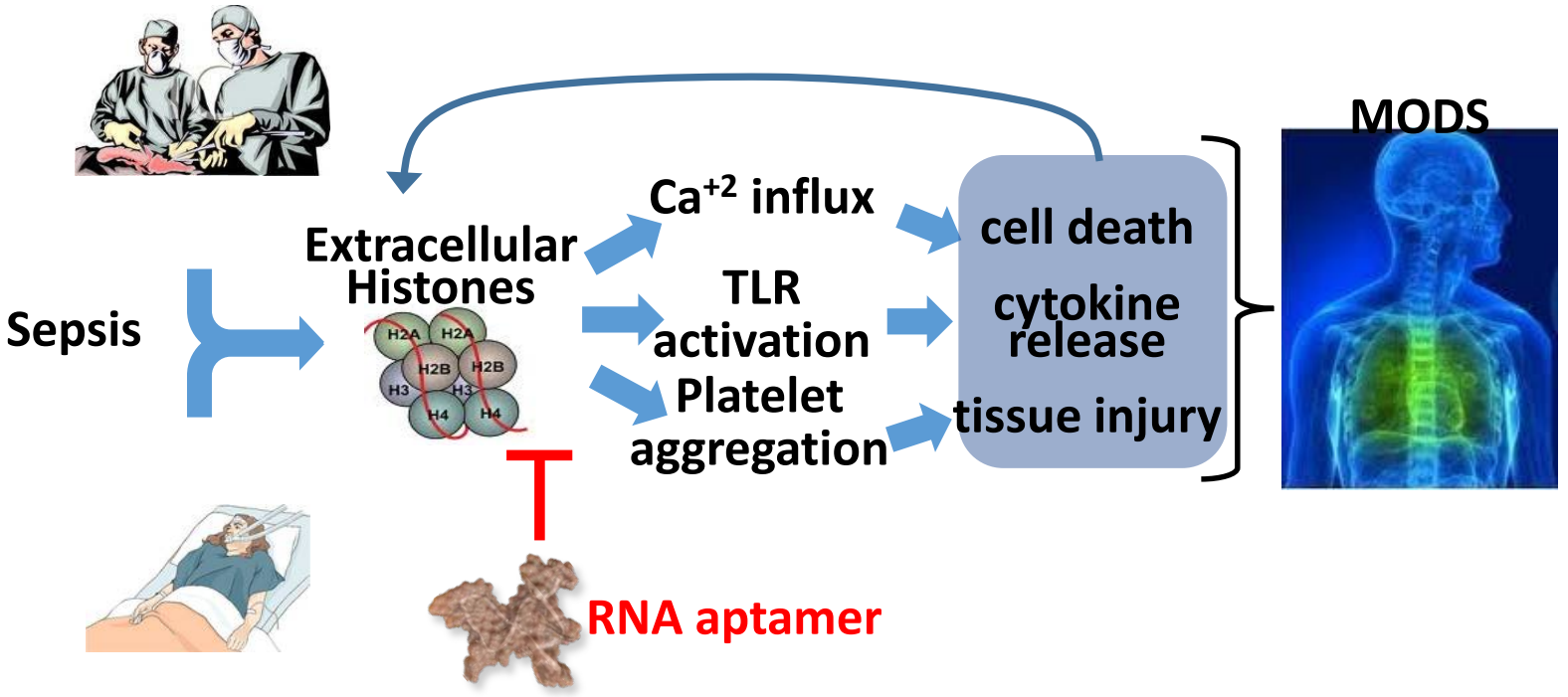
Sepsis
Extracellular Histones
H2A
H2A
H2B
H2B
H3
H3
H4
H4
Ca+2 influx
TLR activation
Platelet aggregation
cell death
cytokine release
tissue injury
MODS
RNA aptamer

RNA Inhibitors of Nuclear Proteins Implicated in Multiple Organ Dysfunction Syndrome

Kevin Urak

ASGCT 20018

5/16/2018

Canonical function of histones

Infection

Trauma

Poor life choices

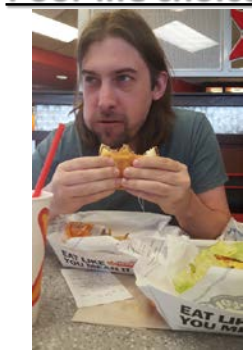

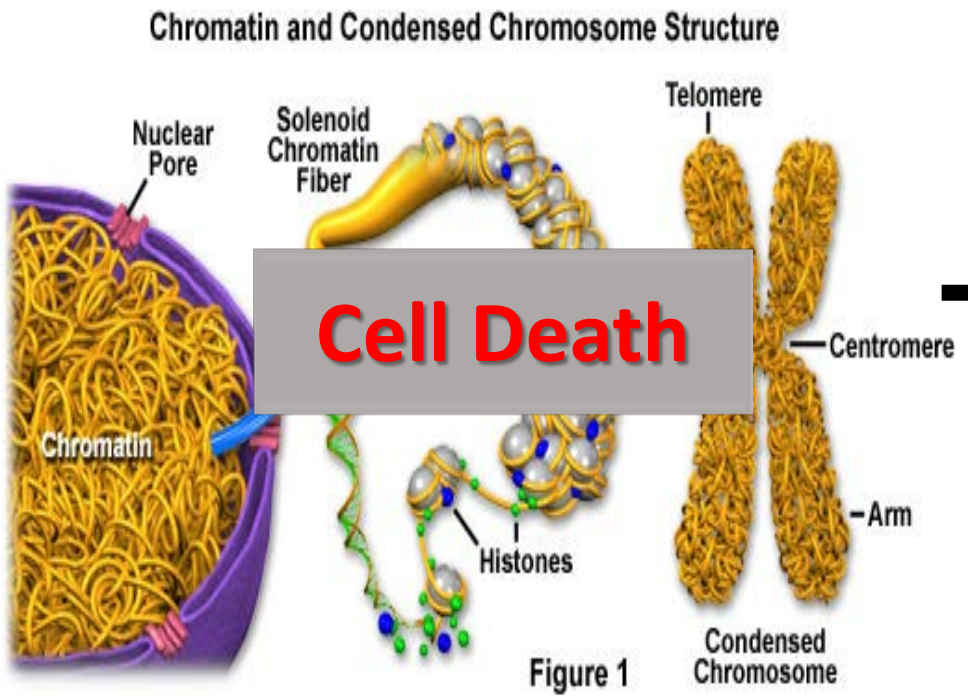

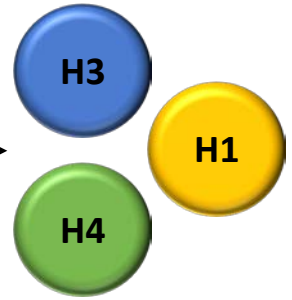

Problems with extracellular histones

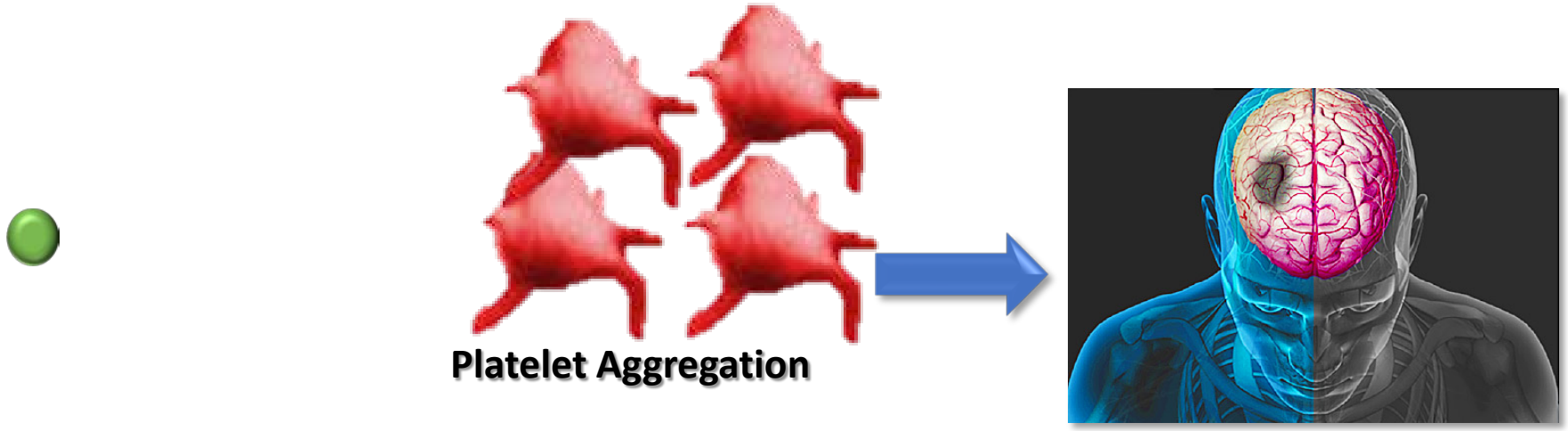

Extracellular histones are major mediators of death in sepsis
Xu et al. Nature Medicine 15, 1318 - 1321 (2009)

Role of extracellular histones in the cardiomyopathy of sepsis
Kalbitz et al. The FASEB Journal *vol. 29 no. 5 2185-2193*

Extracellular histones promote thrombin generation through platelet-dependent mechanisms: involvement of platelet TLR2 and TLR4
Semeraro et al. Blood 2011 118:1952-1961

Histones induce rapid and profound thrombocytopenia in mice
Fuchs et al. Blood 2011 118:3708-3714

Extracellular histones neutralizing agents

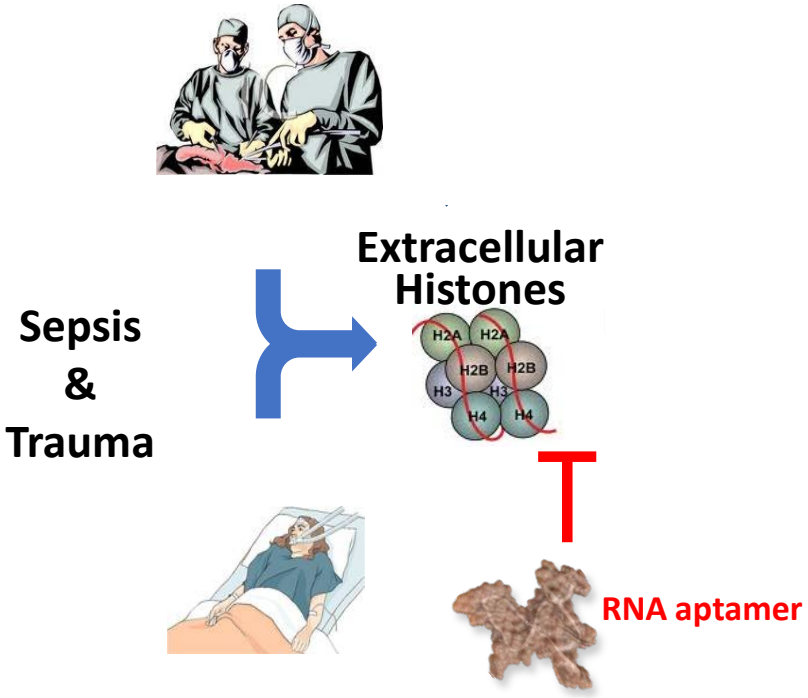

Identification of histone aptamers

Surface Plasmon Resonance

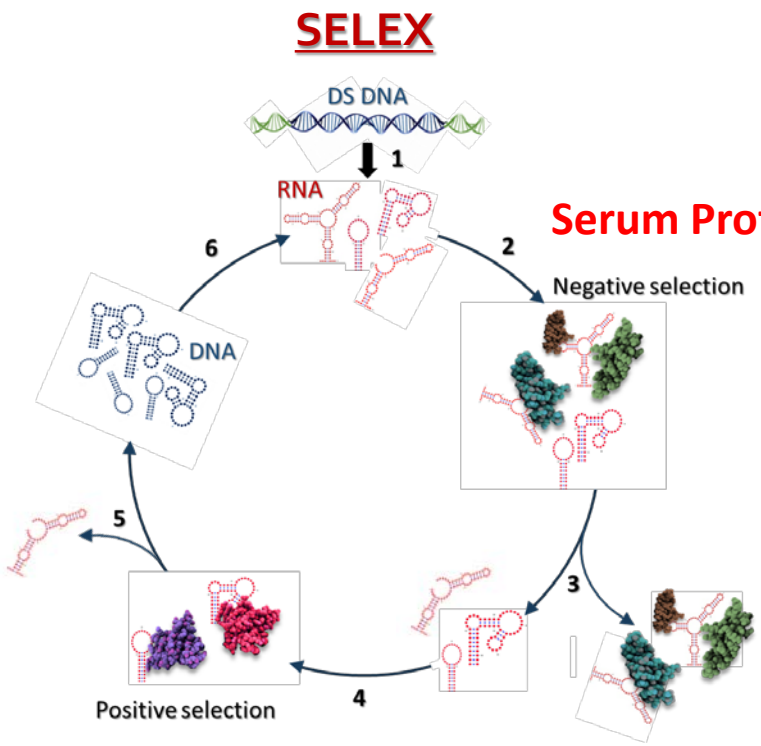

Serum Proteins

Histone H3 & H4

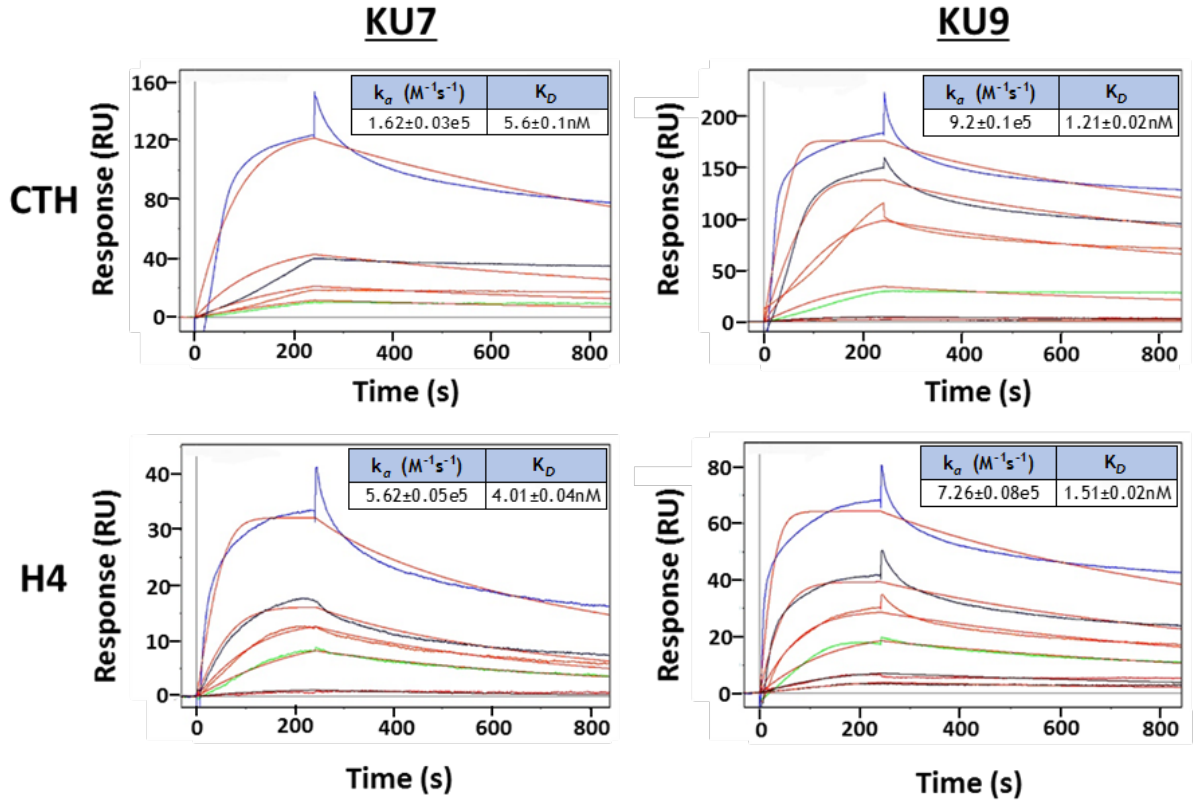

Aptamers inhibit histone-mediated platelet aggregation

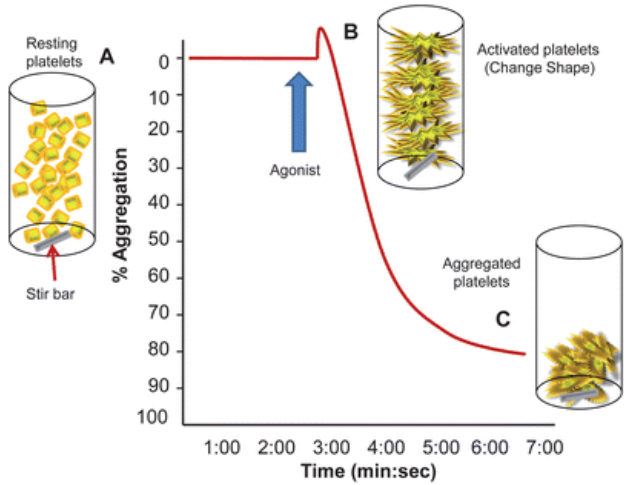

Light transmission aggregometry

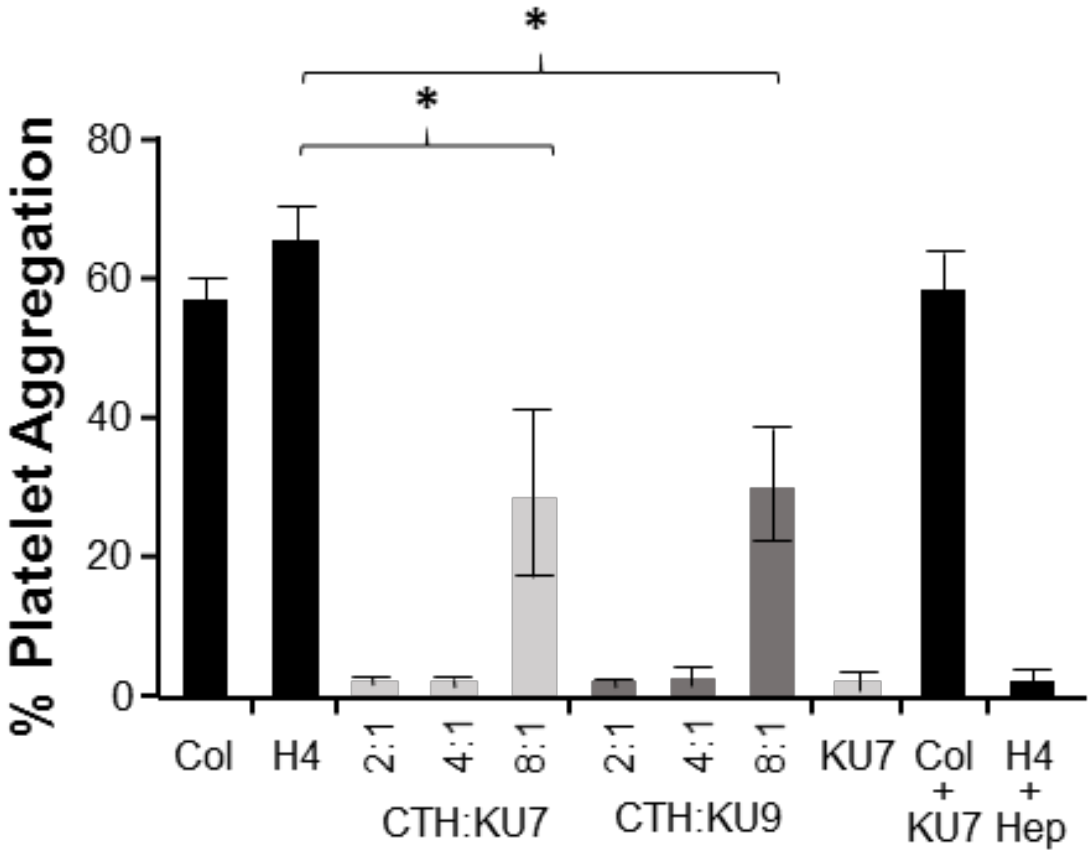

Efficacy of histone aptamers in murine MODS model

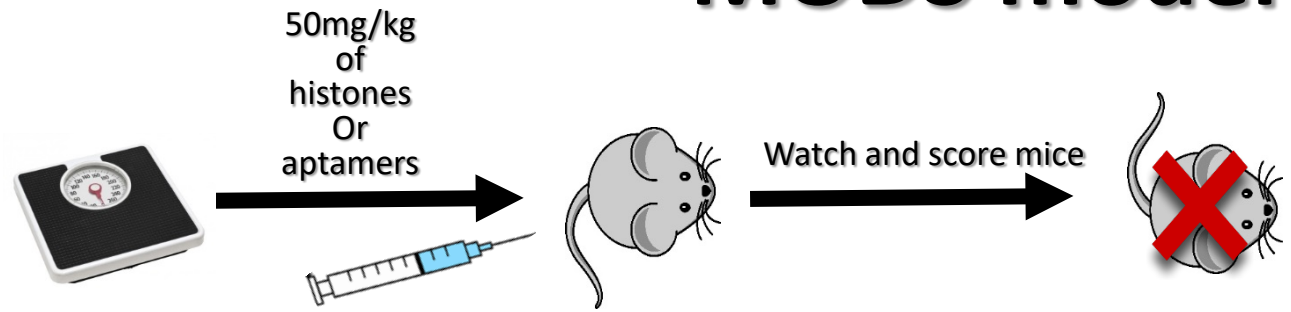

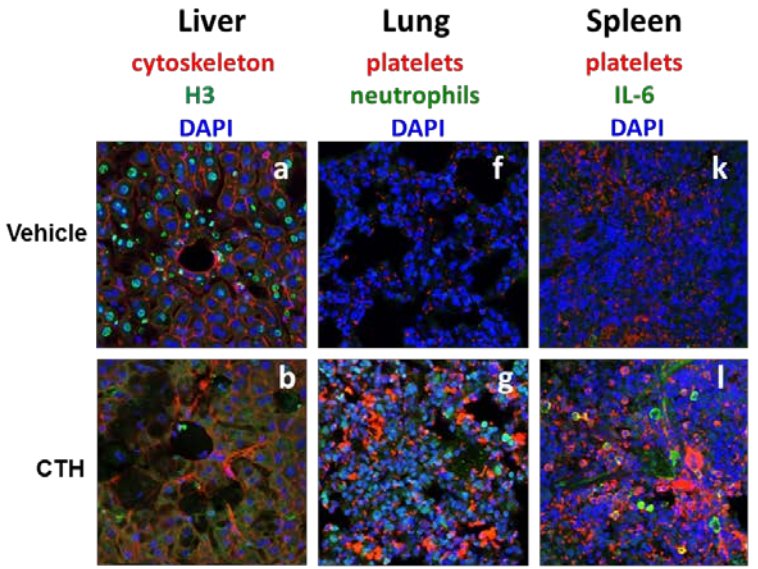

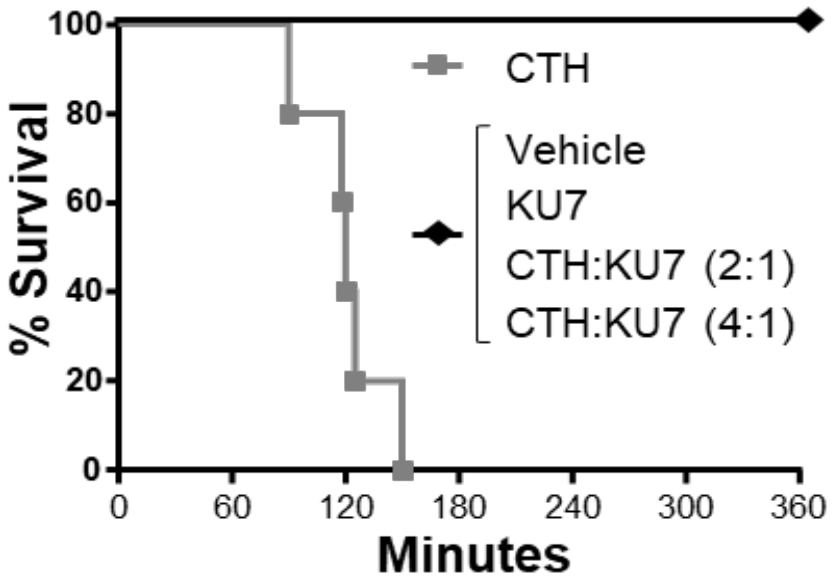

Time dependent inhibition of histone mediated toxicity with aptamers *in vitro*

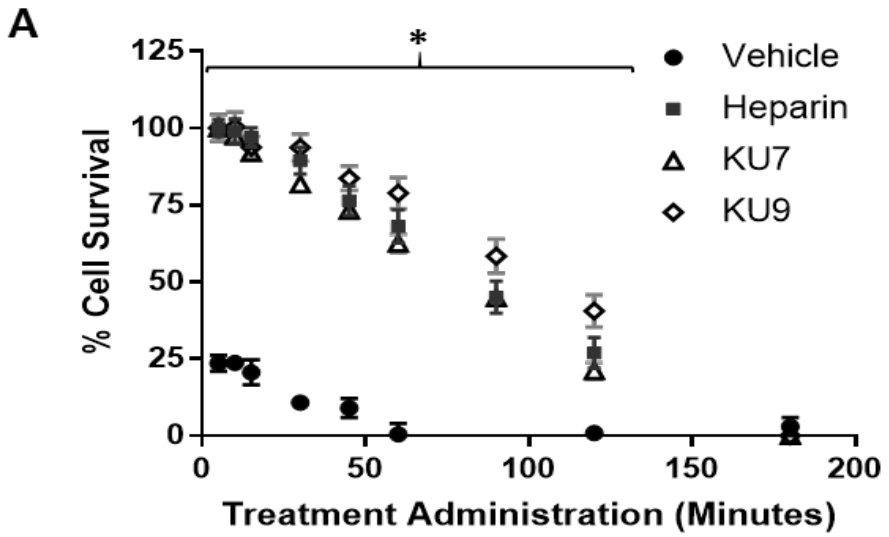

Aptamers protect against histone mediated death in mice

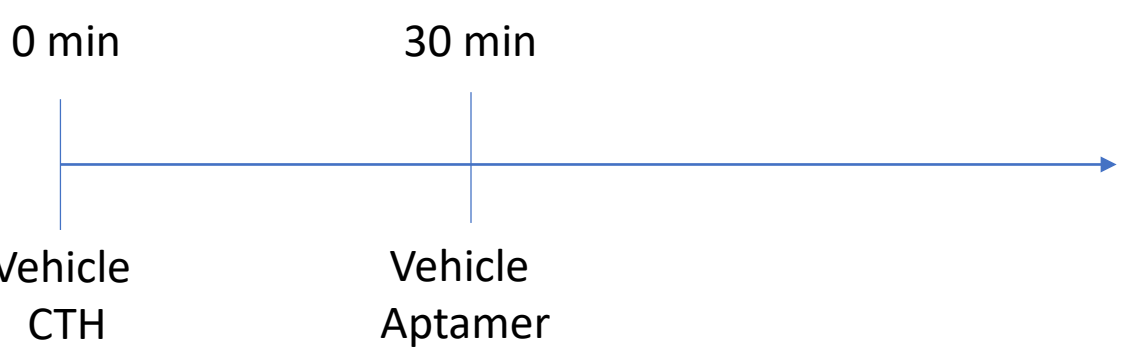

C

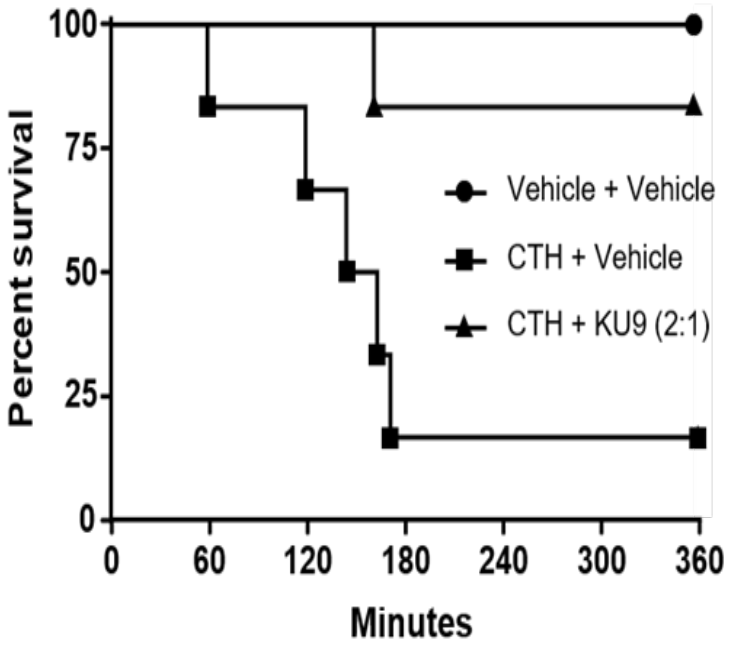

D

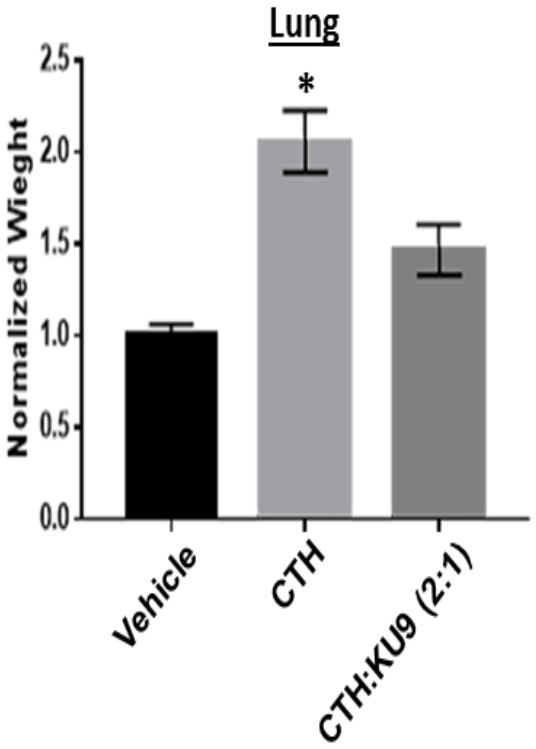

Future Directions

- Short and long term safety studies
- Relevant disease animal models (sepsis)
- Pharmacokinetic studies of the aptamer distributions

THANK YOU!

Giangrande Lab

Giselle Blanco
Justin Dassie
David Dickey
Luiza Hernandez
Craig Howell
Sven Kruspe
Li-Hsien Lin
Xiu Ying (Lisa) Liu
William Rockey
Kristina Wyatt Thiel
William Thiel
Gregory Thomas
Ofonime Udofot
Ryan Whitaker

U Iowa

Vladimir Badovinac
Kent Choi
Julia Klesney-Tait
Patrick McGonagill
David Meyerholz
Sanjana Dayal
Francis Miller

IDT Inc.

Mark Behlke

TriLink

Anton McCaffrey
Richard Hogrefe

Thesis Committee

James McNamara
Kathrine Musselman
Adam Dupey
Mary Wilson

MCB program

Fredrick Domann
Paulette Villhauer

NATIONAL INSTITUTES OF HEALTH
NATIONAL CANCER INSTITUTE
ELSA U. PARDEE FOUNDATION
MARY KAY ASH CHARITABLE FOUNDATION
Roy J. Carver CHARITABLE TRUST
THE UNIVERSITY OF IOWA
PRESIDENTIAL BIOLOGICAL SCHOLAR PROGRAM

Questions?

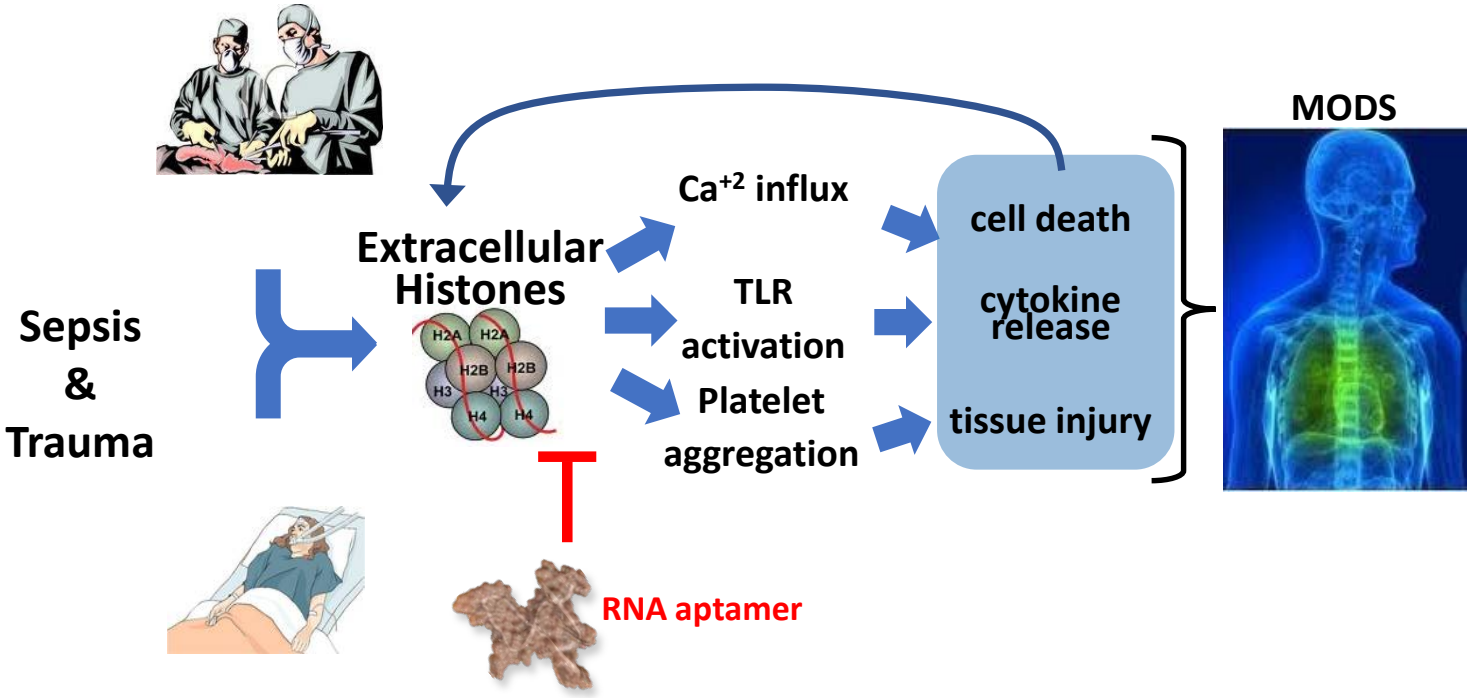
Sepsis
&
Trauma
Extracellular
Histones
H2A
H2A
H2B
H2B
H3
H3
H4
H4
Ca+2 influx
TLR
activation
Platelet
aggregation
cell death
cytokine
release
tissue injury
MODS
RNA aptamer

ABSTRACT

Multiple organ dysfunction syndrome (MODS) is an insidious and life threatening sequelae in patients suffering major trauma or illness. With prompt care patients with major trauma/illness can survive the initial injury, but soon other organs not directly affected by the original injury/illness may become dysfunctional. Breathing problems will develop that require placement on a ventilator, the kidneys will stop working requiring dialysis, and the patient will bleed from every orifice. Coordinated efforts in the intensive care unit (ICU) may reverse MODS at great cost, but there is currently no treatment to prevent MODS. Of those that develop MODS (200,000 case/year in the US), the risk of death is 40%. The most common organ involved in MODS is the lung (referred to as acute respiratory distress syndrome or ARDS). Trauma, smoke inhalation, burns, radiation, severe infection and blood transfusions can each cause ARDS and lead to acute lung injury (ALI). Only recently have investigators recognized that there is a common element to these conditions: damaged tissues releasing histones into the circulation. Histones are basic proteins found in chromatin. They normally reside in the nucleus of the cell and partner with DNA. However, when released from dying cells, histones have toxic effects on the lungs and other organs. We hypothesized that neutralization of extracellular histones with nucleic acid aptamers (anionic molecules) can prevent the morbidity and mortality associated with MODS/ARDS. We have employed Systemic Evolution of Ligands by Exponential Enrichment (SELEX) technology to identify RNA aptamers that bind with high affinity (low nM-pM range) and specificity to those histones (H3 and H4) known to cause MODS/ARDS but not to other proteins present in blood or on cells. We confirmed that histones H3/H4 induce pronounced platelet aggregation, which can be inhibited with the addition of the selected RNA aptamers. Furthermore, we demonstrate that histone-induced cytotoxicity can be reversed by treatment with the RNA aptamers both *in vitro* (lung-derived endothelial and epithelial cells) and *in vivo* in a mouse model of MODS/ARDS. Current efforts are focused on evaluating and the efficacy and safety of these RNA bio-drugs in other established murine models of MODS/ARDS (e.g. inhalation lung injury and influenza). In conclusion, we present robust preclinical data on a novel class of therapeutics against circulating histones that may be potentially effective in a wide-variety of common clinical conditions with high degree of morbidity, mortality and expense and for which, there is currently no effective treatment thus, establishing a paradigm change in the treatment of critically ill patients.

Figure 1. Aptamer Inhibitors of Extracellular Histones for the Treatment of Critical Illness

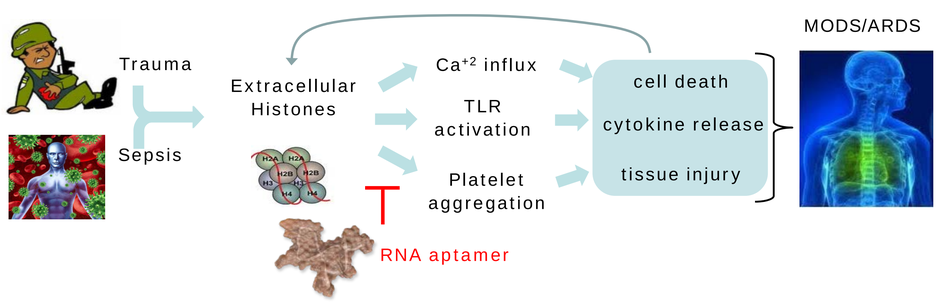

Schematic of aptamer-mediated inhibition of MODS/ARDS

Figure 2. Protein-Based SELEX

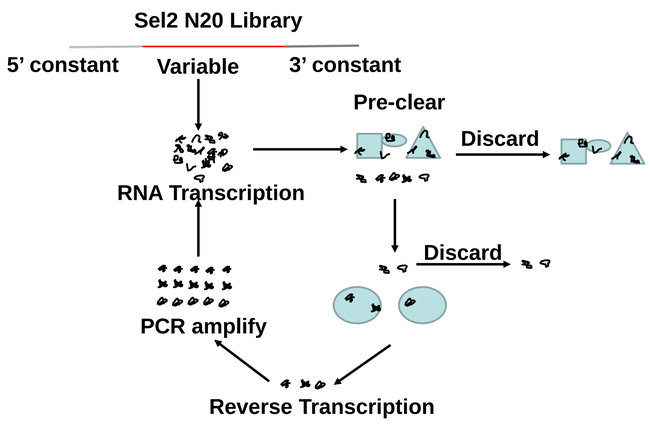

Systematic Evolution of Ligands by EXponential Enrichment (SELEX) is a combinatorial process that has been utilized to isolate aptamers that display high-affinity binding to soluble factors, cell-surface receptors, intracellular proteins and whole cells.

Figure 3. Selected RNA Aptamers Specificity, Sensitivity, and Stability .

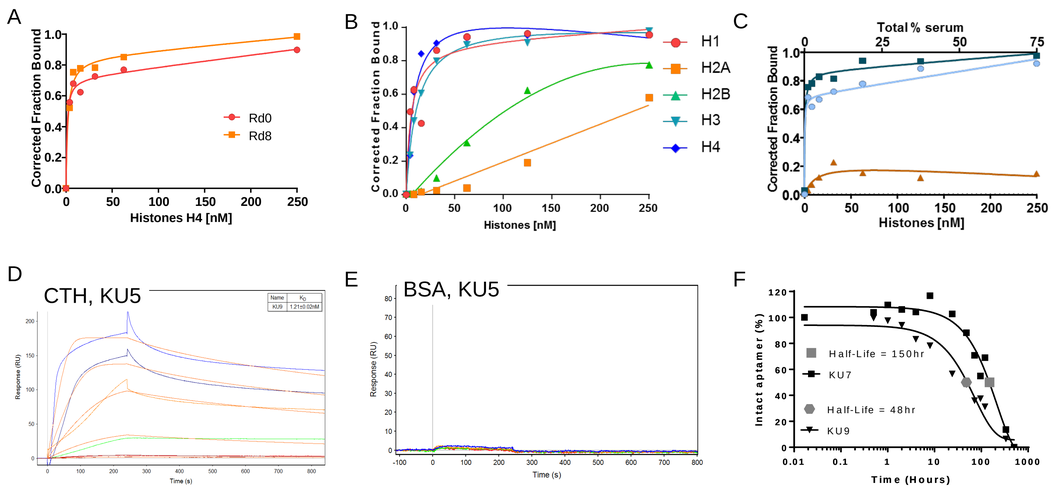

A) Binding affinities of histone H3 to unselected RNA aptamer library (R0) and selected RNA aptamer pool from round 8 of selection (R8) were determined as in part A. **B)** The affinity of aptamer clone KU7 with all histones subtype, **C)** and serum alone. A leftward shit in binding is indicative of enrichment for higher affinity aptamers. **D)** Surface plasmon resonance was used for KU 7 to determine binding to calf thymus histones and **E)** BSA. **F)** The serum stability of the different aptamer clones in 50% serum.

Figure 4. RNA Aptamers Inhibit Histone-Mediated Cytotoxicity

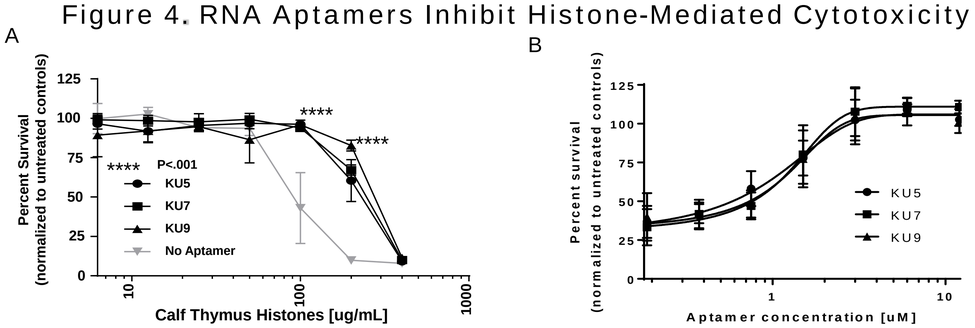

A) EA.Hy926 cells were treated with 1.2uM of the respected aptamer and a decreasing amount of calf thymus histones. Cell viability was determined by MTS assay. A 2way ANOVA test determined that there was a significant difference between all aptamers and the no aptamer treatment at the 100 and 200 µg/ml concentration of calf thymus histones. **B)** EA.Hy926 cells were treated with 180µg/mL of Calf Thymus Histone and a decreasing amount of Aptamer.

Figure 5. RNA Aptamers Inhibit Histone-Mediated Platelet Aggregation

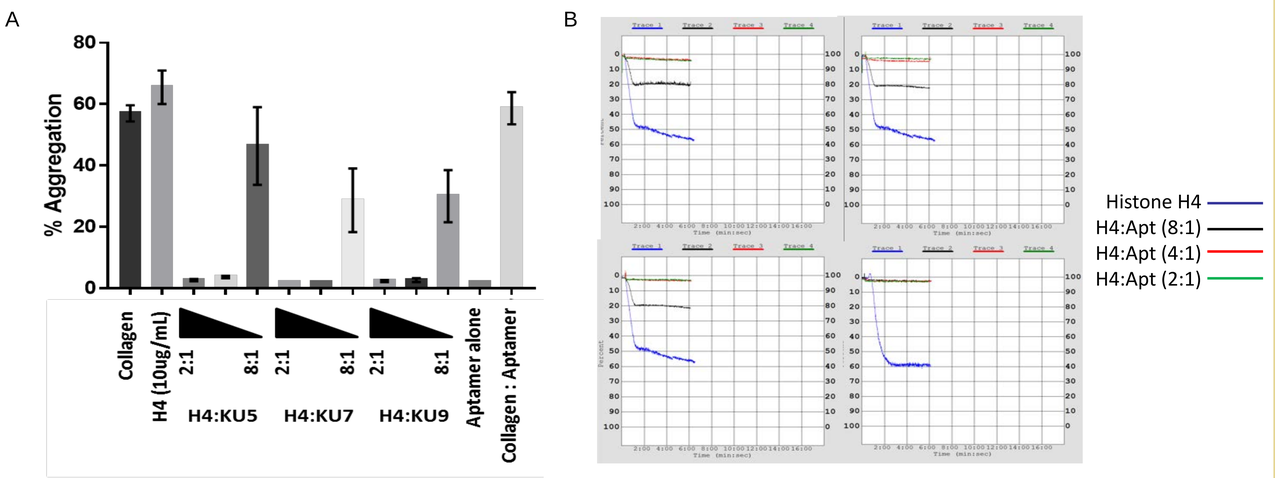

Platelet aggregation was performed with washed human platelets and quantitated using an aggregometer at 2 min intervals. **A)** Analysis of triplicate samples from 3 different donor used for platelet aggregation with collagen, histone H4, and aptamers. **B)** Aggregometry plots of data from figure A.

Figure 6. Murin

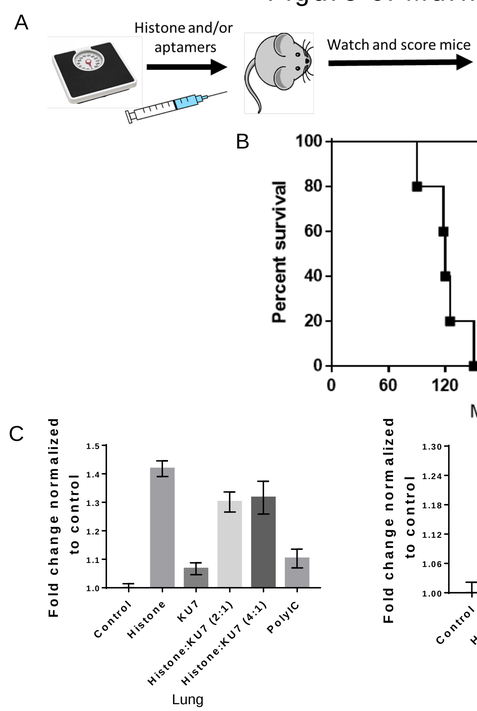

A) Diagram of the Multiple organ dysfunction syn with CTH (50mg/kg), KU7 (25mg/kg), Histone:H determined by taking the body weight of each euthanizing. **D)** The organs were then sectioned a

Future Directions

1. Further investigate the Minimal Effective Dose
2. Explore the treatment time course in vitro
3. Determine the time course with the MODS mur
4. Establish clinically relevant *in vivo* murine mod as sepsis, smoke inhalation, transfusion-relate efficacy of selected aptamers.

Acknowledgements

Funding

- **Carver Collaborative Pilot Grant 2015**
- OVPRED Internal Funding Initiative 2015
- **DOD**